



저작자표시-비영리-변경금지 2.0 대한민국

이용자는 아래의 조건을 따르는 경우에 한하여 자유롭게

- 이 저작물을 복제, 배포, 전송, 전시, 공연 및 방송할 수 있습니다.

다음과 같은 조건을 따라야 합니다:



저작자표시. 귀하는 원저작자를 표시하여야 합니다.



비영리. 귀하는 이 저작물을 영리 목적으로 이용할 수 없습니다.



변경금지. 귀하는 이 저작물을 개작, 변형 또는 가공할 수 없습니다.

- 귀하는, 이 저작물의 재이용이나 배포의 경우, 이 저작물에 적용된 이용허락조건을 명확하게 나타내어야 합니다.
- 저작권자로부터 별도의 허가를 받으면 이러한 조건들은 적용되지 않습니다.

저작권법에 따른 이용자의 권리는 위의 내용에 의하여 영향을 받지 않습니다.

이것은 [이용허락규약\(Legal Code\)](#)을 이해하기 쉽게 요약한 것입니다.

[Disclaimer](#)

이학박사 학위논문

The ICE transcription factors integrate  
environmental signals into developmental  
pathways in *Arabidopsis*

ICE 전사인자에 의한 환경 신호 및  
식물 발달관련 경로의 통합에 관한 연구

2018 년 2 월

서울대학교 대학원

화 학 부

이 재 형

## ABSTRACT

Plants are sessile organisms that must respond to changes in their environments. They should be able to tolerate environmental constraints to survive and propagate. To cope with inadequate environmental conditions, plants have evolved adaptive mechanisms through the gene regulatory network. Many transcriptional regulators including transcription factors directly or indirectly control their downstream gene expressions in response to environmental changes. INDUCER OF CBF EXPRESSION (ICE) transcription factors have a crucial role in transcriptional regulation of their target gene expressions in response to environmental stimuli. However, it is largely unknown how environmental signals are integrated into plant developmental pathways in *Arabidopsis*.

In this study, I investigated function of ICE transcription factors as a molecular knob that integrate environmental signals into plant development. The regulatory mechanisms of the transcription factors, which are critical for temperature and light responses, were identified.

In **Chapter 1**, I examined how the temperature and photoperiod signals are coordinated to modulate timing of flowering during changing seasons. In this study, I demonstrated an elaborate signaling network for fine-tuning of seasonal flowering in plants. I found that the transient-cold effect on flowering is mediated primarily by ICE1. ICE1 directly activates *FLOWERING LOCUS C (FLC)* under short-term cold conditions. By

contrast, under floral promotive conditions, SUPPRESSOR OF OVEREXPRESSION OF CO 1 (SOC1), which is largely known as a floral inducer, inhibited the DNA binding of ICE1 to the *FLC* and *C-REPEAT BINDING FACTOR 3* gene promoters, inducing flowering with a reduction of freezing tolerance. These observations indicate that optimal flowering of plants during changing seasons is fine-tuned by an ICE1-FLC-SOC1 signaling network.

In **Chapter 2**, I investigated how light induces stomatal development. In this study, I found that CONSTITUTIVE PHOTOMORPHOGENIC 1 (COP1) degrades and ubiquitinates ICE proteins under dark conditions. Moreover, light inhibited COP1-mediated degradation of ICE proteins in the abaxial epidermal cells, thus inducing stomatal development. These observations indicate that photostabilization of ICE proteins, via light-mediated inhibition of COP1-mediated protein surveillance systems, is important for stomatal development.

**Keywords:** Transcription factors, flowering, low temperature, light signaling, stomatal development, adaptive responses

**Student Number:** 2010-23096

# CONTENTS

<b>ABSTRACT</b> .....	<b>i</b>
<b>CONTENTS</b> .....	<b>iii</b>
<b>LIST OF FIGURES</b> .....	<b>viii</b>
<b>LIST OF TABLES</b> .....	<b>xi</b>
<b>ABBREVIATIONS</b> .....	<b>xii</b>

## BACKGROUND

<b>1. Temperature-mediated adaptive responses in plants</b> .....	<b>1</b>
<b>1.1 Role of ICE1 in acquiring cold acclimation</b> .....	<b>1</b>
<b>1.2 Short-term exposure to cold temperature delays flowering         in <i>Arabidopsis</i></b> .....	<b>2</b>
<b>1.3 The broader role of ICE1 in plant development</b> .....	<b>3</b>
<b>2. Light-mediated stomatal development in <i>Arabidopsis</i></b> .....	<b>6</b>
<b>2.1 Stomatal differentiation and patterning in <i>Arabidopsis</i></b> .....	<b>6</b>
<b>2.2 Light is required for inducing stomatal development</b> .....	<b>7</b>

2.3 COP1 is a photomorphogenic repressor.....	9
3. The purpose of this study.....	10

## **MATERIALS AND METHODS**

1. Plant materials and growth conditions.....	11
2. Gene expression analysis.....	13
3. Transcriptional regulation activity assay.....	14
4. ICE1 protein stability assay.....	15
5. ChIP assay.....	16
6. Yeast two-hybrid assay.....	16
7. BiFC assay.....	17
8. <i>in vitro</i> pull-down assay.....	17
9. Coimmunoprecipitation assay.....	18
10. Freezing tolerance assay.....	19
11. Flowering time measurement.....	19
12. Intermittent cold treatment and vernalization.....	19
13. Fluorescent imaging and microscopic analysis.....	20
14. Ubiquitination assay.....	20
15. SI measurement.....	20

16. Statistical analysis.....20

**CHAPTER 1: INDUCER OF CBF EXPRESSION 1  
integrates cold signals into the FLOWERING LOCUS  
C-mediated flowering pathways in *Arabidopsis***

**ABSTRACT.....25**

**INTRODUCTION.....26**

**RESULTS**

*FLC* expression is reduced in the early-flowering *ice1-2*  
mutant.....26

ICE1 activates *FLC* by binding to the gene promoter  
.....33

ICE1 activates the *FLC* gene under cold temperature  
conditions.....40

ICE1 interacts with SOC1 in the nucleus.....42

SOC1 inhibits ICE1 binding to *FLC* promoter in  
promoting flowering.....46

SOC1 inhibits ICE1 binding to <i>CBF3</i> promoter in inducing cold acclimation.....	52
<b>DISCUSSION.....</b>	<b>60</b>
 <b>CHAPTER 2: Light inhibits COP1-mediated degradation of ICE transcription factors to induce stomatal development in <i>Arabidopsis</i></b>	
<b>ABSTRACT.....</b>	<b>66</b>
<b>INTRODUCTION.....</b>	<b>67</b>
<b>RESULTS</b>	
<b>Light induces ICE accumulation in the nuclei of leaf     abaxial epidermal cells.....</b>	<b>71</b>
<b>COP1 interacts with ICE proteins.....</b>	<b>74</b>
<b>COP1 ubiquitinates ICE proteins.....</b>	<b>81</b>
<b>COP1 degrades ICE proteins through ubiquitin/proteasome     pathway.....</b>	<b>85</b>

<b>Light inhibits COP1-mediated degradation of ICE proteins</b> .....	<b>98</b>
<b>Light-mediated stabilization of ICE proteins is critical for stomatal development.....</b>	<b>100</b>
<b>ICE proteins integrate light and developmental signals into stomatal development.....</b>	<b>110</b>
<b>DISCUSSION.....</b>	<b>116</b>
<b>REFERENCES.....</b>	<b>121</b>
<b>PUBLICATION LIST.....</b>	<b>138</b>
<b>ABSTRACT IN KOREAN.....</b>	<b>139</b>

## LIST OF FIGURES

Figure 1. The <i>ice1-2</i> mutant exhibited early flowering under LDs and SDs.....	30
Figure 2. Complementation of <i>ice1-2</i> mutant.....	31
Figure 3. Expression of flowering genes in <i>ice1-2</i> mutant.....	32
Figure 4. FLC dependence of flowering in <i>ICE1</i> -overexpressing plants.....	36
Figure 5. ICE1 activates <i>FLC</i> expression by binding to the gene promoter.....	37
Figure 6. Flowering phenotypes of <i>ICE1</i> -overexpressing plants.....	39
Figure 7. Effects of long-term cold on <i>ice1-2</i> flowering.....	41
Figure 8. ICE1 delays flowering by inducing <i>FLC</i> under cold temperature conditions.....	43
Figure 9. Effects of short-term cold on ICE1 protein stability.....	44
Figure 10. Cold temperature accelerates the binding of ICE1 on <i>FLC</i> gene promoter.....	45
Figure 11. ICE1 interacts with SOC1 in yeast cells.....	47
Figure 12. ICE1 interacts with SOC1 <i>in planta</i> .....	48
Figure 13. Inhibition of ICE1 transcriptional activation activity by SOC1..	50
Figure 14. Inhibition of ICE1 binding to <i>FLC</i> promoter by SOC1.....	51
Figure 15. SOC1 inhibits ICE1 function in inducing <i>FLC</i> gene.....	53
Figure 16. Linkage of SOC1 with ICE1 in freezing tolerance.....	55

Figure 17. SOC1 inhibits ICE1 binding to <i>CBF3</i> promoter.....	56
Figure 18. SOC1 inhibits ICE1 in inducing cold acclimation.....	58
Figure 19. An ICE1-mediated signaling network integrates cold signals into flowering time control via a feedback loop.....	59
Figure 20. Kinetics of <i>ICE</i> transcription.....	72
Figure 21. Effects of light on <i>ICE</i> transcription.....	73
Figure 22. Light induces ICE accumulation.....	75
Figure 23. Light-induced ICE accumulation occurs in the nuclei of abaxial epidermal cells of cotyledons.....	76
Figure 24. Effects of light on ICE protein stability in stomata and stomatal lineage cells.....	77
Figure 25. Effects of light on ICE1 accumulation in different plant organs .....	78
Figure 26. ICE proteins interact with COP1 in yeast cells.....	82
Figure 27. ICE proteins interact with COP1 <i>in planta</i> .....	83
Figure 28. COP1 does not interact with SPCH, MUTE, and FAMA.....	84
Figure 29. COP1 ubiquitinates ICE proteins <i>in vitro</i> .....	86
Figure 30. Autoubiquitination activity of COP1 <i>in vitro</i> .....	87
Figure 31. ICE ubiquitination <i>in vivo</i> .....	88
Figure 32. COP1 does not ubiquitinate SPCH, MUTE, and FAMA.....	89
Figure 33. COP1 degrades ICE proteins through ubiquitin/proteasome pathways.....	91
Figure 34. Kinetics of ICE accumulation in abaxial epidermal cells.....	94

Figure 35. SPCH degradation is not associated with ubiquitin/proteasome pathways.....	95
Figure 36. SPCH degradation is not associate with COP1 function.....	97
Figure 37. Light inhibits COP1-mediated degradation of ICE1.....	99
Figure 38. Light-mediated stabilization of ICE1 is important for stomatal development.....	102
Figure 39. Kinetics of stomatal differentiation in 35S: <i>GFP-ICE1 cop1-4</i> plants.....	104
Figure 40. Stomatal phenotype of 35S: <i>GFP-ICE1 cop1-5</i> plants in darkness.....	105
Figure 41. ICE1 and SCRM2 are required for light-mediated induction of stomatal development.....	108
Figure 42. Stomatal phenotypes of <i>ice1-2 scrm2-2</i> mutants harboring <i>cop1-5</i> mutation.....	109
Figure 43. Functional relationship between YDA and ICE1 in light-induced stomatal development.....	111
Figure 44. ICE proteins integrate light signals into stomatal development .....	114
Figure 45. ICE-mediated light signaling scheme during stomatal development.....	115

## LIST OF TABLES

Table 1. Primers used in this study.....	22
Table 2. Flowering phenotypes of flowering mutants in <i>ice1-2</i> background.....	34

## ABBREVIATIONS

ABA	Abscisic acid
BiFC	Bimolecular fluorescence complementation
BP filter	Band pass filter
BS	Binding sequence
CaMV	Cauliflower mosaic virus
cDNA	Complementary DNA
ChIP	Chromatin immunoprecipitation
CO	CONSTANS
CO <sub>2</sub>	Carbon dioxide
C <sub>T</sub>	Threshold cycle
CRY	Cryptochrome
DAG	Days after germination
DIC	Differential interference contrast
EPF2	EPIDERMAL PATTERNING FACTOR 2
FRI	FRIGIDA
FT	FLOWERING LOCUS T
GFP	Green fluorescent protein
GI	GIGANTEA
GST	Glutathione S-transferase
GUS	β-glucuronidase
HA	Hemagglutinin

LDs	Long days
MAPK	Mitogen-activated protein kinase
MBP	Maltose binding protein
MS	Murashige and Skoog
nBS	Non-binding sequence
NLS	Nuclear localization sequence
PEG	Polyethylene glycol
PHY	Phytochrome
PI	Propidium iodide
ProS2	Protein S2
SDs	Short days
SI	Stomatal index
SLGC	Stomatal lineage ground cell
SPCH	SPEECHLESS
T-DNA	Transfer DNA
Ub	Ubiquitin
YDA	YODA
YFP	Yellow fluorescent protein
ZT	Zeitgeber time

# **BACKGROUND**

## **1. Temperature-mediated adaptive responses in plants**

### **1.1 Role of ICE1 in acquiring cold acclimation**

Plant growth and distribution are significantly affected by environmental conditions, such as changes in temperature. Under freezing conditions, plant survival and development are significantly disturbed, thus impeding on crop quality and productivity. To cope with these environmental constraints, they evolved to develop adaptive responses. Cold acclimation is triggered by an exposure to low but non-freezing temperature (Guy, 1990). As a result, the fluidity of the plasma-membrane and levels of cellular metabolic materials are largely affected, which enhance the plant's capacity to tolerate abrupt freezing temperatures (Guy et al., 2008; Medina et al., 2011).

It is well-defined that three tandemly arrayed AP2 family transcription factors, C-repeat binding factors (CBF), have a crucial role in cold acclimation. Low temperature (generally, exposure to 4°C) rapidly induces transcription of *CBF* genes (Gilmour et al., 1998). In turn, CBF transcription factors activate diverse downstream genes that encode osmo-protectant proteins and constituents of plasma-membrane (Gilmour et al., 1998). Therefore, *CBF*-overexpressing plants exhibit enhanced freezing tolerance.

Among several upstream regulators of *CBF* genes, Inducer of CBF expression 1 (*ICE1*) is a well-defined signaling modulator in cold signaling pathways. *ICE1* encodes a basic-helix-loop-helix transcription factor that binds to MYC-like cis-binding elements of *CBF* promoters. Cold triggers the DNA-binding affinity of *ICE1* to *CBF* genes (Chinnusamy et al., 2003), thereby enhancing freezing tolerance. Transcriptomic analysis reveals that many cold-responsive genes were altered in *ICE1*-defective mutant (Lee et al., 2005), implying that *ICE1* is a key transcription factor in acquiring cold acclimation.

The E3 ubiquitin ligase HIGH EXPRESSION OF OSMOTICALLY RESPONSIVE GENES 1 (*HOS1*) degrades *ICE1* during cold acclimation. This regulatory mechanism attenuates exaggerated cold responses and sustains plant development during cold acclimation (Dong et al., 2006).

### **1.2 Short-term exposure to cold temperature delays flowering in *Arabidopsis***

Diverse plants integrate seasonal changes into their developmental transitions, such as flowering. In temperate zones, while temperature and photoperiod signals are encountered in a predictable manner, unpredictable environmental conditions, such as transient cold conditions, are also encountered during changing seasons. In the early spring, exposure of transient-cold temperature delays flowering (Kime et al., 2004; Seo et al., 2009). By contrast, low temperature enhances freezing tolerance (Guy, 1990). To optimize the timing of flowering, plants evolved to ensure an

elaborate signaling network, minimizing unnecessary freezing tolerance and optimizing reproductive success.

The effects of low temperatures on flowering have dual aspects. Long-term exposure to cold temperature, followed by inductive temperature conditions, accelerates flowering by silencing the *FLOWERING LOCUS C* (*FLC*) (Michaels and Amasino, 2001; Henderson and Dean, 2004), which is known to be a floral repressor. By contrast, intermittent cold treatment delays flowering through inducing *FLC* (Seo et al., 2009). *FLC* represses transcript level of floral integrators, such as *SUPPRESSOR OF OVEREXPRESSION OF CO 1* (*SOC1*) and *FLOWERING LOCUS T* (*FT*) (Blazquez and Weigel, 2000; Yoo et al., 2005).

Meanwhile, it is also known that *SOC1* represses freezing tolerance by negatively regulating the expression of *CBF* genes (Seo et al., 2009). Notably, *CBF*-overexpressing plants exhibit delayed flowering (Seo et al., 2009). Therefore, in plants, *SOC1* minimizes unnecessary freezing tolerances and promotes flowering induction in spring seasons. However, it is currently unknown how the low temperature signals are coordinated with the floral inductive signals for seasonal flowering at the molecular level.

### **1.3 The broader role of ICE1 in plant development**

*ICE1* acts as a master regulator in cold signaling pathways (Chinnusamy et al., 2003). *ICE1* transcription factors play a role in the ABA-independent cold signaling pathway (Liang et al., 2015). However, recent studies have

reported that ICE1 has a functional divergence in plant growth and development. It is largely perceived that ABA is directly involved in diverse osmotic stress responses in plants (Kang et al., 2002). Notably, an *ICE1*-defective mutant exhibits retardation of seedling growth under ABA- and sugar-deprived conditions, indicating that ICE1 is also involved in ABA- and sugar-mediated developmental pathways (Shinozaki et al., 2003). These observations indicate that the ICE1-mediated signaling network integrates sugar and hormonal signaling during plant development.

Specific roles of ICE1 in endosperm breakdown have also been proposed. It has been reported that an *ICE1*-defective mutant exhibited endosperm persistence phenotype, which causes significantly impeded embryo growth (Denay et al., 2014). Molecular mechanistic analysis reveals that heterodimerization of ICE1 and ZHOUP1 (ZOU) is required for proper endosperm breakdown. ICE1 and ZOU cooperatively regulate the expression of common target genes that are deeply involved in endosperm breakdown (Denay et al., 2014).

Stomatal differentiation and patterning are also modulated by ICE transcription factors, which are also known as SCREAM (SCRM). ICE1 and its functional paralog ICE2/SCRM2 specify transitional steps of stomatal differentiation (Kanaoka et al., 2008), by forming heterodimers with SPEECHLESS (SPCH), MUTE, and FAMA (Kanaoka et al., 2008). Together with the proposed role of ICE/SCRM, which has been described in cold signaling, diverse developmental processes are modulated by the

ICE-mediated signaling network. These observations strongly suggest that a plausible role for ICE1 in linking plant development and environmental adaptation in plants.

## **2. Light-mediated stomatal development in *Arabidopsis***

### **2.1 Stomatal differentiation and patterning in *Arabidopsis***

The stoma is a microscopic pore, mostly found in the epidermis of leaves. It functions as epidermal opening involving atmospheric gas exchange and water evaporation, which ensures photosynthetic conductance and optimizes plant growth and development. Therefore, proper stomatal development is crucial for plant propagation and global carbon cycle (Hetherington and Woodward, 2003; Driscoll et al., 2006).

Stomatal differentiation and spacing and distribution of stoma in epidermis are temporally and spatially modulated for optimal development. Initiation of stomatal development is conducted by the progenitor cells, also known as meristemoid mother cells. The cells asymmetrically divide and then produce meristemoids (Bergmann and Sack, 2007; MacAlister et al., 2007; Pillitteri and Torii, 2012). These cells, which have a stem-cell-like character, differentiate into the guard mother cells, eventually dividing into the guard cells (Ohashi-Ito and Bergmann, 2006; Pillitteri et al., 2007). It is also notable that the guard cells are not located adjacent to each other (Geisler et al., 2000; Geisler et al., 2003). The spatial regulation of stomatal development is important for stomatal aperture and other physiological conductances in plants (Nadeau and Sack, 2002; Hetherington and Woodward, 2003; Shpak et al., 2005).

Molecular genetic analysis reveals that **SPEECHLESS (SPCH)**,

MUTE, and FAMA proteins trigger sequential steps of stomatal development (Ohashi-Ito and Bergmann, 2006; MacAlister et al., 2007; Pillitteri et al., 2007). These proteins are tightly regulated in a spatiotemporal manner. Interestingly, ICE/SCRM transcription factors specify the transition of stomatal lineage by interacting with the proteins (Kanaoka et al., 2008). These regulatory modules resemble myogenic bHLH proteins in skeletal muscle differentiation in animal systems (Weintraub, 1993). ICE and SPCH transcription factors cooperatively regulate the target gene expression that modulates the stomatal patterning gene, *EPF2*, thus triggering stomatal development (Horst et al., 2015). In addition, several negative regulators are identified by forward genetic analysis (Bergmann et al., 2004; Shpak et al., 2005; Wang et al., 2007). These regulators negatively modulate the activity of SPCH, MUTE, and FAMA (Lampard et al., 2008; Dong and Bergmann, 2010).

## **2.2 Light is required for inducing stomatal development**

Stomatal development integrates environmental information. The concentration of CO<sub>2</sub> affects stomatal formation and density. High concentrations of CO<sub>2</sub> reduce stomatal density in leaf epidermal cells. This is an adaptive strategy for preventing unnecessary gas exchange in the conditions (Engineer et al., 2014). Forward genetic analysis reveals several regulators, which are directly involved in CO<sub>2</sub>-mediated stomatal development. Carbonic anhydrases, EPIDERMAL PATTERNING FACTOR

2 (*EPF2*), and *CO<sub>2</sub> RESPONSE SECRETED PROTEASE (CRPS)* are directly involved in *CO<sub>2</sub>*-mediated stomatal development. They affect *EPF2* gene expression in response to the environmental changes (Engineer et al., 2014).

Stomatal development is also affected by temperature changes. High temperature reduces stomatal density of leaves, despite higher cooling capacity (Crawford et al., 2012). In addition, low temperature delays cell differentiation, thus possibly inhibiting stomatal development (Thomashow, 1999). These adaptive mechanisms provide an additional link between environmental temperatures and stomatal development. In addition, atmospheric humidity also affects stomatal development. However, how the various environmental cues modulate stomatal development at the molecular level is unclear.

Light-mediated stomatal development is extensively studied among the environmental cues. Light induces the transition of stomatal differentiation (Kang et al., 2009; Balcerowicz et al., 2014). Therefore, dark-grown wild-type seedlings exhibit aborted stomatal development (Kang et al., 2009). Specifically, in dark-grown seedlings, aborted stomatal lineage cells are prominently existed, but stomatal formation is significantly disturbed, demonstrating that light induces transitional steps of stomatal development (Kang et al., 2009). Phytochromes and cryptochromes modulate light-mediated stomatal development. (Kang et al., 2009) Additionally, COP1, which acts downstream of the photoreceptors, represses stomatal

development (Kang et al., 2009; Balcerowicz et al., 2014). However, how light signals are integrated with the developmental pathways during stomatal development is currently unknown.

### **2.3 COP1 is a photomorphogenic repressor**

Light is an energy source, which is important for diverse aspect of plant growth and development. Light affects diverse aspect of plant growth, such as hypocotyl and petiole elongation, and flowering time (Lau and Deng, 2012). From the phenotype of seedling photomorphogenesis, COP1 has been identified as a negative regulator of light signaling (von Arnim and Deng, 1994). Notably, COP1-defective mutants exhibit proper cell elongation and development even in the dark (Kang et al., 2009). The E3 ubiquitin ligase COP1 directs degradation of light-regulated transcription factors, such as ELONGATED HYPOCOTYL 5 (HY5), LONG AFTER FAR-RED LIGHT 1 (LAF1), and LONG HYPOCOTYL IN FAR-RED 1 (HFR1) (Osterlund et al., 2000; Seo et al., 2003; Jang et al., 2005).

COP1 forms a heterodimeric protein complex with SUPPRESSOR OF PHYA-105 (SPA) and DDB1 proteins (Saijo et al., 2003). Their activities are synergistically effective on their target proteins (Saijo et al., 2003). Notably, light inhibits COP1 activity by two mechanisms. Light-activated photoreceptors disrupt the COP1-SPA interaction, thereby promoting photomorphogenic development (Lian et al., 2011; Liu et al., 2011; Zuo et al., 2011; Lu et al., 2015; Sheerin et al., 2015). Light

exposure also leads to the loss of nuclear localization of COP1, which is relocated into the cytoplasm (von Arnim and Deng, 1994; Stacey et al., 1999).

COP1 is involved in diverse photomorphogenic development. It is known that COP1 also acts as a negative regulator of stomatal development (Kang et al., 2009). In this signaling network, the COP1/SPA protein complex, which is downstream of photoreceptors, cooperatively modulates stomatal development (Kang et al., 2009). However, it is currently unknown how the signaling module is linked to the central gene regulatory network.

### **3. The purpose of this study**

Due to the nature of plants, they have developed an adaptive strategy to changing environments for their optimal growth and development. It is perceived that diverse regulatory mechanisms could be involved in these adaptive responses. This study describes regulatory mechanisms of adaptive responses in response to changes of temperature and light. How the environmental changes modulate plant growth and development is identified at the molecular level.

## MATERIALS AND METHODS

### Plant materials and growth conditions

All *Arabidopsis thaliana* lines used were in Columbia (Col-0) background except for *cop1-5* mutant, which has been generated in Wassilewskija (Ws-2) background (McNellis et al., 1994). The *ice1-2* and *scrm2-2* mutants have been described previously (Kanaoka et al., 2008; Kim et al., 2015). The *cop1-4* and *cop1-6* mutants have been described previously (Deng et al., 1991). The flowering time mutants used include *co-101* (Takada and Goto, 2003), *gi-2* (Fowler et al., 1999), *ft-10* (Yoo et al., 2005), *soci-2* (Lee et al., 2000), *flc-3* (Michaels and Amasino, 1999), *fve-4* (Ausín et al., 2004), and *fca-9* (Page et al., 1999). Col-0 plant bearing an active *FRI* allele introgressed from the San Feliu-2 accession has been described previously (Lee et al., 1994).

For the complementation of *ice1-2* mutant with a wild-type *ICE1* gene, a genomic *ICE1* gene sequence with its own promoter consisting of ~3.8-kb sequence upstream of the transcription start site was transformed into the mutant. A full-size *SOCI* cDNA was subcloned under the control of the CaMV 35S promoter in the binary pH2GW7 vector, and the expression construct was transformed into Col-0 plants to generate *SOCI*-ox plants. More than 20 independent lines were obtained from each transformation, among which a few representative lines were chosen for subsequent assays. A MYC-coding sequence was fused in-frame to the 5'

ends of *ICE1* and *SCRM2/ICE2* genes, and the fusions were expressed driven by endogenous *ICE* promoters in Col-0 plants, resulting in *pICE1:MYC-ICE1* and *pSCRM2:MYC-SCRM2* plants, respectively. To produce *pICE1:GFP-ICE1*, *pSCRM2:GFP-SCRM2*, and *pSPCH:GFP-SPCH* plants, a green fluorescent protein (GFP)-coding sequence was fused in-frame to the 5' ends of *ICE* and *SPCH* genes, and the fusions were subcloned under the control of endogenous promoters into the modified pBA002a vector (Jung et al., 2013). To produce transgenic plants overexpressing *ICE1* gene, a full-size *ICE1* cDNA was fused in-frame to the 3' end of a MYC-coding sequence, and the fusion construct was overexpressed driven by the CaMV 35S promoter in Col-0 plants, resulting in *35S:MYC-ICE1* plants. The *35S:MYC-ICE* transgenic plants have been described previously (Kim et al., 2015; Lee et al., 2015). A full-size *SPCH* cDNA was fused in-frame to the 3' end of a MYC-coding sequence, and the fusion construct was overexpressed driven by the CaMV 35S promoter in Col-0 background to generate *35S:MYC-SPCH* plants. To produce *35S:GFP-ICE1* plants, a full-size *ICE1* cDNA was fused in-frame to the 3' end of a GFP-coding sequence, and the fusion construct was subcloned under the control of the CaMV 35S promoter into the binary pBA002 vector (Kim et al., 2006). A full-size *ICE1* cDNA was also fused in-frame to the 3' end of a HA-coding sequence, and the fusion construct was overexpressed driven by the CaMV 35S promoter to generate *35S:HA-ICE1* plants. To produce transgenic plants expressing COP1-MYC under the

control of a  $\beta$ -estradiol-inducible promoter, a full size *COP1*-coding sequence was subcloned into the pER8 vector (Zuo et al., 2000). For generating *pICE:NLS-GFP* and *pSPCH:NLS-GFP* plants, the gene promoter sequences were transcriptionally fused to nuclear localization sequence (NLS) and GFP-coding sequence, and the fusion constructs were transformed into Col-0 plants.

*Arabidopsis* seeds were cold-imbibed for 3 days at 4°C in complete darkness and allowed to germinate in a controlled culture room set at 23°C with relative humidity of 60%. They were grown under either LDs (16-hr light and 8-hr dark) or SDs (8-hr light and 16-hr dark) with white-light illumination ( $120 \mu\text{mol photons m}^{-2}\cdot\text{s}^{-1}$ ) provided by FLR40D/A fluorescent tubes (Osram, Seoul, Korea). For treatments with different light wavelengths, plants were grown on 1/2 X Murashige and Skoog-agar (MS-agar) plates with white light ( $50 \mu\text{mol}\cdot\text{m}^{-2}\cdot\text{s}^{-1}$ ), blue ( $35 \mu\text{mol}\cdot\text{m}^{-2}\cdot\text{s}^{-1}$ ), red ( $40 \mu\text{mol}\cdot\text{m}^{-2}\cdot\text{s}^{-1}$ ), or far-red ( $15 \mu\text{mol}\cdot\text{m}^{-2}\cdot\text{s}^{-1}$ ) illumination. *Arabidopsis* transformation was performed by the floral dip method (Clough and Bent, 1998).

### **Gene expression analysis**

Preparation of RNA samples and RT-qPCR were performed according to the rules proposed to ensure reproducible measurements of mRNA levels (Udvardi et al., 2008). RT-qPCR reactions were performed in 96-well blocks with the Applied Biosystems 7500 Real-Time PCR System (Foster

City, CA) using the SYBR Green I master mix in a volume of 20  $\mu$ L. PCR primers used were listed in Table 1. The two-step thermal cycling profile employed was 15 s at 95°C for denaturation and 1 min at 60°C for annealing and polymerization. An *eIF4A* gene (At3g13920) was included as internal control in the PCR reactions in order to normalize the variations in the amounts of cDNA used. All RT-qPCR reactions were performed in biological triplicates using RNA samples extracted from three independent plant materials grown under identical conditions. The threshold cycle ( $C_T$ ) was automatically determined for each reaction by the system set with default parameters. The reaction specificity was determined by the melt curve analysis of amplified products using the standard method installed in the system.

#### **Transcriptional regulation activity assay**

For transient GUS expression assays in *Arabidopsis* protoplasts, a set of reporter and effector plasmids was constructed. The *pMin35S* reporter plasmid contains a minimal CaMV 35S promoter harboring the TATA box and the GUS gene. The *pFLC:GUS* reporter plasmid includes a *FLC* promoter sequence upstream of the 35S minimal promoter. Three copies of binding sequences were fused to the 5' end of the CaMV 35S minimal promoter to produce *pFLC-BS* and *pFLC-mBS* reporter plasmids. To construct the *p35S:ICE1* effector plasmid, the *ICE1* gene was inserted into an expression vector containing the CaMV 35S promoter and a NOS

terminator. The reporter and effector plasmids were cotransformed into *Arabidopsis* protoplasts. GUS activity was measured by the fluorometric method, as described previously (Jefferson et al., 1987). A CaMV 35S promoter-luciferase construct was also cotransformed as an internal control in the assays. The luciferase assay was performed using the Luciferase Assay System kit (Promega, Madison, WI).

### **ICE protein stability assay**

The 35S:*MYC-ICE1* transgenic plants were grown on MS-agar plates under LDs. Protein extracts were prepared from whole plant materials. The protein extracts were separated by SDS-PAGE and transferred to Immobilon-P membrane (Millipore, Bedford, MA), and ICE1 proteins were immunologically detected using an anti-MYC antibody at 1:2000 dilution (Millipore). Five-day-old 35S:*HA-ICE1* pXVE:*COPI-MYC* plants grown on MS-agar plates were incubated in MS liquid medium supplemented with 50  $\mu$ M MG132 and/or 25  $\mu$ M  $\beta$ -estradiol for 16 h in the light. Seedlings were washed three times with fresh MS liquid and transferred to MS liquid medium containing 0.5 mM cycloheximide under either light or dark conditions. Whole seedlings were used for the extraction of total proteins. Western blot hybridization was conducted using specific antibodies, as described previously (Lee et al., 2015).

### **ChIP assay**

The 35S:*MYC-ICE1* transgenic plants were grown either on MS-agar plates or in soil were used for chromatin preparation. CHIP assays were performed as described previously (Jung et al., 2012). Whole plants were vacuum-infiltrated with 1% (v/v) formaldehyde for cross-linking for 20 min on ice and ground in liquid nitrogen after quenching the cross-linking reaction. Chromatin samples were sonicated into ~0.3-kb DNA fragments. An anti-MYC antibody (Millipore) was added to the chromatin solutions, which were precleared with salmon sperm DNA/ Protein A agarose beads (Millipore). The precipitates were eluted from the beads. Cross-links were reversed, and residual proteins were removed by incubation with proteinase K. DNA was recovered using the Promega spin column (Promega). Quantitative PCR was performed to determine the amounts of genomic DNA enriched in each chromatin preparation.

#### **Yeast two-hybrid assay**

Yeast two-hybrid assays were conducted using the BD Matchmaker system (Clontech, Mountain View, CA). The pGADT7 vector was used for GAL4 AD (activation domain), and the pGBKT7 vector was used for GAL4 BD (DNA-binding domain). Yeast strain AH109 (leu-, trp-, ade-, his-), which has the chromosomally integrated reporter genes lacZ and HIS driven by the GAL1 promoter, was used for transformation of the vector constructs. The COP1-ICE interactions were also examined by both cell growth on selective media and measurements of  $\beta$ -galactosidase activity according to

the system procedures.

### **BiFC assay**

BiFC assays were performed by the cotransfection of the YFP<sup>N</sup>-SOC1 and ICE1-YFP<sup>C</sup> vectors into *Arabidopsis* mesophyll protoplasts. The YFP<sup>N</sup>-COP1 and ICE1-YFP<sup>C</sup> construct pair and the YFP<sup>N</sup>-SCRM2 and COP1-YFP<sup>C</sup> construct pair. The subcellular distribution of the SOC1-ICE1 and COP1-ICE1 interactions was visualized by DIC and fluorescence microscopy. Reconstitution of YFP fluorescence was observed using the Zeiss LSM510 confocal microscope (Carl Zeiss, Jena, Germany) with the following YFP filter setup: excitation 515 nm, 458/514 dichroic, and emission 560-615 nm BP filter.

### ***in vitro* pull-down assay**

Recombinant GST and GST-SOC1 fusion proteins were prepared in *E. coli* cells. A full-size *ICE1* cDNA was amplified by RT-PCR and subcloned into the pGADT7 vector. The ICE1 polypeptides were labeled with <sup>35</sup>S-Met by *in vitro* translation using the TNT coupled reticulocyte lysate system (Promega). The protein preparations and GST-binding resin (Novagen, San Diego, CA) were agitated for 12 hr at 4°C in binding buffer (50 mM Tris-Cl, pH8.0, 100 mM NaCl, 10% glycerol, 1% Triton X-100, 1 mM PMSF) containing protease inhibitor cocktail (Roche, Indianapolis, IN). Beads were washed 10 times with TN buffer (25 mM

Tris-Cl, pH8.0, 100 mM NaCl). The bound proteins were eluted with 1X SDS-PAGE loading buffer by boiling for 5 min and subject to SDS-PAGE and autoradiography.

### **Coimmunoprecipitation assay**

The *HA-ICE1* and *SOCI-MYC* gene sequences were transcriptionally fused to the endogenous *ICE1* and *SOCI* promoters consisting of 3.8 kbp and 4.0 kbp, respectively, and the expression constructs were subcloned into the pHGW and myc-pBA vectors (Jung et al., 2013), respectively and transformed into Col-0 plants. The transgenic plants grown on MS-agar plates for 12 days were used for total protein extraction. Protein complexes were coimmunoprecipitated using an anti-MYC antibody (Sigma-Aldrich, St. Louis, MO) and analyzed immunologically using anti-MYC and anti-HA antibodies (Millipore). For coimmunoprecipitation assays in ICE1-COP1 interactions, the *35S:HA-ICE1 pXVE:COP1-MYC* plants grown on MS-agar plates for 5 d were incubated in the presence of 25  $\mu$ M  $\beta$ -estradiol and 50  $\mu$ M MG132 for 1 d in darkness before extracting total proteins from whole seedlings. Protein complexes were coimmunoprecipitated using an anti-HA antibody (Sigma-Aldrich, St Louis, MO), and the precipitates were analyzed immunologically using anti-HA and anti-MYC antibodies (Millipore, Billerica, MA).

### **Freezing tolerance assay**

Approximately 30 plants grown in soil were used for each assay. Two-week-old plants grown under LDs were treated at 0°C for 30 min before exposure to freezing temperatures. Temperature was set to -1°C/30 min decrease. The plants were then incubated for 3 hr at different freezing temperatures. Temperature was restored to 4°C by 1°C increase per 30 min. The freezing temperature-treated plants were incubated at 4°C in the dark overnight for thawing and allowed to recover by incubating at 23°C for 7 days before calculating survival rates.

#### **Flowering time measurement**

Plants were grown in soil at 23°C under either LDs or SDs until flowering. Flowering times were determined by counting the total number of rosette and cauline leaves at the time of bolting. Approximately 14-20 plants were counted for each measurement.

#### **Intermittent cold treatment and vernalization**

For intermittent cold treatment, plants were exposed to 4°C for 6 hr at dawn for 20 days and then grown at 23°C under LDs until flowering.

For vernalization treatment, plants were germinated and grown at 4°C for 40 days under SDs. The plants were then grown at 23°C under LDs until flowering.

#### **Fluorescent imaging and microscopic analysis**

A Leica SP8 confocal laser scanning microscope (Buffalo Grove, IL) was used to capture propidium iodide (PI) staining and GFP fluorescence images. Reconstitution of GFP fluorescence was observed with the following filter setup: excitation 561 nm and emission 570-650 nm for PI; excitation 488 nm and emission 490-540 nm for GFP using HyD detector. Images were taken at the same laser intensity to compare intensities between genotypes. To counter-stain epidermal cell shapes, plant tissues were stained with 50 µg/mL PI for 2 min and rinsed briefly with deionized water before visualization (Kang et al., 2009).

#### **Colocalization assay**

Assays were performed by cotransfection of non-tagged COP1 and GFP-ICE1 constructs into *Arabidopsis* mesophyll protoplasts by a polyethylene glycol (PEG)-calcium transfection method (Yoo et al., 2007). The subcellular distribution of GFP-ICE1 was visualized by fluorescence microscopy.

#### **ICE ubiquitination assays**

Recombinant ProS2-ICE and MBP-COP1 fusion proteins were prepared in *Escherichia coli* cells. Ubiquitination assay *in vitro* was performed using 400 ng ProS2-ICE and 200 ng MBP-COP1 proteins in a reaction buffer (50 mM Tris, pH7.4, 5 mM MgCl<sub>2</sub>, 2 mM ATP, 2 mM DTT) containing 100 ng human E1 (Boston Biochem, Cambridge, MA), 100 ng human E2

UbcH5b (Boston Biochem), and 1  $\mu$ g ubiquitin (Sigma-Aldrich). Recombinant MBP-COP1 protein was pretreated with 20  $\mu$ M ZnCl<sub>2</sub> before assays. Reactions were performed at 30°C for 2.5 h with gentle shaking and terminated by adding SDS-PAGE loading buffer. The reaction mixtures were separated on 6% SDS-PAGE, and ubiquitinated ProS2-ICE proteins were detected using an anti-ProS2 (Takara Bio) or an anti-ubiquitin (Sigma-Aldrich) antibody. Ubiquitination assays *in vivo* were performed as described previously (Kim et al., 2015).

### **SI measurement**

SI is given as the percentage number of stomata as compared to total pavement cells per unit area of leaf (Kang et al. 2009). It was measured using the central area of abaxial epidermis of cotyledons. Only stomata having visible pores were counted.

### **Statistical analysis**

The statistical significance between two means of measurements were determined using Student's *t*-test with P values of <0.01.

Primers	Sequences	Usage
eIF4A-F	5'-TGACCACACAGTCTCTGCAA	qRT-RCR
eIF4A-R	5'-ACCAGGGAGACTTGTTGGAC	qRT-RCR
CO-F	5'-GATGACGACGTATCGTTATGGA	qRT-RCR
CO-R	5'-TACTCTCGTTTCTCAGTTTACAAAC	qRT-RCR
GI-F	5'-TGGCGATGTTTGTCTTCAT	qRT-RCR
GI-R	5'-AGCCATTGCTCCGAATAGT	qRT-RCR
FT-F	5'-GGTGGAGAAGACCTCAGGAA	qRT-RCR
FT-R	5'-GGTTGCTAGGACTTGAACATC	qRT-RCR
SOC1-F	5'-GGATCTCATGAAAGCGAAGTTT	qRT-RCR
SOC1-R	5'-TCACTTTCTTGAAGAACAAGGTA	qRT-RCR
FLC-F	5'-CCCTCTCCGTGACTAGAGCC	qRT-RCR
FLC-R	5'-TGGGAGAGTCACCGGAAGAT	qRT-RCR
ICE1-F	5'-AATTGGGGAACAGGGATTG	qRT-RCR
ICE1-R	5'-CAACGGAGCTGTGAAACCAC	qRT-RCR
ICE2-F	5'-TCTTCAAGCTTGCATCCGTT	qRT-RCR
ICE2-R	5'-GTTGGCCTTTAGGACTTGGC	qRT-RCR
GFP-ICE1-F	5'-CGACAACCACTACCTGAGCA	qRT-RCR
GFP-ICE1-R	5'-CACCACCGTTTAACCAAACC	qRT-RCR
FLC P1-F	5'-TTCCCATCGTTTGAAGTCC	qRT-RCR
FLC P1-R	5'-TATTTCTTGGATCCGCCACT	ChIP-RCR
FLC P2-F	5'-AGTGGCGGATCCAAGAAATAA	ChIP-RCR
FLC P2-R	5'-TAGTGCCCCACATCAATCCA	ChIP-RCR
FLC P3-F	5'-GGATTGATGTGGGGCACTAT	ChIP-RCR
FLC P3-R	5'-ATTTGCATTCTTTGCTCGT	ChIP-RCR
FLC P4-F	5'-TGGAGGGAACAACCTAATGC	ChIP-RCR
FLC P4-R	5'-TCGCATACAATTTCAATTGGAC	ChIP-RCR
FLC P5-F	5'-GGTAGCCAAAGATTTGGTTAAA	ChIP-RCR
FLC P5-R	5'-TGTTAAAATTTTGTGAGAACAAGC	ChIP-RCR
FLC P6-F	5'-GTTGATTATATATGATTCA	ChIP-RCR
FLC P6-R	5'-AGTGGGTGAAACTGATTACT	ChIP-RCR
FLC P7-F	5'-GTGAAATGTTTGTGTGGCTCC	ChIP-RCR
FLC P7-R	5'-TTTGAATGGTAACACAATAAACGA	ChIP-RCR
FLC P8-F	5'-GCTGATACAAGCATTTCACCAA	ChIP-RCR
FLC P8-R	5'-AATGTTGCGGAGATTAACACAAA	ChIP-RCR
FLC P9-F	5'-TTGATGACGTAGGCGAGTGG	ChIP-RCR
FLC P9-R	5'-AAAGAACCTCCACTCTACAT	ChIP-RCR
FLC P10-F	5'-CCGTATCGTAGGGGAGGAAA	ChIP-RCR
FLC P10-R	5'-TCGTGCGGCCAGATATTTTT	ChIP-RCR
CBF3 M1-F	5'-AGATCTTAATGAGTGAATCC	ChIP-RCR
CBF3 M1-R	5'-TAAGGATTCACTCATTAAAGA	ChIP-RCR
CBF3 M2-F	5'-GCCACACATTCATACGCAAAG	ChIP-RCR
CBF3 M2-R	5'-TAAGGATTCACTCATTAAAGA	ChIP-RCR
CBF3 M3-F	5'-ACTGTTTATTAATCAACCG	ChIP-RCR
CBF3 M3-R	5'-CACCAAGTAGTTTTGGCGGA	ChIP-RCR
CBF3 M4-F	5'-GTTTCGCGATCCGATCTACA	ChIP-RCR
CBF3 M4-R	5'-TCACAAAAATGATGATTGAG	ChIP-RCR
CBF3 nBS-F	5'-GGATGTGCTATAAGAATGGGAGA	ChIP-RCR
CBF3 nBS-R	5'-CGTTAATTGTTACCCCGTGTAT	ChIP-RCR
35S:MYC-ICE1-F	5'-CAACCCGGGCGATGGGTCTTGACGGAAACAATGG	Subcloning
35S:MYC-ICE1-R	5'-GATGGATCCAGATCATACCAGCATACCCTGCTGT	Subcloning
ICE1-Y2H-Full-F	5'-ACTGAATTCATGGGTCTTGACGGAAACAATGGTG	Subcloning
ICE1-Y2H-Full-R	5'-CAGGATCCATCAGATCATACCAGCATACCCTGCTG	Subcloning
ICE1-Y2H-N-R	5'-ACTGGATCCCATTGTGAAGATCATTGATCCTTTG	Subcloning
ICE1-Y2H-C-F	5'-AGGGAATTCGATCTTCACAATGAACCTTGAGTCAA	Subcloning

Primers	Sequences	Usage
SOC1-Y2H-Full-F	5'-GAACATATGGTGAGGGGCAAAACTCAGATGAAGA	Subcloning
SOC1-Y2H-Full-R	5'-TGAGGATCCATCACTTTCTTGAAGAACAAGGTAA	Subcloning
SOC1-Y2H-M-R	5'-GCAGGATCCCTTCAGAAACCGGTTTGGTGCTGAC	Subcloning
SOC1-Y2H-K-F	5'-ACTCATATGCGAGTCAGCACAAACCGGTTTCTG	Subcloning
SOC1-Y2H-K-R	5'-CGCGGATCCGAGATCCCACTTTTCAGAGAGCTT	Subcloning
SOC1-Y2H-C-F	5'-CTCCATATGAAGTGGGGATCTCATGAAAGCGAAG	Subcloning
ICE1-BiFC-F	5'-ACTGTCGACATGGGTCTTGACGGAAACAATGGTG	Subcloning
ICE1-BiFC-R	5'-AGGGGATCCTCAGATCATACCAGCATACCCTGCT	Subcloning
SOC1-BiFC-F	5'-AGACCCGGGTATGGTGAGGGGCAAAACTCAGATG	Subcloning
SOC1-BiFC-R	5'-GAGGGATCCTCACTTTCTTGAAGAACAAGGTAAAC	Subcloning
pICE1-F	5'-GTCAGGTCCCTAGTTAAAAGGAATAACAATTAAT	Subcloning
pICE1-R	5'-TCGCCTAGGTTGACACCTTTACCCCAAAGTCTGA	Subcloning
pICE2-F	5'-TCTAGGTCCCGCTCTCTGCTTCATCTTCTTCTT	Subcloning
pICE2-R	5'-AGTCTAGGGTCAAACCTAGTAGAGAGAGAGAGAG	Subcloning
MYC-ICE-F	5'-GAGGGCGCGCCTGTACAGACGTCTCGACGGTATC	Subcloning
GFP-ICE-F	5'-AAAGGCGCGCCCATGGTGAGCAAGGGCGAGGAGC	Subcloning
MYC(GFP)-ICE1-R	5'-TCCACTAGTTCAGATCATACCAGCATACCCTGCT	Subcloning
MYC(GFP)-ICE2-R	5'-TTCTTAATTAATAATCAAACCAAACAGCGTAACC	Subcloning
MYC-ICE1-ox-F	5'-CAACCCGGGCGATGGGTCTTGACGGAAACAATGG	Subcloning
MYC-ICE1-ox-R	5'-GATGGATCCAGATCATACCAGCATACCCTGCTGT	Subcloning
MYC-ICE2-ox-F	5'-TACGGCGCGCCCATGAACAGCGACGGTGTGGCC	Subcloning
MYC-ICE2-ox-R	5'-CGCGACGTACCAAACAGCGTAACCTGCTGTAT	Subcloning
pXVE:COP1-MYC-F	5'-GAACTCGAGATGGAAGAGATTTGACGGATCCGG	Subcloning
pXVE:COP1-MYC-F	5'-TAGTTAATTAAGACGCGTCTAGGCTACGTAGGA	Subcloning
ICE2-Y2H-F	5'-TAGGAATTCATGAACAGCGACGGTGTGGCTTG	Subcloning
ICE2-Y2H-R	5'-TTCGGATCCGCAATCAAACCAAACAGCGTAACC	Subcloning
COP1-Y2H-Full-F	5'-GAAGAATTCATGGAAGAGATTTGACGGATCCGG	Subcloning
COP1-Y2H-Full-R	5'-TCTGTCGACATCAGCAGCGAGTACCAGAATTT	Subcloning
COP1-Y2H-ΔR-F	5'-TTGGAATTCACCTCAGCTCGGCATGTGTCAAAA	Subcloning
COP1-Y2H-ΔRC-F	5'-TCTGAATTCCTGCGGATGCTCGGAGATGATCCAA	Subcloning
COP1-Y2H-ΔW-R	5'-TTTGTCGACGATAATTGCCTACAAAATTTCTCC	Subcloning
MYC-SPCH-ox-F	5'-GATGGATCCTCATGCAGGAGATAATACCGGATTT	Subcloning
MYC-SPCH-ox-R	5'-CGTCTTAGGAGCTAGCAGAATGTTTGCTGAATTT	Subcloning
GFP-ICE1-ox-F	5'-CAACCCGGGCGATGGGTCTTGACGGAAACAATGG	Subcloning
GFP-ICE1-ox-R	5'-ATCGGATCCTTCAGATCATACCAGCATACCCTGC	Subcloning
pSPCH-F	5'-TCAAGTCCCAGAAGTATAATTTATGTTATTTCT	Subcloning
pSPCH-R	5'-CTGCCTAGGGATTAGAGATATATCCTTCTCTCTC	Subcloning
GFP-SPCH-F	5'-AAAGGCGCGCCCATGGTGAGCAAGGGCGAGGAGC	Subcloning
GFP-SPCH-R	5'-TCCACTAGTCTAGCAGAATGTTTGCTGAATTTGT	Subcloning

**Table 1. Primers used in this work**

The PCR primers were designed using Primer3 software (version 0.4.0, <http://primer3.sourceforge.net/releases.php>) so that they have calculated melting temperatures in the range of 55–60°C. F, forward primer; R, reverse primer.

## **CHAPTER 1**

**INDUCER OF CBF EXPRESSION 1 integrates cold signals into the FLOWERING LOCUS C-mediated flowering pathways in *Arabidopsis***

## ABSTRACT

Plants constantly monitor changes in photoperiod and temperature throughout the year to synchronize flowering with optimal environmental conditions. In the temperate zones, both photoperiod and temperature fluctuate in a somewhat predictable manner through the season, although a transient shift to low temperature is also encountered during changing seasons, such as early spring. While low temperatures are known to delay flowering by inducing the floral repressor *FLOWERING LOCUS C (FLC)*, it is not fully understood how temperature signals are coordinated with photoperiodic signals in the timing of seasonal flowering. Here, I show that the cold signaling activator INDUCER OF CBF EXPRESSION 1 (ICE1), FLC, and the floral promoter SUPPRESSOR OF OVEREXPRESSION OF CO 1 (SOC1) constitute an elaborate signaling network that integrates cold signals into flowering pathways. The cold-activated ICE1 directly induces the gene encoding FLC, which represses *SOC1* expression, resulting in delayed flowering. In contrast, under floral promotive conditions, SOC1 inhibits the binding of ICE1 to the promoters of *FLC* gene, inducing flowering with a reduction of freezing tolerance. These observations indicate that the ICE1-FLC-SOC1 signaling network contributes to the fine-tuning of flowering during changing seasons.

## INTRODUCTION

In plants, the timing of flowering is coordinated by endogenous developmental cues, such as plant aging (Wang et al., 2009), and environmental signals, including seasonal changes in photoperiod and temperature (Sung and Amasino, 2004; Valverde et al., 2004). The flowering signals are incorporated into flowering genetic pathways through the actions of floral integrators FLOWERING LOCUS T (FT) and SUPPRESSOR OF OVEREXPRESSION OF CO 1 (SOC1) (Blázquez and Weigel, 2000; Yoo et al., 2005).

In the temperate zones, photoperiod and temperature fluctuate in a somewhat predictable pattern throughout the seasons. However, a transient shift to low temperatures also occurs frequently during changing seasons, such as early spring (Kim et al., 2004; Seo et al., 2009). Therefore, plants should monitor both predictable and subtle changes in the seasonal cues to determine when to flower. In blooming spring seasons, when photo-inductive signals are enriched, the long-day (LD) plant *Arabidopsis* initiates flowering by inducing *CONSTANS* (*CO*) and *GIGANTEA* (*GI*) genes (Sawa and Kay, 2011; Suárez-López et al., 2001). The photoperiodic signals activate a set of floral meristem identity genes (Blázquez et al., 1997), leading to flowering induction.

Plants also sense diurnal and seasonal changes in environmental temperature to regulate flowering. Low ambient temperatures delay

flowering through the thermosensory pathway without causing discernible growth and developmental defects (Blázquez et al., 2003; Lee et al., 2007). It has been shown that high ambient temperatures accelerate flowering by triggering the PHYTOCHROME INTERACTING FACTOR 4 transcription factor to activate *FT* gene (Kumar and Wigge, 2010).

A prolonged exposure to low nonfreezing temperatures accelerates flowering through the vernalization pathway, which silences the floral repressor *FLOWERING LOCUS C (FLC)* (Henderson and Dean, 2004; Michaels and Amasino, 2001). In contrast, *Arabidopsis* flowering is delayed under transient cold conditions, which are often experienced during changing seasons (Kim et al., 2004; Seo et al., 2009). The effects of cold temperatures on flowering are mediated primarily by FLC through a signaling pathway that is distinct from the vernalization pathway (Bond et al., 2011).

Plants develop tolerance to freezing temperatures in response to low nonfreezing temperatures, a process known as cold acclimation (Guy, 1990). In a well-established cold signaling pathway, INDUCER OF CBF EXPRESSION1 (*ICE1*) and its targets C-REPEAT BINDING FACTOR (*CBF*) transcription factors activate downstream cold-responsive targets, including *COLD-REGULATED (COR)* genes (Gilmour et al., 1998). The E3 ubiquitin ligase HIGH EXPRESSION OF OSMOTICALLY RESPONSIVE GENES 1 (*HOS1*) attenuates cold signaling by degrading *ICE1* (Dong et al., 2006).

Accumulating evidence support that plant cold response is intimately associated with flowering time control. It has been reported that HOS1 regulates flowering time by modulating CO abundance under cold temperature conditions (Jung et al., 2012). Conversely, under LDs, SOC1 suppresses *CBF* expression (Seo et al., 2009). However, molecular and biochemical mechanisms underlying integration of signaling pathways between flowering timing and cold response are not fully understood.

Here, I demonstrated that the cold signaling activator ICE1, the floral repressor FLC, and the floral promoter SOC1 constitute a feedback loop that integrates cold signals into flowering time control for optimal timing of seasonal flowering under changing seasons. Under cold temperature conditions, ICE1 activated *FLC* expression, resulting in *SOC1* suppression and thereby delayed flowering. In contrast, under floral promotive conditions, SOC1 inhibited the DNA binding of ICE1, causing suppression of *CBF* and *FLC* genes and thus promoting flowering. I propose that the ICE1-FLC-SOC1 signaling module provides an adaptation strategy by which the timing of flowering is fine-tuned during changing seasons.

## RESULTS

### **FLC expression is reduced in the early-flowering *ice1-2* mutant**

Cold response is closely linked with flowering time control in *Arabidopsis* (Jung et al., 2012; Seo et al., 2009). ICE1 is a master regulator of plant cold response. However, it is not known whether and how ICE1 is associated with flowering time control.

I found that the loss-of-function *ice1-2* mutant, which harbors a single copy of T-DNA insertion in the third exon of *ICE1* gene (Kanaoka et al., 2008), exhibited early flowering under both LDs and short days (SDs) (Figures 1A and 1B). The early flowering phenotype of *ice1-2* was completely rescued by the expression of a wild-type *ICE1* gene driven by its own promoter (Figure 2), indicating that the *ice1* mutation is the molecular cause of the flowering phenotype of *ice1-2*. Gene expression assays revealed that whereas *FT* and *SOC1* genes were upregulated, *FLC* gene was suppressed in the mutant (Figures 3A and 3B).

To examine the functional relationship between *ICE1* and flowering time genes, the *ice1-2* mutant was crossed with various flowering mutants, and flowering times of the resultant plants were compared with those of parental mutants. The flowering times of *ice1-2 ft-10* and *ice1-2 soc1-2* double mutants were similar to those of *ft-10* and *soc1-2* mutants (Table 2), respectively.

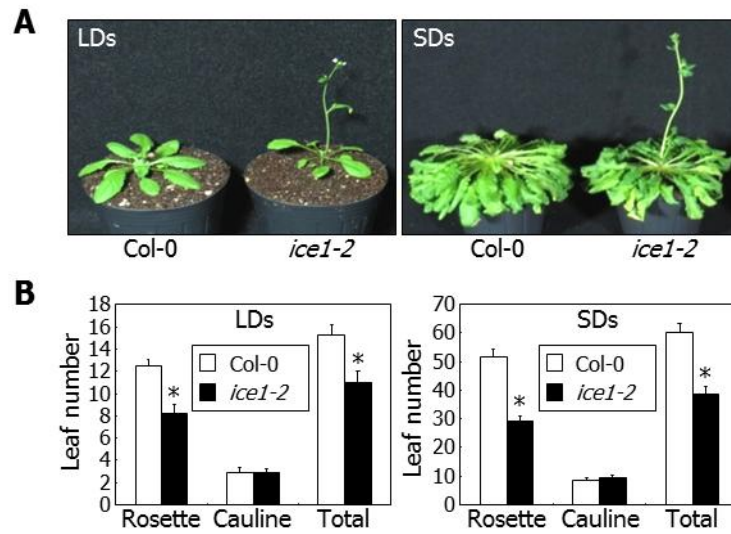


**Figure 1. The *ice1-2* mutant exhibited early flowering under LDs and SDs**

**(A and B)** Flowering phenotypes. Plants were grown in soil at 23°C under either LDs or SDs until flowering **(A)**. Leaf numbers of ~20 plants were averaged and statistically analyzed using Student *t*-test ( $*P < 0.01$ ) **(B)**. Bars indicate standard error of the mean.

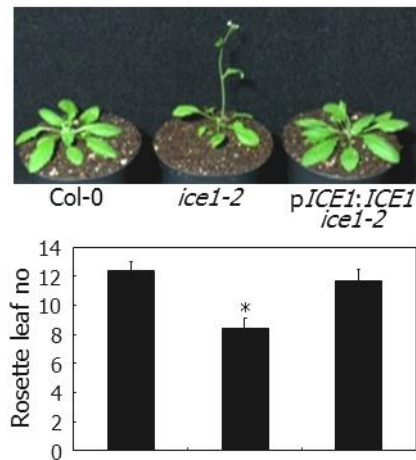


**Figure 2. Complementation of *ice1-2* mutant**

The *ice1-2* mutant (SALK-003155), which has been described previously (Kanaoka et al., 2008), was isolated from the *Arabidopsis* T-DNA insertional mutant pool deposited in the *Arabidopsis* Biological Resource Center (Ohio State University, OH). The mutant was transformed with a genomic *ICE1* sequence driven by its own promoter consisting of ~3.8-kb sequence upstream of the transcription start site, resulting in *pICE1:ICE1 ice1-2*. Plants were grown under long days (LDs, 16-h light and 8-h dark) until flowering (upper panel). Rosette leaves of ~20 plants were averaged and statistically analyzed using Student *t*-test ( $*P < 0.01$ ) (lower panel). Bars indicate standard error of the mean.

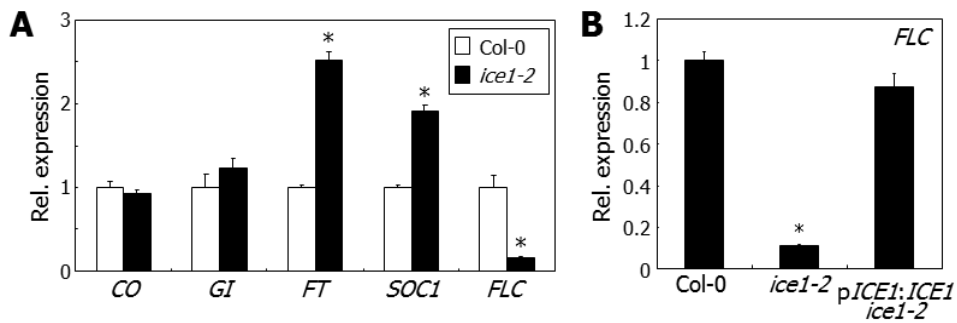


**Figure 3. Expression of flowering genes in *ice1-2* mutant**

**(A)** Expression of flowering genes. Ten-day-old whole plants grown on MS-agar plates harvested at ZT14 were used for total RNA extraction. Transcript levels were examined by qRT-PCR. Biological triplicates were averaged and statistically analyzed (*t*-test,  $*P < 0.01$ ). Bars indicate standard error of the mean.

**(B)** *FLC* expression. Ten-day-old whole plants grown on 1/2 X Murashige and Skoog-agar (MS-agar) plates were used for total RNA extraction. Transcript levels were examined by quantitative real-time RT-PCR (qRT-PCR). Biological triplicates were averaged and statistically analyzed (*t*-test,  $*P < 0.01$ ). Bars indicate standard error of the mean.

The *ice1-2 flc-3* double mutant flowered slightly earlier than the parental mutants, suggesting that the *ice1-2* flowering phenotype is associated with *FLC* gene, although it is possible that a FLC-independent pathway is also involved. In contrast, the genetic crosses of the *ice1-2* mutant with *co-101* and *gi-2* mutants and the gene mutations belonging to the autonomous and vernalization flowering pathways, such as *fve-4*, *fca-9*, and *Col-FRI*, exhibited additive flowering phenotypes (Table 2). These observations indicate that ICE1 is linked with *FT*, *SOC1*, and *FLC* genes in regulating flowering time.

#### **ICE1 activates *FLC* by binding to the gene promoter**

I found that whereas the levels of *FT* and *SOC1* transcripts were elevated approximately two-fold, that of *FLC* transcripts was reduced by more than 80% in *ice1-2* mutant (Figure 3A). *FLC* is a negative regulator of *FT* and *SOC1* genes (Michaels and Amasino, 1999). I therefore suspected that the suppression of *FLC* gene is the primary cause of the early flowering phenotype of *ice1-2*.

To clarify whether the biologically significant effect by ICE1 is mainly through *FLC*, I examined the expression of *FT*, *SOC1*, and *FLC* genes in *ICE1*-overexpressing plants. *FT* and *SOC1* gene expressions are reduced by approximately 20-60% compared with those of Col-0 plants (Figures 4A and 4B). The expressions of *FLC* gene were increased by two to four fold changes

Genotype	Rosette leaf	Genotype	Rosette leaf
Col-0	12.4±0.6	<i>ft-10 soc1-2</i>	61.4±6.1
<i>ice1-2</i>	8.2±0.8	<i>ice1-2 ft-10 soc1-2</i>	56.7±5.2
<i>co-101</i>	37.1±2.9	<i>flc-3</i>	10.5±0.9
<i>ice1-2 co-101</i>	22.4±1.6	<i>ice1-2 flc-3</i>	6.7±0.6
<i>gi-2</i>	42.7±4.2	Col- <i>FRI</i>	67.4±7.2
<i>ice1-2 gi-2</i>	26.3±2.0	Col- <i>FRI ice1-2</i>	49.6±5.1
<i>ft-10</i>	39.2±3.4	<i>five-4</i>	38.4±3.6
<i>ice1-2 ft-10</i>	37.3±3.3	<i>ice1-2 five-4</i>	25.4±2.3
<i>soc1-2</i>	21.1±1.3	<i>fca-9</i>	52.3±4.7
<i>ice1-2 soc1-2</i>	19.4±1.2	<i>ice1-2 fca-9</i>	36.1±2.5

**Table 2. Flowering phenotypes of flowering mutants in *ice1-2* background**

Plant growth under LDs and counting of rosette leaf numbers were performed as described in Figure 1. Values represent mean ± standard error.

compared with that of Col-0 plants (Figure 4C). Notably, the late flowering phenotype of 35S:*MYC-ICE1* plants was largely eliminated by *flc-3* mutation (Figure 4D). These results indicate that *FLC* gene is a major target in ICE1-mediated flowering time control.

I first examined whether ICE1 induces *FLC* gene by transient  $\beta$ -glucuronidase (GUS) expression assays in *Arabidopsis* protoplasts. Sequence analysis revealed that *FLC* promoter contains a series of potential MYC-recognition sequences within the 2-kbp sequence region from the transcription start site (Figure 5A). Reporter constructs harboring *FLC* promoter sequence regions of 400b to 2kb, which were transcriptionally fused to the GUS reporter, and effector construct having *ICE1* gene driven by the cauliflower mosaic virus (CaMV) 35S promoter were cotransformed into *Arabidopsis* protoplasts. GUS activity assays showed that ICE1 activates *FLC* gene, perhaps binding to the promoter sequences (Figure 5B).

Chromatin immunoprecipitation (ChIP) assays were employed to directly examine the binding of ICE1 to *FLC* promoter. ChIP assays showed that ICE1 binds to a subset of the MYC-recognition sequences, which were P5, P7, P8, and P10 sequences (Figure 5C), indicating that ICE1 directly binds to the MYC-recognition sequences in the *FLC* promoter.

Consistent with the binding of ICE1 to *FLC* promoter to activate its expression, transgenic plants overexpressing *ICE1* gene exhibited late flowering in a dosage-dependent manner (Figures 6A and 6B).

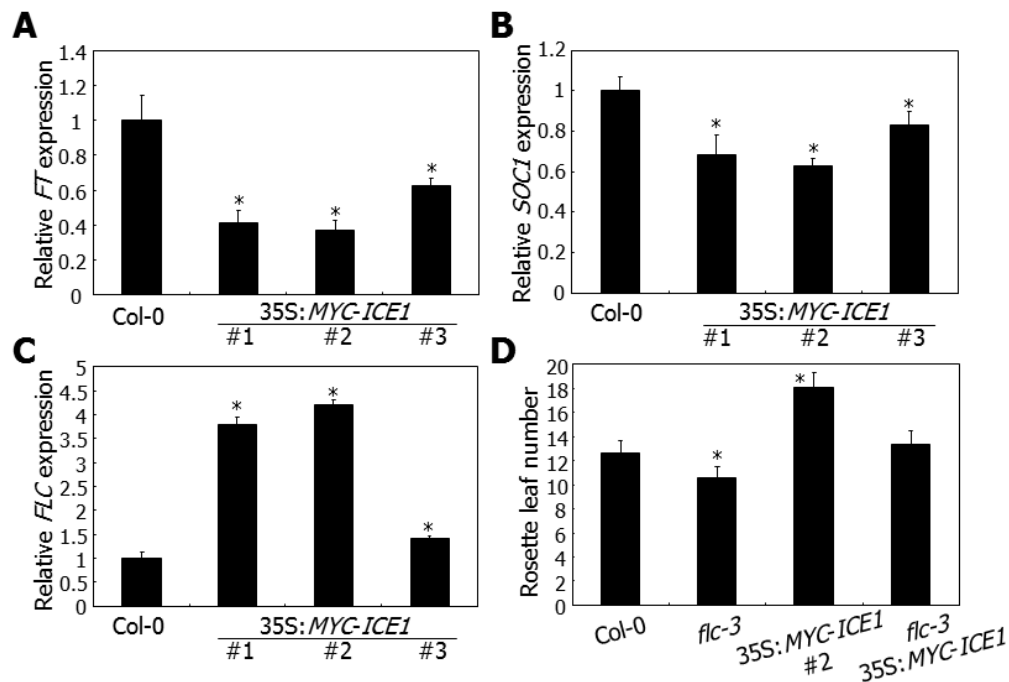


**Figure 4. FLC dependence of flowering in *ICE1*-overexpressing plants**

(A, B, and C) Expression of *FT*, *SOC1*, and *FLC* genes. Ten-day-old whole plants grown on MS-agar plates were used for total RNA extraction. Transcript levels were examined by qRT-PCR, as described in Figure 3. Bars indicate standard error of the mean (*t*-test, \**P* < 0.01).

(D) Flowering phenotypes of *ICE1*-overexpressing plants in *flc-3* background. Flowering time measurements were performed as described in Figure 1. Bars indicate standard error of the mean (*t*-test, \**P* < 0.01).

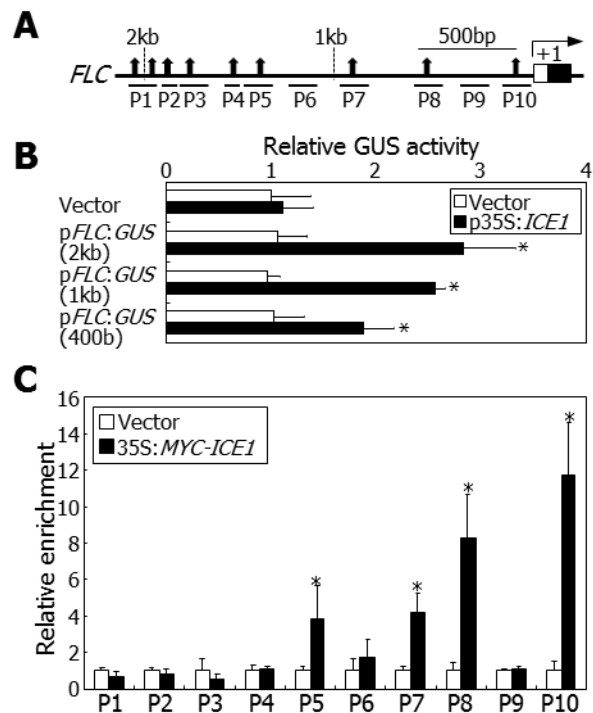


**Figure 5. ICE1 activates *FLC* expression by binding to the gene promoter**

**(A)** MYC-recognition sequences in *FLC* promoter. Potential MYC-recognition sequences (CANNTG) are marked by vertical arrows. The P1 to P10 sequences were analyzed in CHIP assays. Black and white boxes indicate exon and untranslated region, respectively.

**(B)** Transcriptional regulation of *FLC* by ICE1. The *FLC* promoter sequences covering 2-kbp, 1-kbp, or 400bp region upstream of the transcription start site were fused upstream of a CaMV 35S minimal promoter in the reporter vectors. The reporter vectors and the p35S:*ICE1* effector vector were cotransformed into *Arabidopsis* protoplasts. Three measurements were averaged and statistically analyzed (*t*-test, \* $P < 0.01$ ). Bars indicate standard error of the mean.

(C) ChIP assay on ICE1 binding to *FLC* promoter. A *MYC-ICE1* fusion was overexpressed driven by the CaMV 35S promoter in Col-0 plants. Seven-day-old whole plants grown on MS-agar plates under LDs were used for chromatin preparation. Three measurements were averaged and statistically analyzed (*t*-test, \**P* < 0.01). Bars indicate standard error of the mean.

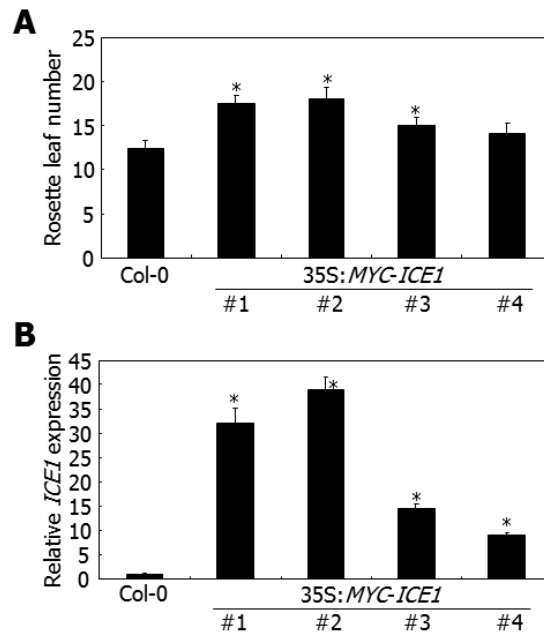


**Figure 6. Flowering phenotypes of *ICE1*-overexpressing plants**

An *ICE1*-coding sequence was fused in-frame to the 3' end of a MYC-coding sequence, and the *MYC-ICE1* fusion was overexpressed driven by the cauliflower mosaic virus (CaMV) 35S promoter in Col-0 plants. More than 40 independent lines were obtained, among which 4 lines were randomly selected for the measurements.

**(A)** Flowering phenotypes. Flowering time measurements were performed as described in Figure 1. Bars indicate standard error of the mean (*t*-test,  $*P < 0.01$ ).

**(B)** Expression of *ICE1* gene. Ten-day-old whole plants grown on MS-agar plates were used for total RNA extraction. Transcript levels were examined by qRT-PCR, as described in Figure 3. Bars indicate standard error of the mean (*t*-test,  $*P < 0.01$ ).

### **ICE1 activates *FLC* gene under cold temperature conditions**

My data showed that ICE1, which is otherwise a central inducer of cold response, activates *FLC* by directly binding to the gene promoter. Therefore, a question was whether ICE1 regulates flowering time in response to cold temperatures.

I examined whether long-term exposure to cold temperatures or vernalization influences the flowering time of *ice1-2* mutant. The *ice1-2* flowering was accelerated by vernalization, as was observed with the flowering of Col-0 and Col-*FRI* plants (Figures 7A and 7B). Accordingly, *FLC* expression was significantly reduced in both Col-0 and *ice1-2* plants after vernalization treatments (Figure 7C), suggesting that ICE1 is not involved in the vernalization response of flowering.

I next examined the effects of cold temperature on *ice1-2* flowering. To eliminate indirect effects caused by cold stress response, I employed intermittent cold treatment, which delays flowering without discernibly affecting plant growth and development (Kim et al., 2004; Seo et al., 2009). Whereas intermittent cold induced *FLC* expression in Col-0 plants, the inductive effects of intermittent cold disappeared in *ice1-2* mutant (Figure 8A). In addition, while Col-0 flowering was delayed by the treatments, *ice1-2* flowering was not affected under the same assay conditions, like *flc-3* flowering (Figure 8B). Moreover, the intermittent cold-insensitive flowering of the *ice1-2* mutant was rescued by the

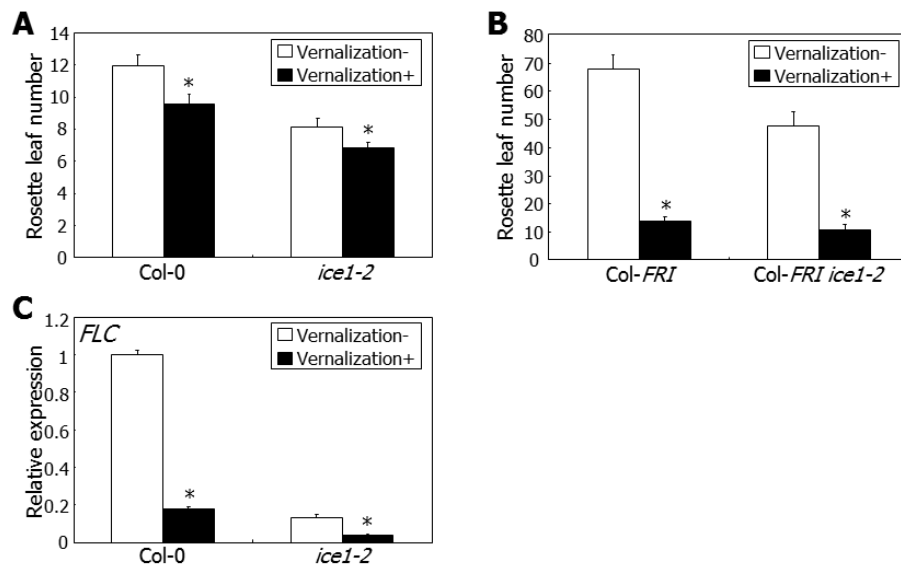


**Figure 7. Effects of long-term cold on *ice1-2* flowering**

**(A and B)** Effects of long-term cold (vernalization) on *ice1-2* flowering. *Arabidopsis* seeds were germinated and grown in soil at 23°C for 2 days under LDs and vernalized for 40 days under short days (SDs, 8-h light and 16-h dark). The vernalization-treated plants were grown at 23°C until flowering under LDs. Flowering time measurements were performed as described in Figure 1. Bars indicate standard error of the mean (*t*-test,  $*P < 0.01$ ) **(A)**. Col-*FRI* and Col-*FRI ice1-2* plants were also assayed **(B)**.

**(C)** *FLC* expression. Non-vernalized and vernalized plants were grown for 10 days under LDs. Total RNA extraction and qRT-PCR were performed as described in Figure 3. Bars indicate standard error of the mean (*t*-test,  $*P < 0.01$ ).

expression of *ICE1* gene driven by its own promoter (Figure 8B). These observations indicate that ICE1 mediates the effects of cold temperature on flowering time.

The next question was how ICE1 regulates the cold-responsive flowering. It is known that ICE1 is degraded at cold temperature (Dong et al., 2006). Immunological analysis using transgenic plants overexpressing a MYC-ICE1 fusion revealed that the level of ICE1 decreases at cold temperature, but it was rapidly recovered upon transfer to normal temperature (Figure 9A). I prepared chromatin samples at zeitgeber time 14 (ZT14), when the level of ICE1 was fully recovered (Figure 9B). ChIP assays revealed that ICE1 binding to *FLC* promoter was elevated approximately 2-fold after cold treatments (Figure 10A). I also found that the up-regulation of *FLC* by ICE1 is elevated by intermittent cold compared with that of normal temperature conditions in *ICE1*-overexpressing plants (Figure 10B). Together, these observations indicate that cold temperature triggers the binding of ICE1 to *FLC* promoter, thereby causing its induction and delayed flowering.

### **ICE1 interacts with SOC1 in the nucleus**

It is known that CBFs activate *FLC* gene and *FLC* suppresses *SOC1* expression, causing delayed flowering under cold temperature conditions (Michaels and Amasino, 2001; Seo et al., 2009). I found that ICE1 activates *FLC* gene. It was therefore hypothesized that SOC1 and ICE1

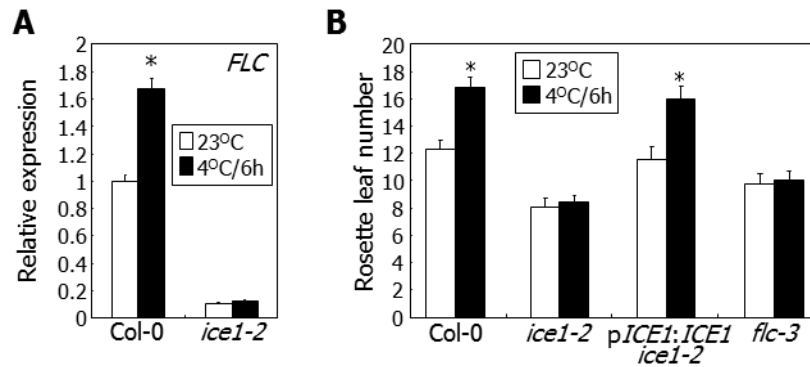


**Figure 8. ICE1 delays flowering by inducing *FLC* under cold temperature conditions**

**(A)** Effects of short-term cold on *FLC* expression. Plants were treated with intermittent cold at 4°C for 6h at dawn for 15 days before harvesting whole plant materials at ZT14 for total RNA extraction. Transcript levels were examined by qRT-PCR. Biological triplicates were averaged and statistically analyzed using Student *t*-test ( $*P < 0.01$ ). Bars indicate standard error of the mean.

**(B)** Effects of short-term cold on flowering time. Plants were treated with intermittent cold for 20 days and grown under normal conditions until flowering. Rosette leaves of ~20 plants were counted and statistically analyzed (*t*-test,  $*P < 0.01$ ).

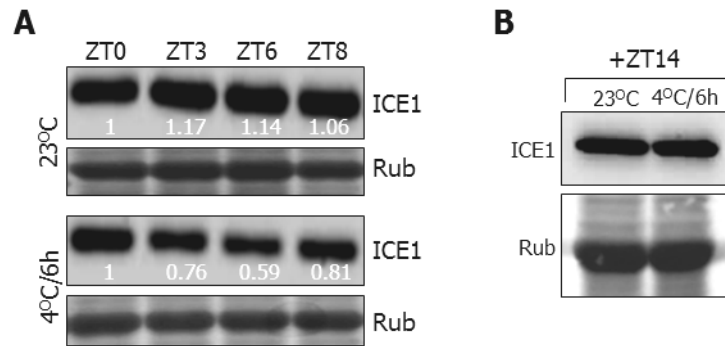


**Figure 9. Effects of short-term cold on ICE1 protein stability**

**(A and B)** The *35S:MYC-ICE1* transgenic plants were treated with intermittent cold for 15 days, and whole plants were harvested at the indicated ZT points of the 15<sup>th</sup> day for the preparation of protein extracts. An anti-MYC antibody was used to detect ICE1. Part of Coomassie blue-stained gel containing Rubisco (Rub) was displayed as loading control.

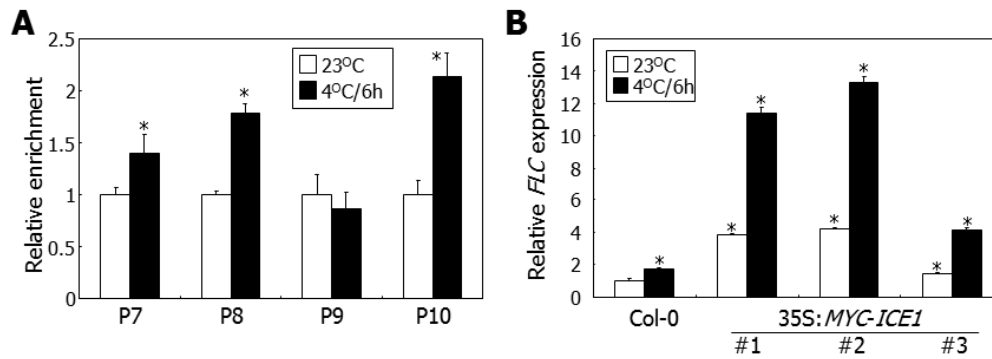


**Figure 10. Cold temperature accelerates the binding of ICE1 on *FLC* gene promoter**

**(A)** ChIP assay on ICE1 binding to *FLC* promoter. The 35S:MYC-ICE1 transgenic plants described in Figure 9 were used for chromatin preparation. ChIP assays were conducted as described in Figure 5C.

**(B)** Effects of short-term cold on *FLC* expression in ICE1-overexpressing plants. Plants were treated with intermittent cold at 4°C for 6h at dawn for 20 days before harvesting whole plant materials at ZT14 for total RNA extraction. Transcript levels were examined by qRT-PCR, as described in Figure 3. Bars indicate standard error of the mean (*t*-test, \**P* < 0.01).

might be functionally interrelated in regulating flowering time.

I tested whether ICE1 directly interacts with SOC1. Gene sequences encoding a series of ICE1 and SOC1 deletion forms were produced (Figure 11A). Yeast two-hybrid assays showed that full-size SOC1 does not interact with ICE1 proteins (Figure 11B). In contrast, SOC1 deletions containing K-box or C-terminal domain or both interacted with the C-terminal domain of ICE1 harboring the leucine zipper (ZIP) motif. Notably, SOC1 deletions containing MADS-box did not interact with ICE1, suggesting that MADS-box interferes with the ICE1-SOC1 interaction in yeast cells, as has been observed previously (Dong et al., 2006; Jung et al., 2012).

Consistent with the interaction data in yeast cells, bimolecular fluorescence complementation (BiFC) assays revealed that the full-size SOC1 interacts with ICE1 in the nucleus (Figure 12A). The ICE1-SOC1 interaction was also verified by *in vitro* pull-down assays using recombinant glutathione-S-transferase (GST)-SOC1 fusion prepared in *E. coli* cells and *in vitro* translated 35S-labeled ICE1 polypeptides (Figure 12B).

To examine whether the ICE1 interacts with SOC1 *in vivo*, I performed coimmunoprecipitation assays using transgenic plants that express genes encoding hemagglutinin (HA)-ICE1 and SOC1-MYC fusions driven by the endogenous promoters. It was found that the ICE1-SOC1 interaction occurs *in planta* (Figure 12C).

### **SOC1 inhibits ICE1 binding to *FLC* promoter in promoting flowering**

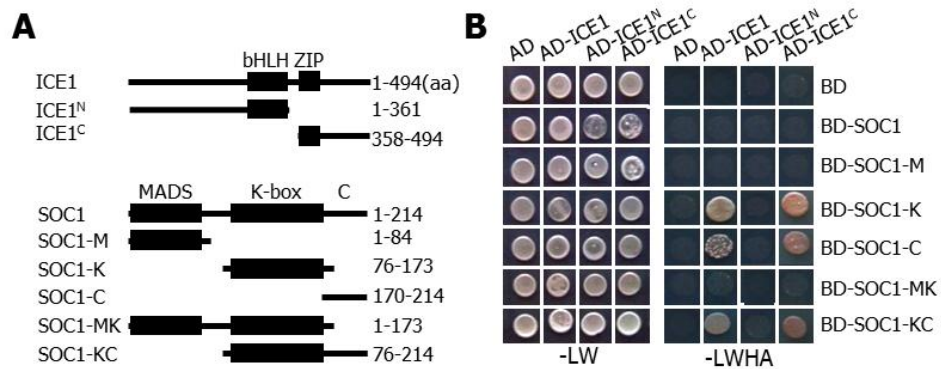


**Figure 11. ICE1 interacts with SOC1 in yeast cells**

**(A)** ICE1 and SOC1 constructs used. Numbers indicate residue positions. ZIP, leucine zipper. bHLH, basic helix-loop-helix. C, C-terminal region.

**(B)** Interaction of ICE1 with SOC1 in yeast cells. -LW indicates Leu and Trp dropout plates. -LWHA indicates Leu, Trp, His, and Ade dropout plates.

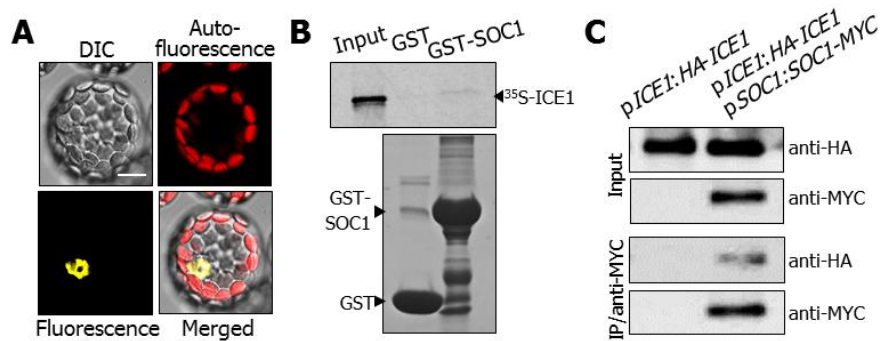


**Figure 12. ICE1 interacts with SOC1 in planta**

**(A)** BiFC assay. The YFP<sup>N</sup>-SOC1 and ICE1-YFP<sup>C</sup> constructs were coexpressed transiently in *Arabidopsis* protoplasts and visualized by differential interference contrast (DIC) and fluorescence microscopy. Bar, 10  $\mu$ m.

**(B)** *in vitro* pull-down assay. Recombinant GST-SOC1 fusion produced in *E. coli* cells and *in vitro* translated <sup>35</sup>S-labeled ICE1 polypeptides were used (upper panel). The input represents 5% of the radiolabeled protein used in the assays. Recombinant GST protein was used as negative control. Part of Coomassie blue-stained gel was displayed as loading control (lower panel).

**(C)** Coimmunoprecipitation assay. Total proteins were extracted from transgenic plants grown on MS-agar plates for 12 days. Protein complexes were immunoprecipitated using an anti-MYC antibody and analyzed immunologically using anti-MYC and anti-HA antibodies. IP, immunoprecipitation.

I investigated the functional relationship between ICE1 and SOC1 by performing transient GUS expression assays in *Arabidopsis* protoplasts. In effector vectors, a full-size *ICE1* cDNA was fused in-frame to the 3' end of the GAL4 DNA binding domain (DB)-coding sequence, and the *GAL4 DB-ICE1* and *SOC1* sequences were transcriptionally fused to the CaMV 35S promoter (Figure 13A). The results showed that SOC1 coexpression reduced the transcriptional activation activity of ICE1 by more than 60% (Figure 13B). In contrast, ICE1 did not affect the transcriptional regulatory activity of SOC1 (Figures 13C and 13D).

I next examined whether SOC1 influences the DNA-binding property of ICE1. For the assays, a MYC-ICE1 fusion was transformed into *soc1-2* mutant, *SOC1*-overexpressing plant (*SOC1-ox*), and Col-0 plants. Among the transgenic lines, those producing similar levels of ICE1 protein were selected for ChIP assays. The assays showed that ICE1 binding to *FLC* promoter increased in Col-0 background (Figure 14). It was further elevated in *soc1-2* background. In contrast, it decreased by ~80% in *SOC1-ox* background (Figure 14), indicating that SOC1 inhibits the binding of ICE1 to *FLC* promoter.

ICE1 induces *FLC* gene by binding to the gene promoter. I therefore examined whether SOC1 influences the ICE1-mediated induction of *FLC* gene. The level of *FLC* transcripts was higher by ~1.5 fold in *soc1-2* mutant than in Col-0 plants at normal temperature conditions (Figure 15A). However, the inductive effects of the *soc1* mutation on *FLC*

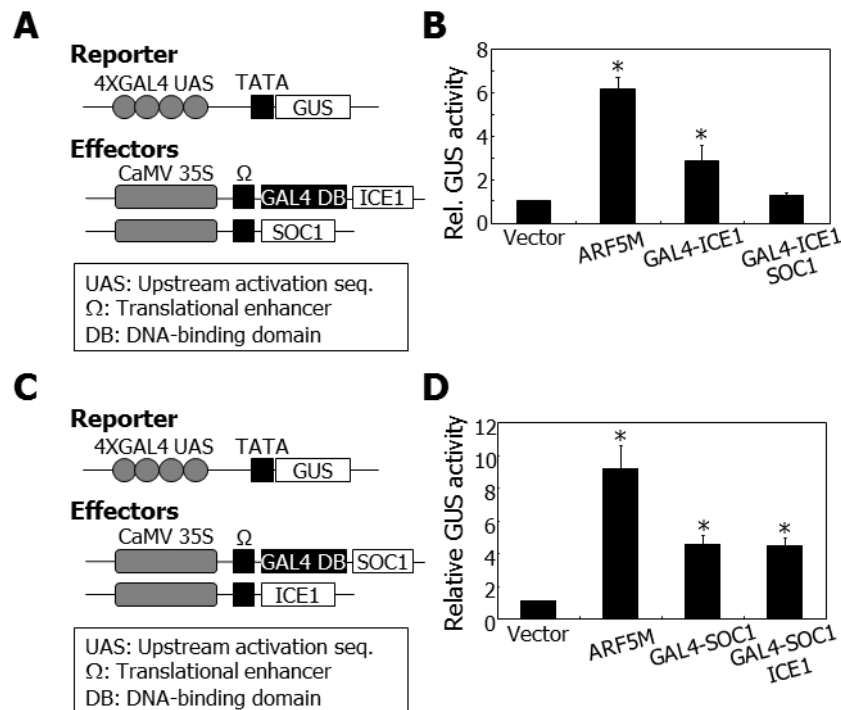


**Figure 13. Inhibition of ICE1 transcriptional activation activity by SOC1**

**(A and B)** A full-size *ICE1* cDNA was fused in-frame to the 3' end of GAL4 DNA-binding domain (DB)-coding sequence **(A)**. The reporter and effector constructs were expressed transiently in *Arabidopsis* protoplasts **(B)**. ARF5M was used as positive control (Miura et al., 2007). Five measurements were averaged and statistically analyzed (*t*-test,  $*P < 0.01$ ). Bars indicate standard error of the mean.

**(C and D)** Effects of ICE1 on SOC1 transcriptional activation activity. A full-size *SOC1* cDNA was fused in-frame to the 3' end of the GAL4 DNA-binding domain (DB)-coding sequence **(C)**. The reporter and effector constructs were expressed transiently in *Arabidopsis* protoplasts **(D)**. ARF5M was used as positive control (Miura et al., 2007). Three measurements were averaged and statistically analyzed (*t*-test,  $*P < 0.01$ ). Bars indicate standard error of the mean.

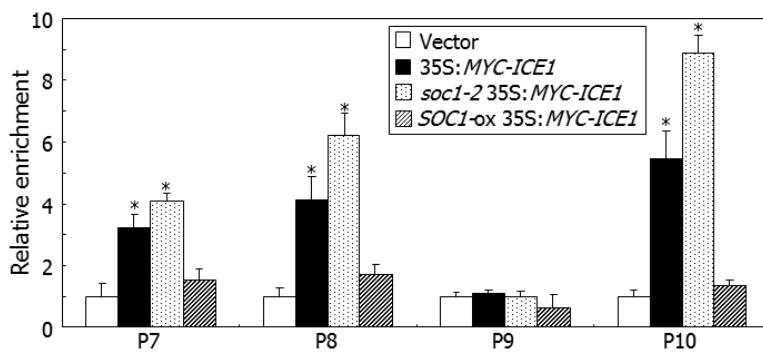


**Figure 14. Inhibition of ICE1 binding to *FLC* promoter by SOC1**

Ten-day-old plants grown on MS-agar plates under LDs were used for ChIP assays. Three measurements were averaged and statistically analyzed (*t*-test,  $*P < 0.01$ ). Bars indicate standard error of the mean.

expression largely disappeared in *ice1-2* mutant and *soc1-2 ice1-2* double mutant. In addition, whereas *FLC* expression was slightly elevated in Col-0 plants overexpressing *ICE1* gene, it was significantly elevated in *soc1-2* mutant overexpressing *ICE1* gene (Figure 15B), indicating that SOC1 suppresses ICE1 function in inducing *FLC* gene at normal temperature conditions.

Under intermittent cold conditions, *FLC* gene was induced in both Col-0 plants and *soc1-2* mutant (Figure 15A). Notably, the inductive effects of intermittent cold on *FLC* expression were not observed in *ice1-2* mutant and *soc1-2 ice1-2* double mutant, showing that SOC1 is not associated with the ICE1-mediated induction of *FLC* gene under cold temperature conditions. Consistent with the independence of SOC1 from the ICE1-mediated induction of *FLC* gene at cold temperature, flowering time was delayed by intermittent cold in *soc1-2* mutant, as was observed in Col-0 plants (Figure 15C). In contrast, flowering times of *ice1-2* mutant and *soc1-2 ice1-2* double mutant were not affected under the same assay conditions, certainly due to the lack of ICE1-mediated *FLC* induction.

### **SOC1 inhibits ICE1 binding to *CBF3* promoter in inducing cold acclimation**

ICE1 activates *CBF3* gene by binding to the gene promoter under cold temperature conditions. Meanwhile, it is known that *CBF* genes are suppressed at floral-inductive temperatures (Zarka et al., 2003). I observed

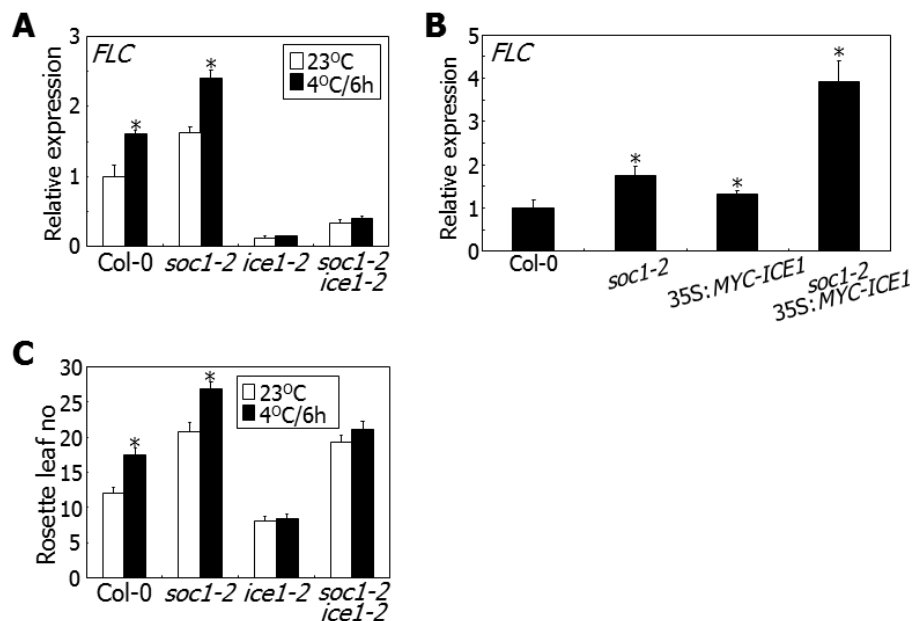


**Figure 15. SOC1 inhibits ICE1 function in inducing *FLC* gene**

**(A)** Effects of short-term cold on *FLC* expression in *soc1-2* and *ice1-2* mutants. Intermittent cold treatments were performed as described in Figure 8. Transcript levels were examined by qRT-PCR. Biological triplicates were averaged and statistically analyzed (*t*-test,  $*P < 0.01$ ). Bars indicate standard error of the mean.

**(B)** *FLC* expression in *soc1-2* 35S:MYC-ICE1 plants. Ten-day-old whole plants grown on MS-agar plates under LDs were used for total RNA extraction. Expression of *FLC* gene was examined by qRT-PCR. Bars indicate standard error of the mean (*t*-test,  $*P < 0.01$ ).

**(C)** Effects of short-term cold on flowering time in *soc1-2* and *ice1-2* mutants. Flowering times were measured as described in Figure 1. Bars indicate standard error of the mean (*t*-test,  $*P < 0.01$ ).

that *SOC1-ox* plants exhibit reduced freezing tolerance, as observed in *ice1-2* plants (Figure 16A). It was notable that the freezing tolerance was further reduced in *SOC1-ox ice1-2* plants. Meanwhile, the expression of *CBF3* gene was elevated in *soc1-2* mutant by more than 2-fold (Figure 16B). In addition, whereas the level of *CBF3* transcripts was only slightly higher in 35S:*MYC-ICE1* transgenic plants compared to that in Col-0 plants, the transcript level in *soc1-2* 35S:*MYC-ICE1* plants was comparable to that in *soc1-2* mutant. These observations suggest that SOC1 suppresses *CBF3* expression possibly by inhibiting ICE1 function. I therefore asked whether SOC1 affects the binding of ICE1 to *CBF3* promoter.

*CBF3* promoter has several copies of potential MYC-recognition sequences, designated M1 to M4 in this work, within the 1-kbp sequence region from the transcription start site (Figure 17A). I prepared chromatin samples from 35S:*MYC-ICE1* and *soc1-2* 35S:*MYC-ICE1* plants at ZT8 under LDs, when *CBF3* transcription reaches the diurnal peak (Lee and Thomashow, 2012). ChIP assays showed that ICE1 binds to M1 and M4 sequences (Figure 17B). Notably, ICE1 binding to *CBF3* promoter was further enhanced by more than 2-fold in *soc1-2* 35S:*MYC-ICE1* plants, indicating that SOC1 inhibits the ICE1 binding to *CBF3* promoter.

I examined whether the SOC1-mediated inhibition of ICE1 binding to *CBF3* promoter is associated with freezing tolerance. Under nonacclimated conditions, *soc1-2* mutant exhibited enhanced freezing tolerance (Figures 18A and 18B), and the level of *CBF3* transcripts was

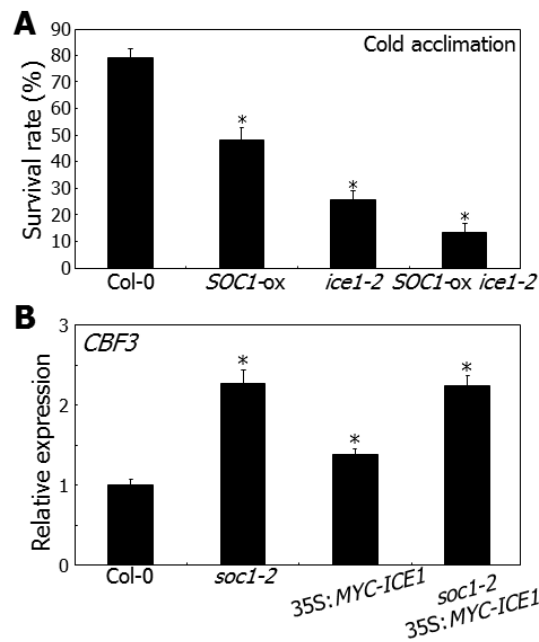


**Figure 16. Linkage of SOC1 with ICE1 in freezing tolerance**

The *ice1-2* mutant was crossed with *SOC1-ox* plants, in which a full-size *SOC1* cDNA was overexpressed driven by the CaMV 35S promoter in Col-0 background, resulting in *SOC1-ox ice1-2* plants. Twelve-day-old plants grown on MS-agar plates at 23°C were transferred to soil and grown for 3 additional days under LDs. They were cold-acclimated by incubating at 4°C for 10 days. They were then incubated at 0°C for 1 h before exposure to -8°C for 3 h. They were transferred to 23°C for 7 days before calculating survival rates (A). Three measurements, each consisting of ~30 plants, were averaged and statistically analyzed using Student *t*-test (\**P* < 0.01). Bars indicate standard error of the mean. For *CBF3* expression assays, ten-day-old whole plants grown on MS-agar plates under LDs were harvested at ZT8 for total RNA extraction (B). Expression of *CBF3* gene was examined by qRT-PCR, as described in Figure 3. Bars indicate standard error of the mean (*t*-test, \**P* < 0.01).

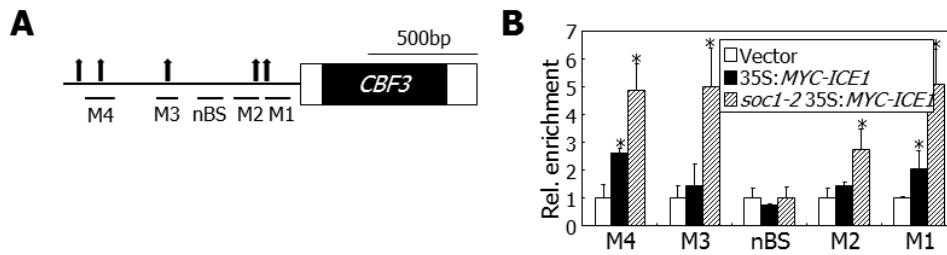


**Figure 17. SOC1 inhibits ICE1 binding to *CBF3* promoter**

**(A)** MYC-recognition sequences in *CBF3* promoter. The M1 to M4 sequences covering putative MYC-recognition sequences in *CBF3* promoter were used in ChIP assays. nBS, nonbinding sequence. Black and white boxes indicate exon and untranslated regions, respectively.

**(B)** ChIP assay on ICE1 binding to *CBF3* promoter in *soc1-2* background. Plant growth and ChIP assays were conducted as described in Figure 5C. Bars indicate standard error of the mean (*t*-test, \**P* < 0.01).

accordingly higher by 1.8-fold in the mutant (Figure 18C). Notably, the enhanced freezing tolerance and the elevated *CBF3* transcription were largely compromised in *ice1-2* background (Figures 18B and 18C). These observations support that the SOC1-mediated suppression of ICE1 function is physiologically important for acquiring basal freezing tolerance.

I next examined freezing tolerance response after cold acclimation. The *soc1-2* mutant still exhibited enhanced freezing tolerance compared to that of Col-0 plants (Figures 18D and 18E). Interestingly, the enhancement of freezing tolerance in the *soc1-2* mutant was not as prominent as that observed under nonacclimated conditions, although the level of *CBF3* transcripts was also higher in the mutant (Figure 18F). Together, these observations indicate that SOC1 inhibits ICE1 binding to *CBF3* promoter to reduce basal freezing tolerance primarily under nonacclimation conditions but plays a limited role under cold acclimation conditions.

Altogether, my data demonstrate that the cold signaling mediator ICE1 and the floral integrator SOC1 constitute an intricate signaling network, which incorporates cold signals into the flowering pathways to achieve optimal timing of seasonal flowering (Figure 19). Under floral promotive conditions, such as LDs, SOC1 suppresses ICE1 activity in regulating *FLC* gene, leading to flowering induction. In contrast, under cold temperature conditions, ICE1 induces *FLC* expression, resulting in *SOC1* suppression and delayed flowering.

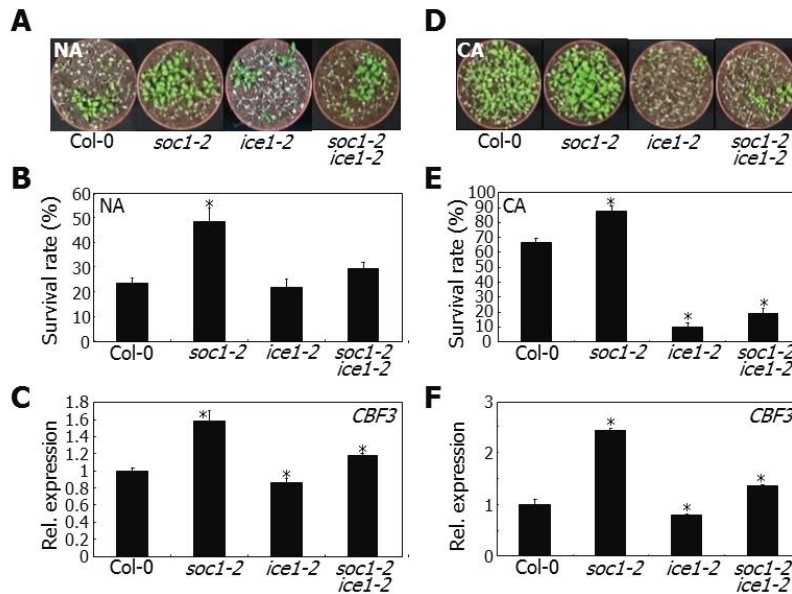


**Figure 18. SOC1 inhibits ICE1 in inducing cold acclimation**

**(A, B, and C)** Freezing tolerance of nonacclimated (NA) *soc1-2* and *ice1-2* mutants. Two-week-old plants grown in soil were exposed to  $-5^{\circ}\text{C}$  for 3 hr. The plants were then incubated at  $4^{\circ}\text{C}$  overnight before allowing to recover by incubating at  $23^{\circ}\text{C}$  for 7 days **(A)**. Survival rates were calculated using ~30 plants **(B)**. Three measurements were averaged and statistically analyzed (*t*-test,  $*P < 0.01$ ). For *CBF3* expression assays, ten-day-old whole plants grown on MS-agar plates were harvested at ZT8 **(C)**. Transcript levels were examined by qRT-PCR (*t*-test,  $*P < 0.01$ ).

**(D, E, and F)** Freezing tolerance of cold-acclimated (CA) *soc1-2* and *ice1-2* mutants. Before freezing tolerance assays, plants were cold-acclimated by incubating at  $4^{\circ}\text{C}$  for 10 days. They were exposed to  $-9^{\circ}\text{C}$  for 3 hr **(D)**. Calculation of survival rates and *CBF3* expression assays were conducted as described above **(E and F, respectively)** (*t*-test,  $*P < 0.01$ ).

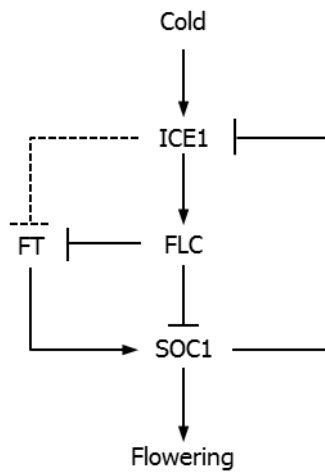


**Figure 19. An ICE1-mediated signaling network integrates cold signals into flowering time control via a feedback loop**

The cold-activated ICE1 induces *FLC* gene by directly binding to the gene promoter resulting in delayed flowering. Under floral promotive conditions, such as LDs, SOC1 inhibits the binding of ICE1 to *FLC* promoter, thus promoting flowering.

## DISCUSSION

### **Functional divergence of ICE1: Recognizing of flowering timing during changing seasons**

The ICE1 transcription factor integrates low temperature into plant development (Chinnusamy et al., 2003; Denay et al., 2014). Among the several stress responses during their development, it is well-defined that the pivotal role of ICE1 in acquiring cold acclimation (Chinnusamy et al., 2003). Notably, plants must respond to environmental conditions in their development to adjust their fitness and optimize their growth. To support this notion, several recent studies also revealed the functional divergence of ICE1 in adaptive responses during developmental processes (Kanaoka et al., 2008; Denay et al., 2014; Lee et al., 2015).

In this study, I found that the ICE1 transcription factor modulates the timing of flowering under transient-cold conditions. The *ICE1*-defective mutant exhibited early flowering, indicating repressive role of ICE1 in flowering time control. Notably, the flowering of *ICE1*-defective mutant was not affected by transient-cold temperature, demonstrating the importance of ICE1 in temperature-mediated adaptive responses of flowering. I also demonstrated that ICE1 transcription factor is directly associated with *FLC* promoter. Furthermore, cold signals induced ICE1 binding on *FLC*, thereby elevating *FLC* transcript and delaying timing of flowering. In this aspect, it is prominent that ICE1 plays a developmental role by acting as a signaling

integrator that links cold adaptation with flowering time control, not simply acting in stress responses.

I also found that the *ICE*-defective mutant exhibited altered timing of flowering in normal temperature conditions. An explanation would be that ICE1 acts as a general transcription factor to maintain *FLC* and other flowering time gene expressions in a cold-independent manner.

It is notable that low temperature affects the status of *FLC* chromatin (Henderson and Dean, 2004). HOS1, which is also known to be a cold attenuator, induces *FLC* transcription by antagonizing its interaction partners FVE and histone deacetylase 6 (HDA6) (Jung et al., 2013). Interestingly, the ICE1 binding site is proximal to the transcriptional start site of *FLC*, which is also known to be the HOS1 binding region. Several adaptive responses are governed by transcriptional changes and epigenetic controls under changing environments, which are coordinately modulated by transcription factors and chromatin modification factors (Xiao et al., 2017). Therefore, interplay between ICE1 and the HOS1-FVE-HDA6 signaling module or chromatin modifiers is to be tested for specifying functional linkage between flowering time control and cold adaptation.

### **Two aspects of low temperature-mediated flowering time control by ICE1 transcription factor**

There are two different aspects of flowering time control in response to low temperature: cold acclimation and vernalization. The cold acclimation

response is induced by three or five days of cold temperature conditions (Guy, 1990). The short-term cold conditions enhance the tolerance of freezing, but delay flowering timing (Kim et al., 2004; Seo et al., 2009). This response is recognized as an adaptive mechanism. Another aspect of exposure to cold temperature is a winter cold, long-term cold temperature. Exposure to a long-term cold following optimal temperature conditions, such as spring, accelerates flowering (Michaels and Amasino, 2001; Henderson and Dean, 2004). This response is called vernalization (Sung et al., 2003). During winter cold, polycomb-like chromatin-modifying complex initiates modification of *FLC* chromatin, thereby silencing its gene level. Vernalization-mediated *FLC* silencing is associated with H3K27me3 and H3K9me3 status (Sung et al., 2003). Cold-mediated induction of *VERNALIZATION INSENSITIVE 3 (VIN3)* triggers vernalization responses by silencing *FLC* (Sung et al., 2003).

There are some common factors that mediate short-term cold and vernalization in flowering. The former induces *FLC*, which is known to be a repressor of flowering (Henderson and Dean, 2004). Therefore, short-term cold delays flowering. By contrast, long-term cold following inductive temperature conditions, silences *FLC*, thus ensuring flowering. Notably, vernalization responses are regulated by the duration of cold temperature. The early steps of vernalization is that *VIN3* induction, the gene product represses *FLC* (Sung et al., 2003). Although cold acclimation and vernalization are independent of each other (Bond et al., 2014), it is

possible that certain common factors exist that regulate both responses. I found that ICE1 transcription factors play a key role in short-term cold responses. Therefore, it is potentially interested to test ICE1 function in the early step of vernalization responses. A plausible scenario is that ICE1 initiates vernalization through directly activating *VIN3* transcription.

### **Attenuation of ICE1 function in cold adaptation**

SOC1, which is known to be a transcriptional activator, also has a repressive activity on its downstream targets. Liu and colleagues reveal that SOC1 possesses a conserved C-terminal motif, which is directly linked to the transcriptional repressor complex in modulating floral organ formation (Liu et al., 2009). In addition, the transcription of *CBF* is also repressed by SOC1, sustaining and attenuating freezing tolerance (Seo et al., 2009).

In this study, I found that SOC1 inhibits the cold response through suppression of ICE1 binding of the *CBF3* promoter. The floral integrator as well as inducer, SOC1, inhibits ICE1 activity during floral inductive conditions, such as LDs. By contrast, under non-inductive conditions, SOC1 activity is inhibited, thus delaying flowering. A previous report also reveals that E3 ubiquitin ligase HOS1 degrades ICE1 under cold temperature conditions, thus attenuating the exaggerated cold response and sustaining plant development (Dong et al., 2006). My results provide an additional layers of regulatory mechanism on attenuating cold responses by SOC1.

It is well-known that the MyoD family of bHLH transcription

factors and myocyte enhancer binding factor 2 (MEF2) family of MADS-box transcription factors cooperatively regulate target gene expressions in mammalian systems (Molkentin and Olson, 1996). *SOC1* encodes MADS-box transcription factors. Therefore, the SOC1-ICE1 module provides a distinct molecular mechanism of target gene regulation in plants, which is distinct from previous heterodimeric transcription factors.

### **Integration of photoperiod and cold temperature signals into flowering time control in *Arabidopsis***

In this study, I found that photoperiod and temperature signals are coordinated into the flowering genetic pathways during changing seasons. They optimize and fine-tune the timing of flowering, but minimize the unnecessary freezing tolerance. However, I have not fully addressed the molecular linkages between photoperiod and temperature signals in modulating flowering timing. Notably, I found that reduced expression of *FT*, which is downstream of *CO*, in *ICE1*-defective mutant. Therefore, it is also plausible that *CO*, which is a central modulator in photoperiod signaling pathway, is also possibly linked with *ICE1*. It will be interesting to prove the more direct linkage between the photoperiod and temperature signals using *CO*- and *FT*-deficient mutants.

## **CHAPTER 2**

**Light inhibits COP1-mediated degradation of ICE  
transcription factors to induce stomatal development in  
*Arabidopsis***

## **ABSTRACT**

Stomata are epidermal openings that facilitate plant-atmosphere gas exchange during photosynthesis, respiration, and water evaporation. Stomatal differentiation and patterning is spatially and temporally regulated by the master regulators *SPEECHLESS* (*SPCH*), *MUTE*, and *FAMA*, which constitute a central gene regulatory network along with Inducer of CBF Expression (*ICE*) transcription factors for this developmental process. Stomatal development is also profoundly influenced by environmental conditions, such as light, temperature, and humidity. Light induces stomatal development, and various photoreceptors modulate this response. However, it is unknown how light is functionally linked with the master regulatory network. Here, I demonstrate that, under dark conditions, the E3 ubiquitin ligase *CONSTITUTIVE PHOTOMORPHOGENIC 1* (*COP1*) degrades *ICE* proteins through ubiquitination pathways in leaf abaxial epidermal cells in *Arabidopsis*. Accordingly, the *ICE* proteins accumulate in the nuclei of leaf abaxial epidermal cells in *COP1*-defective mutants, which constitutively produce stomata. Notably, light in the blue, red, and far-red wavelength ranges suppresses the *COP1*-mediated degradation of the *ICE* proteins to induce stomatal development. These observations indicate that light is directly linked with the *ICE*-directed signaling module, via the *COP1*-mediated protein surveillance system, in the modulation of stomatal development.

## INTRODUCTION

Stomata are epidermal openings that facilitate the shoot-atmosphere gas exchange in plants. Therefore, stomatal development is critical for photosynthesis, which ensures plant propagation and is a key factor in the global carbon cycle (Hetherington and Woodward, 2003; Driscoll et al., 2006). It is also important for respiration and water circulation in plants (Lawson and Blatt, 2014).

In *Arabidopsis*, the stomatal development is initiated by an asymmetric cell division in stomatal progenitor cells, named meristemoid mother cells, thereby producing meristemoids (Bergmann and Sack, 2007; MacAlister et al., 2007; Pillitteri and Torii, 2012). The meristemoids subsequently differentiate into guard mother cells, which divide symmetrically and finally differentiate into guard cells (Ohashi-Ito and Bergmann, 2006; Pillitteri et al., 2007). A pair of guard cells forms a stoma, which is more prevalent in the abaxial epidermis of leaves. Notably, mature stomata are never formed adjacent to each other. Asymmetric cell divisions occur only in those stomatal lineage ground cells (SLGCs) that are located away from existing stomata (Geisler et al., 2000; Geisler et al., 2003). It is now thought that the spatial regulation of stomatal development is important for proper stomatal physiology, such as modulation of stomatal aperture by osmosis, and water and ion supply to guard cells by SLGCs (Nadeau and Sack, 2002; Hetherington and Woodward, 2003; Shpak et al.,

2005).

Stomatal formation and patterning is mediated by several developmental regulators, including mitogen-activated protein kinase (MAPK) signaling components and leucine-rich repeat receptor-like proteins (Bergmann et al., 2004; Shpak et al., 2005; Wang et al., 2007). In addition, a group of basic helix-loop-helix (bHLH) transcription factors, SPEECHLESS (SPCH), MUTE, and FAMA, act sequentially during stomatal development by spatially and temporally triggering the initiation, proliferation, and termination of the stomatal lineage cells, respectively (Ohashi-Ito and Bergmann, 2006; MacAlister et al., 2007; Pillitteri et al., 2007). Interestingly, they interact with Inducer of CBF Expression (ICE) transcription factors (Kanaoka et al., 2008), also known as SCREAM (SCRM) proteins (Kanaoka et al., 2008), to induce stomatal development.

Stomatal development is also modulated by environmental signals, such as light, temperature, humidity, and atmospheric CO<sub>2</sub> concentration (Gray et al., 2000; Crawford et al., 2012; Tricker et al., 2012; Casson and Hetherington, 2014), among which the effects of light have been most extensively studied. Light triggers the division of stomatal lineage cells (Kang et al., 2009). Consequently, the division of stomatal lineage cells is halted in the epidermis of etiolated seedlings (Kang et al., 2009; Balcerowicz et al., 2014).

The E3 ubiquitin ligase CONSTITUTIVE PHOTOMORPHOGENIC 1 (COP1) is a photomorphogenic repressor that directs the degradation of

light-regulated transcription factors (Osterlund et al., 2000; Jang et al., 2005). Notably, it also acts as a negative regulator of stomatal development (Kang et al., 2009). It is known that the photoactivation of the red and far-red light photoreceptors phytochromes (phyA to phyE) and the blue light photoreceptors cryptochromes (CRY1 and CRY2) suppresses the action of COP1, inducing stomatal development (Boccalandro et al., 2009; Kang et al., 2009; Lian et al., 2011; Casson and Hetherington, 2014). The phyA, phyB, and CRY photoreceptors inhibit the activity of COP1 by disrupting the formation of COP1-SUPPRESSOR OF phyA-105 (SPA) protein complex during photomorphogenic development (Lian et al., 2011; Liu et al., 2011; Zuo et al., 2011; Lu et al., 2015; Sheerin et al., 2015). As a result, just like the COP1-defective mutants (Kang et al., 2009), transgenic plants overexpressing the COP1-interacting domain of CRY1 and SPA-defective mutants produce stomata even in darkness, supporting the suppressive role of COP1 in light-induced stomatal development.

Here, I demonstrate that COP1 degrades the ICE transcription factors through ubiquitin-proteasome pathways in darkness to inhibit stomatal development. The ICE proteins accumulated in the nuclei of leaf abaxial epidermal cells in COP1-defective mutants that constitutively produce stomata under both light and dark conditions. Notably, light suppresses the COP1-mediated degradation of ICE proteins, triggering stomatal development. My observations indicate that, via the ICE-mediated signaling network, the COP1-mediated light signals are directly linked with

the developmental programs that regulate stomatal development.

## RESULTS

### **Light induces ICE accumulation in the nuclei of leaf abaxial epidermal cells**

Light triggers stomatal differentiation (Casson et al., 2009; Kang et al., 2009). ICE transcription factors are core components of the gene regulatory networks that specify stomatal differentiation through interactions with SPCH, MUTE, and FAMA (Kanaoka et al., 2008). Therefore, the first objective was to determine how the ICE-mediated signaling module is linked with light signaling.

I examined the effects of different light wavelengths on *ICE* gene transcription. Reverse transcription-mediated quantitative real-time RT-PCR (RT-qPCR) assays revealed that the transcription of *ICE* genes is slightly altered by different light wavelengths (Figure 20). Fluorescent examination of gene promoter activities in the abaxial epidermal cells of cotyledons showed that the *ICE* gene transcription is only marginally affected by the light regimes examined (Figures 21A and 21B). I therefore concluded that light does not play a prominent role in regulating the *ICE* gene transcription.

I next asked whether light influences the accumulation of ICE proteins. Seedlings expressing either a MYC-ICE1 or MYC-SCRM2/ICE2 gene fusion driven by their own promoters were exposed to various light wavelengths, and the levels of ICE proteins were examined. It was found

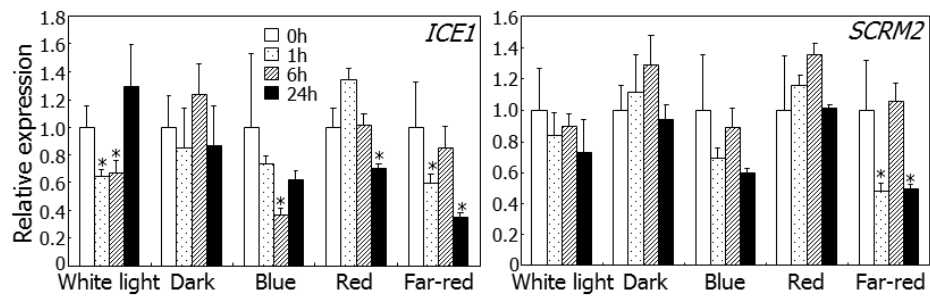


**Figure 20. Kinetics of *ICE* transcription**

Light regimes tested were white light ( $50 \mu\text{mol}\cdot\text{m}^{-2}\cdot\text{s}^{-1}$ ), blue ( $35 \mu\text{mol}\cdot\text{m}^{-2}\cdot\text{s}^{-1}$ ), red ( $40 \mu\text{mol}\cdot\text{m}^{-2}\cdot\text{s}^{-1}$ ), and far-red ( $15 \mu\text{mol}\cdot\text{m}^{-2}\cdot\text{s}^{-1}$ ).

Four-day-old Col-0 seedlings grown on MS-agar plates in darkness were exposed to different light wavelengths for the indicated time periods before harvesting whole seedlings for total RNA extraction. Transcript levels were examined by reverse transcription-mediated quantitative real-time RT-PCR (RT-qPCR). Biological triplicates using independent seedling samples grown under identical conditions were statistically analyzed ( $t$ -test,  $*P < 0.01$ ). Bars indicate standard error of the mean (SE).

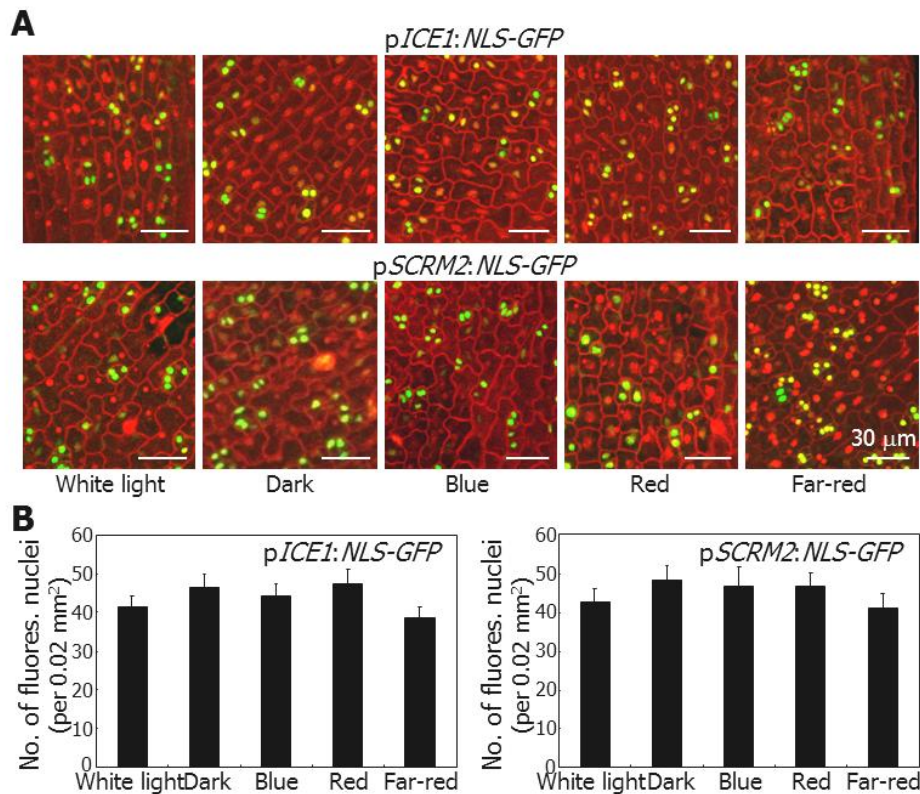


**Figure 21. Effects of light on *ICE* transcription**

**(A)** Fluorescence-assisted detection of *ICE* promoter activity. The *pICE:NLS-GFP* transgenic seedlings were grown on MS-agar plates in darkness for 4 d and then exposed to different light wavelengths for 6 h. Confocal images of abaxial epidermal cells of cotyledons were obtained.

**(B)** Quantification of fluorescent signals in the nuclei of abaxial epidermal cells. Countings of fluorescent nuclei were performed using the plant samples described in **(A)**. Three independent measurements, each consisting of ten countings, were averaged. Bars indicate SE.

that the levels of ICE proteins were higher in seedlings exposed to red, far-red, and blue lights, compared with the etiolated seedlings (Figure 22A). Kinetic analysis of ICE1 accumulation revealed that its level gradually increases in the light and reaches the peak value at 4 h of light exposure (Figure 22B).

To verify the effect of light on ICE accumulation, dark-grown *pICE1:GFP-ICE1* and *pSCRM2:GFP-SCRM2* seedlings, in which GFP-ICE gene fusions were expressed with endogenous gene promoters, were exposed to different light wavelengths. Fluorescence microscopy showed that both ICE1 and SCRM2/ICE2 accumulate in the nuclei of abaxial epidermal cells of cotyledons following light illumination (Figures 23A and 23B). Accumulation of ICE1 was more prominent than SCRM2 accumulation. The light-induced ICE accumulation was also evident in guard cells and stomatal lineage cells (Figure 24). These observations indicate that light stimulates ICE accumulation in leaf abaxial epidermal cells during stomatal development.

I also examined the patterns of ICE1 accumulation in hypocotyl and root cells. Fluorescent detection of ICE1 proteins showed that, while light-induced ICE1 accumulation occurs in hypocotyl guard cells (Figure 25A), ICE1 accumulation and its gene transcription were not discernibly affected by light in the root cells (Figures 25B to 25D).

### **COP1 interacts with ICE proteins**

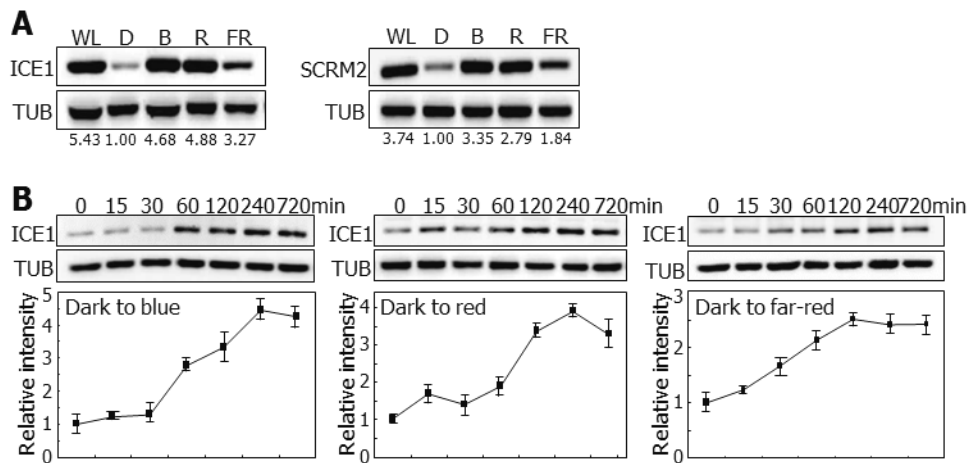


**Figure 22. Light induces ICE accumulation**

**(A)** Light-induced accumulation of ICE proteins. Four-day-old *pICE1:MYC-ICE1* and *pSCRM2:MYC-SCRM2* transgenic seedlings grown on MS-agar plates in darkness were exposed to different light wavelengths for 12 h before extracting total proteins from whole seedlings. ICE proteins were detected immunologically using an anti-MYC antibody. Tubulin (TUB) was detected similarly as loading control. WL, white light. D, dark. B, blue. R, red. FR, far-red. Blots on the membranes were quantitated using the ImageJ software.

**(B)** Kinetics of ICE1 accumulation. Four-day-old *35S:MYC-ICE1* transgenic seedlings grown on MS-agar plates in darkness were exposed to different light wavelengths for up to 12 h before extracting total proteins from whole seedlings. Immunological detection of ICE1 and quantitations were performed as described in **(A)**. Quantitations of three blots from independent biological samples were averaged. Bars indicate standard error of the mean (SE).

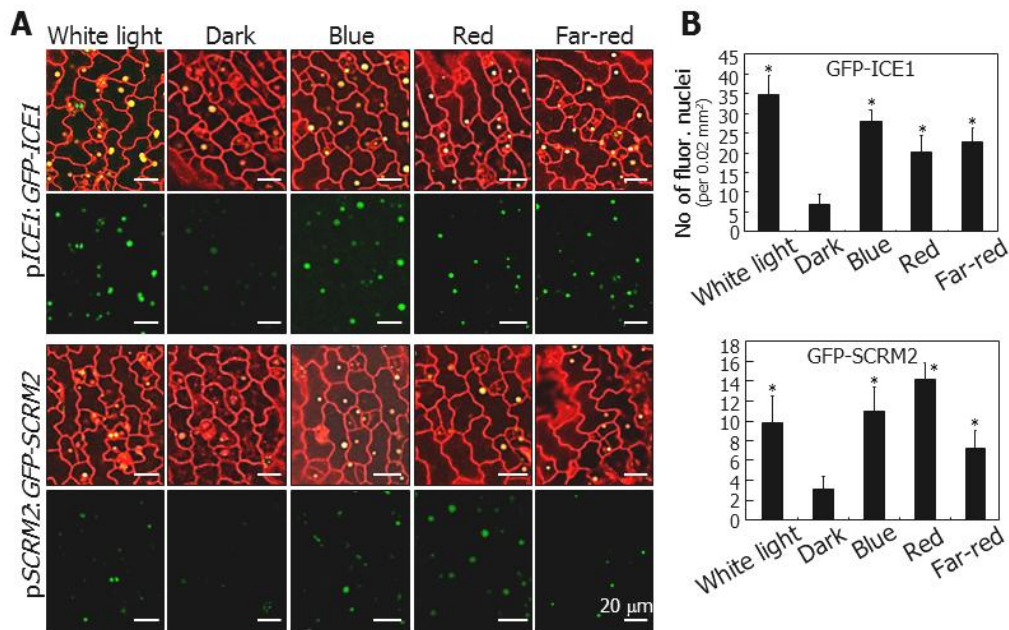


**Figure 23. Light-induced ICE accumulation occurs in the nuclei of abaxial epidermal cells of cotyledons**

**(A)** ICE accumulation in the nuclei of abaxial epidermal cells. Five-day-old *pICE1:GFP-ICE1* and *pSCRM2:GFP-SCRM2* seedlings grown on MS-agar plates in darkness were exposed to different light wavelengths for 4 h before obtaining confocal images.

**(B)** Counting of fluorescent nuclei in abaxial epidermal cells. Countings were performed using the cotyledon samples described in **(A)**. Three independent countings, each consisting of ten seedlings, were averaged and statistically analyzed (*t*-test,  $*P < 0.01$ ). Bars indicate SE.

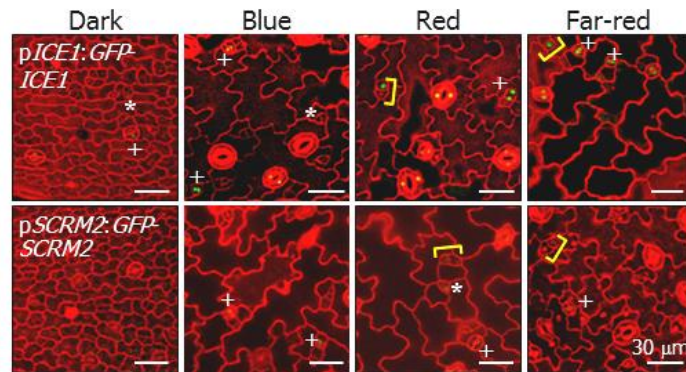


**Figure 24. Effects of light on ICE protein stability in stomata and stomatal lineage cells**

The *pICE1:GFP-ICE1* and *pSCRM2:GFP-SCRM2* transgenic seedlings were grown on MS-agar plates for 5 d under different light wavelengths. Confocal images of abaxial epidermal cells of cotyledons were displayed. Asterisks indicate meristemoids. Brackets indicate guard mother cells. (+) indicates immature stomata.

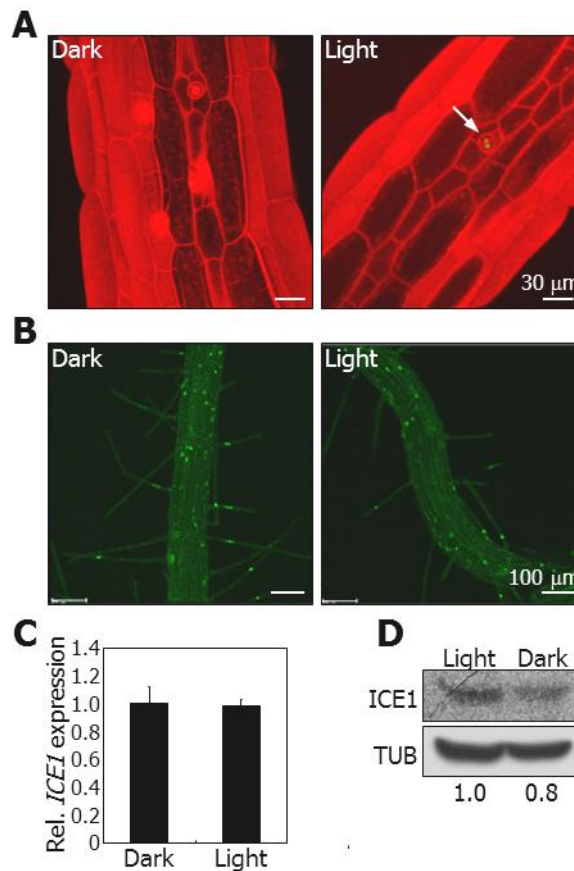


**Figure 25. Effects of light on ICE1 accumulation in different plant organs**

**(A)** ICE1 accumulation in hypocotyl cells. Four-day-old *pICE1:GFP-ICE1* transgenic seedlings grown on MS-agar plates in the light were further incubated either in the light or darkness for 2 d. Confocal images of hypocotyl cells were obtained.

**(B)** ICE1 accumulation in root cells. Four-day-old *pICE1:GFP-ICE1* transgenic seedlings grown on MS-agar plates in darkness were exposed to white light for 12 h. Confocal fluorescent images of root cells were obtained.

**(C)** Transcript levels of *GFP-ICE1* transgene in root cells. Four-day-old

*pICE1:GFP-ICE1* transgenic seedlings grown on MS-agar plates in darkness were exposed to white light for 12 h before harvesting root samples for total RNA extraction. Transcript levels were examined by RT-qPCR, as described in Figure 3. Biological triplicates using independent seedling samples grown under identical conditions were averaged. Bars indicate SE.

**(D)** Light-induced ICE1 accumulation in root cells. Five-day-old *pICE1:GFP-ICE1* seedlings grown in the light were incubated either in darkness or in white light for 24 h before extracting total proteins from root cells. An anti-GFP antibody was used to detect ICE1 proteins. Blots on the membranes were quantitated using the ImageJ software.

COP1 acts as a repressor of light-induced stomatal development (Kang et al., 2009; Balcerowicz et al., 2014). I found that ICE accumulation diminishes in the dark, when a large proportion of COP1 proteins is nuclear-localized (Stacey et al., 1999), raising a possibility that the reduction of ICE levels in the dark is associated with COP1 function.

Yeast two-hybrid assays using genes encoding a set of ICE and COP1 proteins, including their full-size forms, showed that full-size ICE1 and SCRM2/ICE2 forms physically interact with COP1 (Figures 26A and 26B). Assays using truncated ICE1 forms revealed that the ICE1-COP1 interactions occur via the leucine zipper motif of ICE1 (Figures 26A to 26C). Meanwhile, assays using truncated forms of COP1 suggested that, for the ICE-COP1 interactions, the intact conformation of COP1 protein is more important than its specific protein domain(s), as discussed previously (Ang et al., 1998; Torii et al., 1998).

Bimolecular fluorescence complementation (BiFC) assays using *Arabidopsis* protoplasts showed that the ICE-COP1 interactions occur in the nuclei (Figure 27A). To confirm the ICE1-COP1 interactions *in vivo*, I performed coimmunoprecipitation assays using transgenic plants expressing a hemagglutinin (HA)-ICE1 fusion driven by the Cauliflower Mosaic Virus (CaMV) 35S promoter and a COP1-MYC fusion under the control of a  $\beta$ -estradiol-inducible promoter. The ICE1-COP1 interactions occurred when the expression of COP1-MYC gene was induced (Figure 27B), whereas the protein-protein interactions were not detected in the absence of the inducer.

These observations indicate that COP1 interacts with ICE proteins in plant cells.

To investigate the ICE-COP1 interactions further, we transiently expressed p35S:*GFP-ICE1* and p35S:*COP1* constructs separately or together in *Arabidopsis* protoplasts. Fluorescent assays showed that ICE1 is evenly distributed in the nuclei in the absence of COP1 (Figure 27C). When the two constructs were coexpressed, nuclear speckles emitting bright green fluorescence were observed in the nuclei, similar to the nuclear localization patterns of COP1 (Jang et al., 2005), supporting the interactions of ICE1 with COP1 *in planta*. In contrast, I found no discernible interactions of COP1 with SPCH, MUTE, and FAMA in yeast two-hybrid and BiFC assays (Figures 28A and 28B, respectively).

### **COP1 ubiquitinates ICE proteins**

COP1 is a well-characterized E3 ubiquitin ligase that targets a variety of proteins involved in light responses, including phytochrome photoreceptors (Osterlund et al., 2000; Jang et al., 2010). Based on the interactions of COP1 with ICE1 and SCRM2/ICE2, it was postulated that ICE proteins would be subjected to COP1-mediated ubiquitination.

Using recombinant proteins, I examined *in vitro* whether COP1 ubiquitinates ICE proteins. Immunological assays using an anti-ubiquitin antibody showed that protein bands having higher molecular weights compared with those of native ICE1 and SCRM2 proteins were observed in

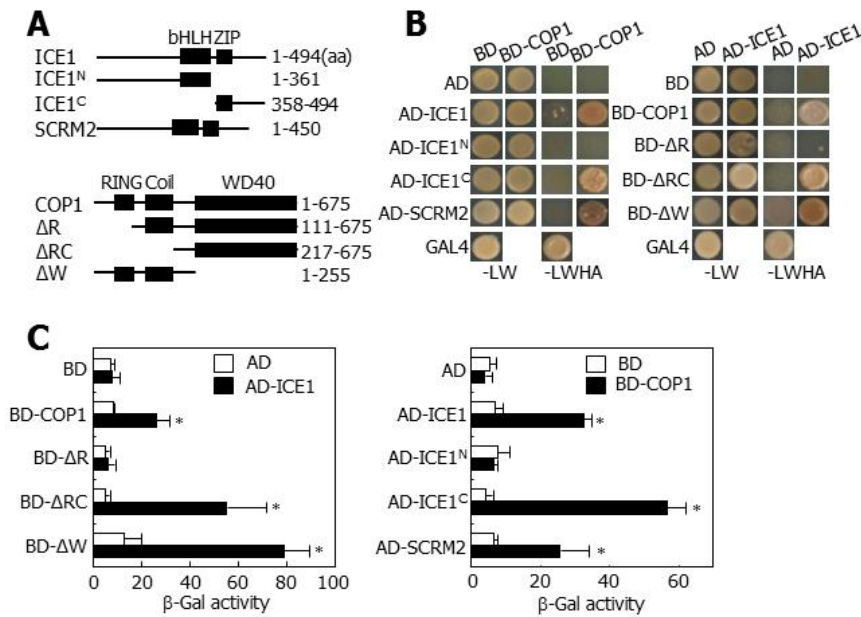


**Figure 26. ICE proteins interact with COP1 in yeast cells**

**(A)** ICE and COP1 constructs. Numbers indicate amino acid (aa) positions.

bHLH, basic helix-loop-helix. ZIP, leucine zipper. RING, ring domain. Coil, coiled-coil.

**(B)** ICE-COP1 interactions in yeast cells. -LW indicates Leu and Trp dropout plates. -LWHA indicates Leu, Trp, His, and Ade dropout plates.

**(C)** β-Gal activity assays. Interactions of ICE proteins with COP1 in yeast cells were examined by measurements of β-Gal activity. Five measurements were averaged and statistically analyzed (*t*-test, \**P* < 0.01). Bars indicate SE.

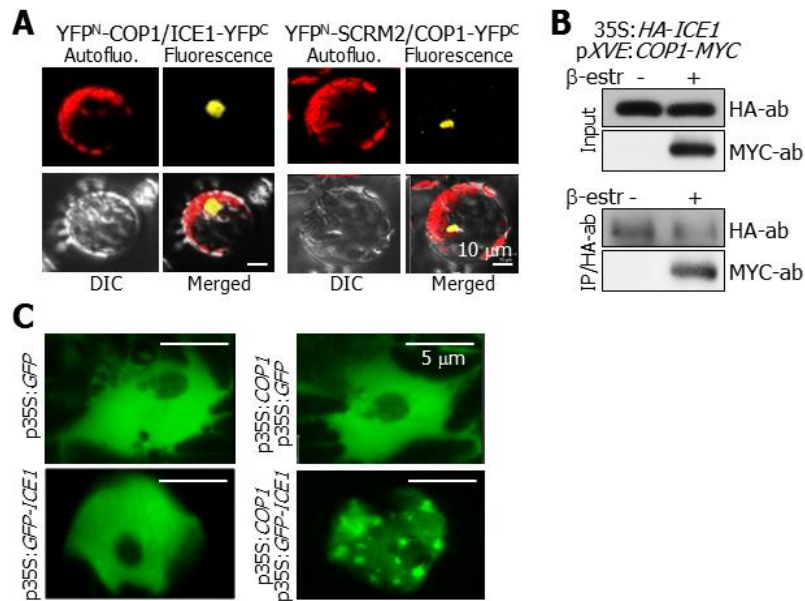


**Figure 27. ICE proteins interact with COP1 in planta**

**(A)** COP1-ICE interactions in *Arabidopsis* protoplasts. The YFP<sup>N</sup>-COP1 and ICE1-YFP<sup>C</sup> constructs and the YFP<sup>N</sup>-SCRM2 and COP1-YFP<sup>C</sup> constructs were coexpressed transiently in *Arabidopsis* protoplasts and visualized by differential interference contrast (DIC) and fluorescence microscopy.

**(B)** Coimmunoprecipitation. Five-day-old 35S:*HA-ICE1* p*XVE*:*COP1-MYC* seedlings were incubated in the presence of 25 μM β-estradiol and 50 μM MG132 for 1 d in darkness before extracting total proteins from whole seedlings. Immunoprecipitation (IP) was performed using an anti-HA antibody. ICE1 and COP1 were detected immunologically using anti-HA and anti-MYC antibodies, respectively.

**(C)** Localization of ICE1 into nuclear speckles. The COP1 and GFP-ICE1 constructs were coexpressed transiently in *Arabidopsis* protoplasts, and the nuclei were visualized by fluorescence microscopy.

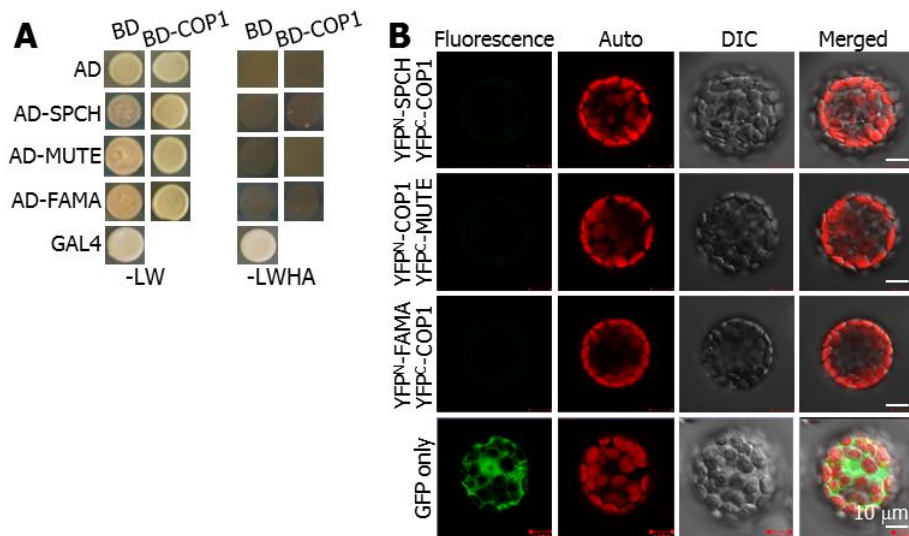


**Figure 28. COP1 does not interact with SPCH, MUTE, and FAMA**

**(A)** Protein-protein interactions in yeast cells. -LW indicates Leu and Trp dropout plates. -LWHA indicates Leu, Trp, His, and Ade dropout plates.

**(B)** BiFC assays. A series of different combinations between YFP<sup>N</sup>-SPCH, YFP<sup>C</sup>-COP1, YFP<sup>N</sup>-COP1, YFP<sup>C</sup>-MUTE, YFP<sup>N</sup>-FAMA, and YFP<sup>C</sup>-COP1 constructs was coexpressed transiently in *Arabidopsis* protoplasts and visualized by DIC and fluorescence microscopy.

the presence of COP1 but not detected in the absence of COP1 (Figure 29 and Figure 30), indicating that COP1 ubiquitinates ICE proteins. To further examine the COP1-mediated ubiquitination of ICE proteins, I performed *in vivo* ubiquitination assays. The 35S:*HA-ICE1* pXVE:*COP1-MYC* plants expressing HA-ICE1 and COP1-MYC fusions were incubated in darkness in the presence of MG132, a potent 26S proteasome inhibitor (Lee and Goldberg, 1998). ICE1 was immunoprecipitated using an anti-HA antibody, and ubiquitinated proteins were detected immunologically using an anti-ubiquitin antibody. The results showed that a ladder of ubiquitinated ICE1 proteins was evident in the presence of  $\beta$ -estradiol, indicating that COP1-mediated ubiquitination of ICE1 occurs *in planta* (Figure 31). I also verified in a similar way that SCRM2 is ubiquitinated *in vivo* but to a lesser extent than ICE1, suggesting that the primary target of the COP1-mediated ubiquitination is ICE1.

The ICE transcription factors form heterodimers with SPCH, MUTE, and FAMA (Kanaoka et al., 2008; Horst et al., 2015). Therefore, I examined whether SPCH, MUTE, and FAMA proteins are the substrates of the COP1-mediated ubiquitination. COP1 did not ubiquitinate SPCH, MUTE, and FAMA *in vitro* (Figure 32).

### **COP1 degrades ICE proteins through ubiquitin/proteasome pathways**

I observed that COP1 ubiquitinates ICE proteins. Therefore, I examined whether COP1 directs the degradation of ICE proteins through

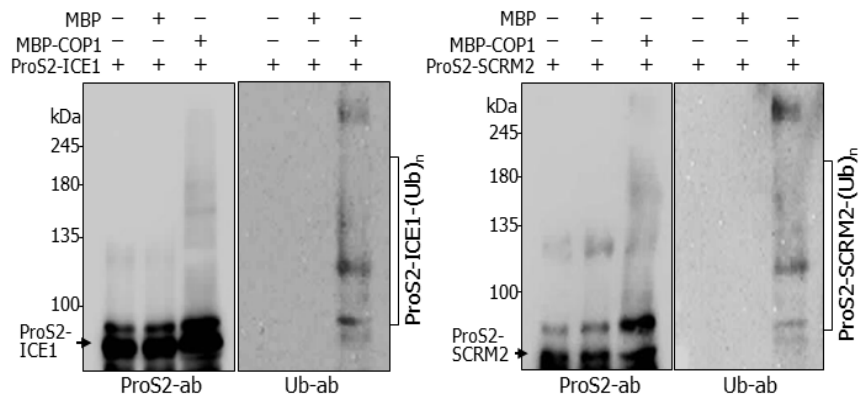


**Figure 29. COP1 ubiquitinates ICE proteins *in vitro***

Ubiquitination assays on ProS2 fusions *in vitro* were performed using human E1, E2, and recombinant MBP-COP1 that was pretreated with 20  $\mu$ M ZnCl<sub>2</sub> prior to the reactions. MBP protein was included as negative control. Ubiquitinated ICE1 and SCRM2 proteins were detected immunologically using an anti-ubiquitin (Ub) antibody (left and right panels, respectively). kDa, kilodalton.

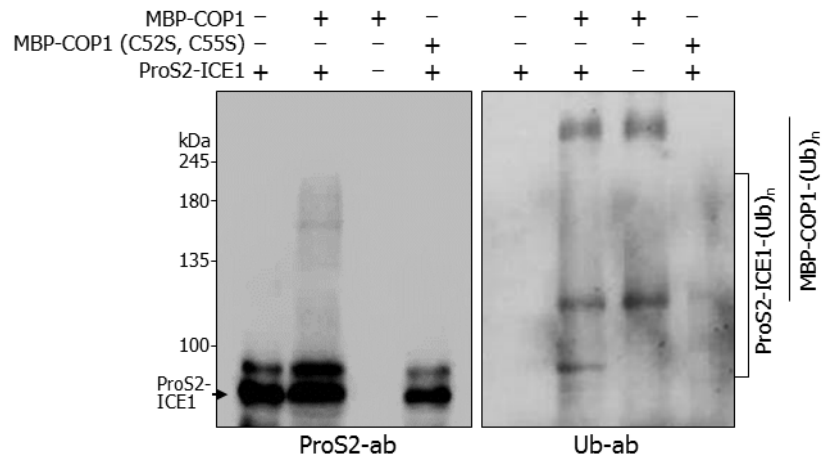


**Figure 30. Autoubiquitination activity of COP1 *in vitro***

The mutant COP1 form harboring C52S and C55S substitutions lacks E3 ubiquitin ligase activity (Seo et al., 2003; Xu et al., 2014). Either the wild-type or mutant cop1 form was included in the *in vitro* ubiquitination assays using ICE1 as substrate. Ubiquitinated ICE1 and COP1 proteins were detected immunologically using an anti-ubiquitin (Ub) antibody. kDa, kilodalton. Note that COP1 exhibits self-ubiquitination activity (Saijo et al., 2003).

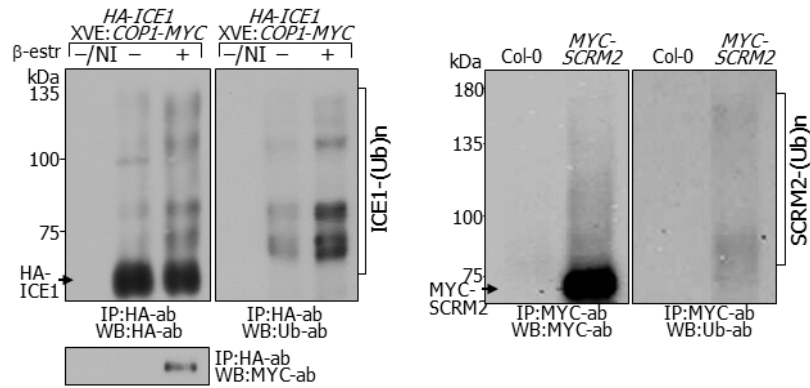


**Figure 31. ICE ubiquitination *in vivo***

Ten-day-old 35S:*HA-ICE1* p*XVE:COPI-MYC* seedlings were incubated in the presence of 25  $\mu$ M  $\beta$ -estradiol and 50  $\mu$ M MG132 for 24 h in darkness before extracting total proteins from whole seedlings (left panel). IP was performed using an anti-HA antibody. Ubiquitinated ICE1 proteins were detected by western blot hybridization (WB) using an anti-Ub antibody. NI, no immunoprecipitation. Ten-day-old 35S:*MYC-SCRM2* seedlings were incubated in the presence of 50  $\mu$ M MG132 for 24 h in darkness before extracting total proteins from whole seedlings (right panel). IP and detection of ubiquitinated SCRM2 were performed as described above.

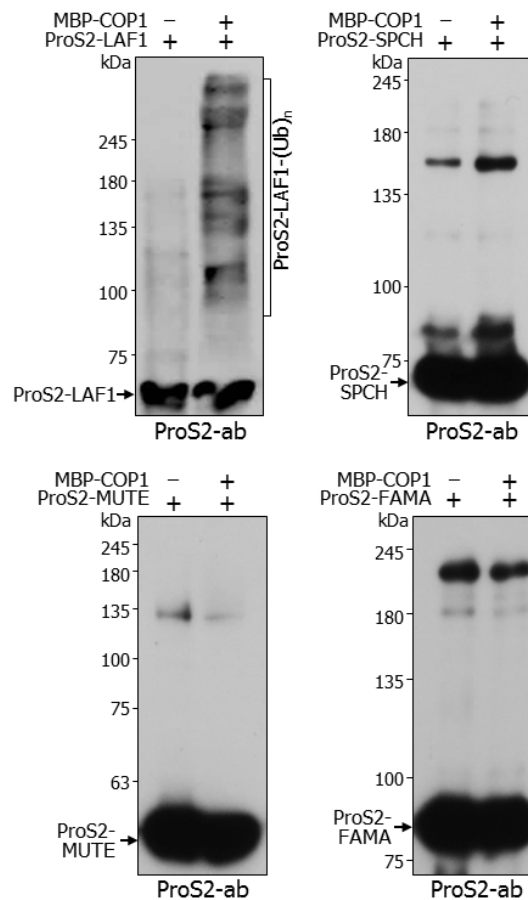


**Figure 32. COP1 does not ubiquitinate SPCH, MUTE, and FAMA**

SPCH, MUTE, and FAMA proteins were prepared as recombinant ProS2 fusions in *Escherichia coli* cells and partially purified by affinity chromatography. Ubiquitination assays on ProS2 fusions *in vitro* were performed using human E1, E2, and recombinant MBP-COP1. Prior to reactions, recombinant MBP-COP1 was pretreated with 20  $\mu$ M ZnCl<sub>2</sub>. They were detected immunologically using an anti-ProS2 antibody (2<sup>nd</sup> to 4<sup>th</sup> panels). kDa, kilodalton. The Long After Far-red light 1 (LAF1) protein, which is ubiquitinated by COP1 (Seo et al., 2003), was included as positive control (1<sup>st</sup> panel).

ubiquitin/proteasome pathways.

Using 35S:*MYC-ICE* transgenic plants, I first investigated whether ubiquitinated ICE proteins undergo degradation. The plants were incubated in darkness with or without MG132, and the levels of ICE proteins were analyzed immunologically. It was found that the levels of ICE1 and SCRM2/ICE2 in MG132-treated plants in darkness were comparable to those in light-grown plants (Figure 33A). However, the protein levels were significantly lower in dark-grown plants without MG132 treatments, indicating that ICE degradation occurs through ubiquitin- and proteasome-dependent pathways.

To test whether the ubiquitin-mediated degradation of ICE proteins is mediated by COP1, I overexpressed the *MYC-ICE* construct driven by the CaMV 35S promoter in COP1-defective mutants, and the levels of ICE proteins were investigated. I found that ICE degradation was significantly reduced in *cop1-4* and *cop1-6* mutants (Figure 33B). I also examined the COP1-mediated degradation of ICE1 using the 35S:*HA-ICE1* p*XVE*:*COP1-MYC* plants. The ICE1 levels were considerably lower when *COP1* expression was induced by  $\beta$ -estradiol (Figure 33C), confirming that COP1 is responsible for the ubiquitin-mediated degradation of ICE proteins.

My data showed that ICE proteins accumulate in cotyledon epidermal cells in the light but disappear in darkness. To examine whether the COP1-mediated degradation of ICE1 occurs in abaxial epidermal cells, I produced transgenic plants expressing a GFP-ICE1 fusion in Col-0 and

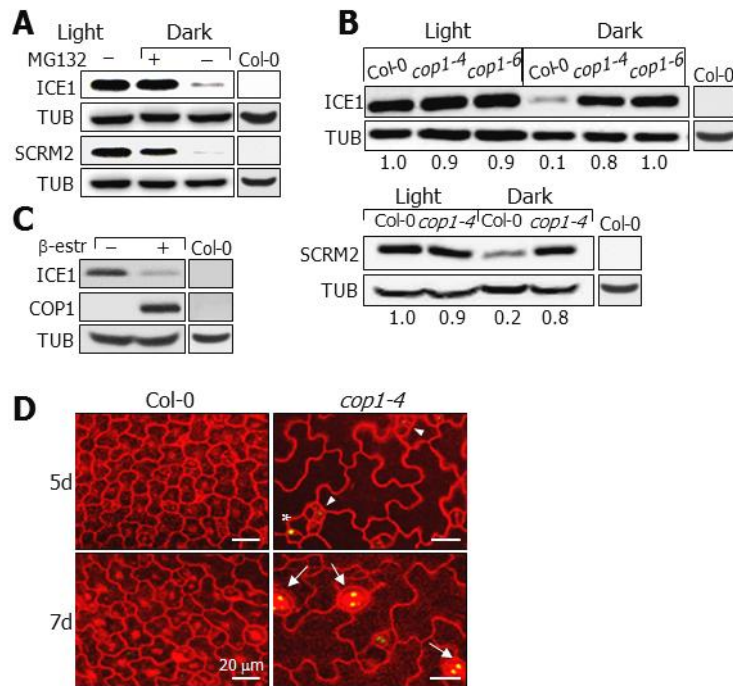


**Figure 33. COP1 degrades ICE proteins through ubiquitin/proteasome pathways**

**(A)** Ubiquitin-mediated ICE degradation. Ten-day-old 35S:*MYC-ICE1* and 35S:*MYC-SCRM2* seedlings were incubated in the presence of 50  $\mu$ M MG132 for 24 h in darkness before extracting total proteins from whole seedlings. An anti-MYC antibody was used to detect ICE proteins. Nontransformed Col-0 seedlings were also included in the assays.

**(B)** Reduced ICE degradation in COP1-defective mutants. The 35S:*MYC-ICE1* and 35S:*MYC-SCRM2* plants were crossed with Col-0 plants and *cop1* mutants (upper and lower panels, respectively). Seedling growth and detection of ICE proteins were performed as described in **(A)**. Nontransformed Col-0 seedlings were also included in the assays.

**(C)** COP1-mediated degradation of ICE1. Ten day-old *35S:HA-ICE1* *pXVE:COP1-MYC* seedlings were incubated in darkness for 24 h in the presence of 10  $\mu$ M MG132 and 25  $\mu$ M  $\beta$ -estradiol before extracting total proteins from whole seedlings. Anti-HA and anti-MYC antibodies were used to detect ICE1 and COP1 proteins, respectively. Nontransformed Col-0 seedlings were also included in the assays.

**(D)** ICE1 accumulation in *cop1-4* stomatal lineage cells. The *pICE1:GFP-ICE1* and *pICE1:GFP-ICE1 cop1-4* seedlings were grown for 5 or 7 d in darkness. Confocal images of abaxial epidermal cells were obtained. Arrowheads indicate division-competent cells. Asterisk indicates meristemoid. Arrows indicate stomata.

*cop1-4* backgrounds. While GFP signals were evident in the stomata lineage cells of *cop1-4* in darkness, the fluorescent signals were not detected in Col-0 background under identical conditions (Figure 33D), indicating that the COP1-mediated degradation of ICE1 occurs in the nuclei of abaxial epidermal cells in darkness. I next examined the kinetics of ICE1 accumulation. The GFP signals appeared rapidly in the stomatal precursor cells following light illumination in Col-0 background (Figure 34). In contrast, GFP signals were evident in the stomatal precursor cells and immature stomata in *cop1-4* background even in darkness, confirming that COP1-mediated degradation of ICE1 occurs in the nuclei of abaxial epidermal cells in darkness.

SPCH forms protein complexes with ICE proteins (Kanaoka et al., 2008; Horst et al., 2015), whose accumulation is enhanced by light during stomatal development. Promoter activity assays using *pSPCH:NLS-GFP* and *pSPCH:GFP-SPCH* constructs revealed that while *SPCH* transcription is not discernibly affected by light, its protein abundance was elevated in the light, as indicated by the numbers of green fluorescent nuclei (Figures 35A to 35C). Notably, the reduction in SPCH abundance in darkness could not be undone by MG132 (Figure 35D). Similar assays showed that the number of green fluorescent nuclei was higher by 2.2-fold in *cop1-4* background than in Col-0 background under dark conditions (Figures 36A and 36B). In addition, light increased the SPCH abundance in both Col-0 plants and *cop1-4* mutants (Figures 36A to 36C). Therefore, I concluded

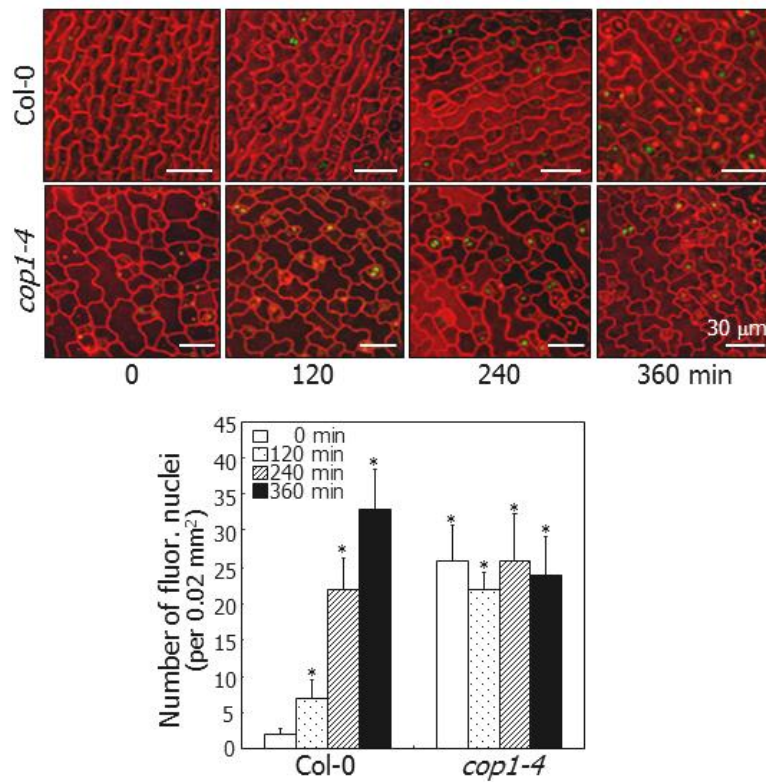


**Figure 34. Kinetics of ICE accumulation in abaxial epidermal cells**

Three-day-old *pICE1:GFP-ICE1* and *pICE1:GFP-ICE1 cop1-4* seedlings grown in darkness were exposed to white light for the indicated time periods before obtaining confocal images (left panel). Three independent measurements, each consisting of ten countings of fluorescent nuclei in abaxial epidermal cells, were averaged and statistically analyzed ( $t$ -test,  $*P < 0.01$ ) (right graph). Bars indicate SE.

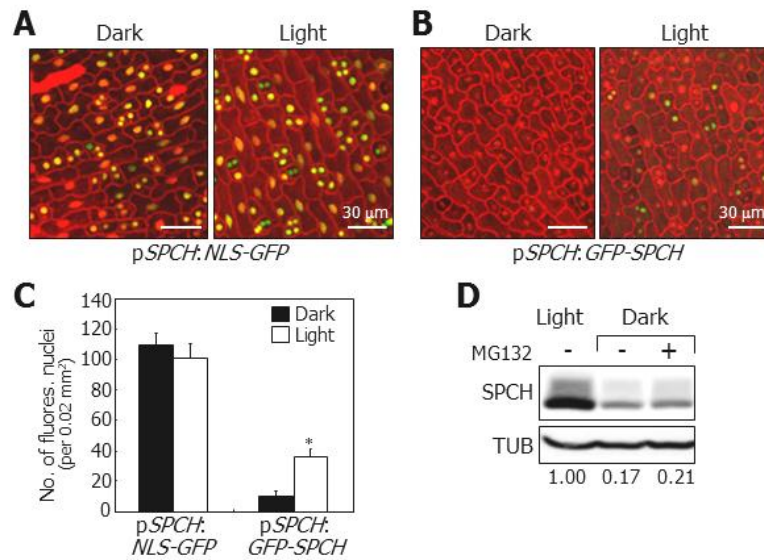


**Figure 35. SPCH degradation is not directly associated with ubiquitin/proteasome pathways**

**(A)** Fluorescence-assisted detection of *SPCH* promoter activity. Three-day-old pSPCH:NLS-GFP transgenic seedlings grown in darkness were exposed to white light for 6 h. Confocal images of abaxial epidermal cells of cotyledons were obtained. NLS, nuclear localization sequence.

**(B and C)** SPCH accumulation in the nuclei of abaxial epidermal cells of cotyledons. Three-day-old pSPCH:GFP-SPCH transgenic seedlings grown in darkness were exposed to white light for 6 h before obtaining confocal images **(B)**. Fluorescent nuclei in abaxial epidermal cells were counted **(C)**. Three independent measurements, each consisting of ten countings, were averaged and statistically analyzed (*t*-test, \**P* < 0.01). Bars indicate SE.

**(D)** Effects of MG132 on SPCH degradation. Five-day-old transgenic seedlings overexpressing a MYC-SPCH fusion were incubated in darkness

for 24 h in the presence of 50  $\mu$ M MG132 before extracting total proteins from whole seedlings. Immunological detection of SPCH proteins was performed using an anti-MYC antibody. Blots on the membranes were quantitated using the ImageJ software.

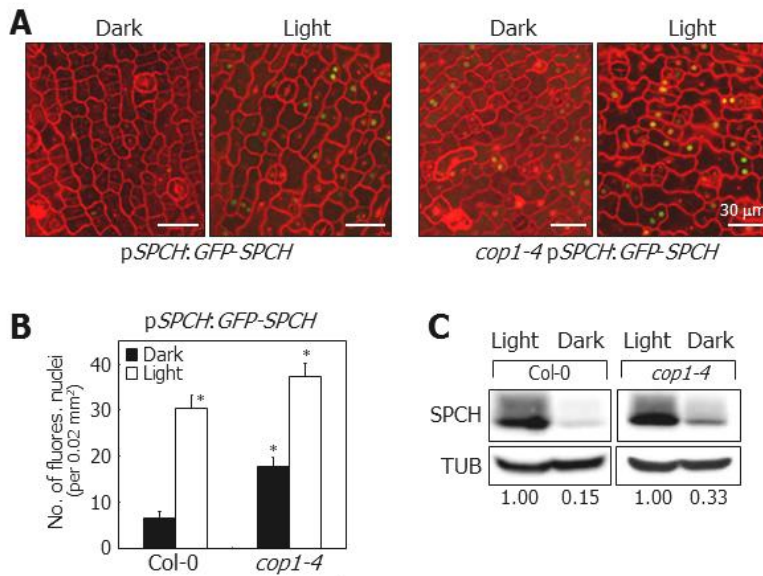


**Figure 36. SPCH degradation is not associate with COP1 function**

**(A and B)** Dark-induced degradation of SPCH in *cop1-4* stomatal lineage cells. Three-day-old pSPCH:GFP-SPCH and *cop1-4* pSPCH:GFP-SPCH seedlings grown in darkness were exposed to white light for 6 h before obtaining confocal images of abaxial epidermal cells of cotyledons **(A)**. Fluorescent nuclei in abaxial epidermal cells were counted **(B)**. Three independent measurements, each consisting of fifteen countings, were averaged and statistically analyzed (*t*-test, \**P* < 0.01). Bars indicate SE.

**(C)** SPCH accumulation in *cop1-4* background. Five-day-old 35S:MYC-SPCH seedlings were incubated in darkness for 24 h. Immunological detection of SPCH proteins was performed as described in Figure 35D. Blots on the membranes were quantitated as described above.

that, while the protein abundance of SPCH is elevated by light, the dark-induced degradation of SPCH is not mediated by ubiquitin/proteasome pathways, unlike ICE proteins.

### **Light inhibits COP1-mediated degradation of ICE proteins**

Light inhibits the nuclear function of COP1 during photomorphogenic responses and stomatal development (Stacey et al., 1999; Kang et al., 2009; Sheerin et al., 2015). Therefore, it was hypothesized that light would inhibit the COP1-mediated degradation of ICE proteins during stomatal development.

To investigate the effects of light on the COP1-mediated degradation of ICE1, the *35S:HA-ICE1 pXVE:COP1-MYC* transgenic plants were pretreated with MG132 in the presence or absence of  $\beta$ -estradiol, and the degradation kinetics of ICE1 were investigated in the presence of cycloheximide. In the absence of the inducer, ICE1 degradation was slower in light than that in the dark (Figures 37A and 37C), consistent with the degradation of ICE1 in darkness. In the inducer-pretreated plants, the degradation rate of ICE1 was discernibly faster than that in plants without the induction of COP1 production in the light (Figures 37B and 37C). Similarly, in darkness, the rate of ICE1 degradation in the inducer-treated plants was faster than that in mock-treated plants, indicating that light inhibits the COP1 activity in degrading ICE1. ICE1 degradation still occurred slowly in the light regardless of the induction of COP1

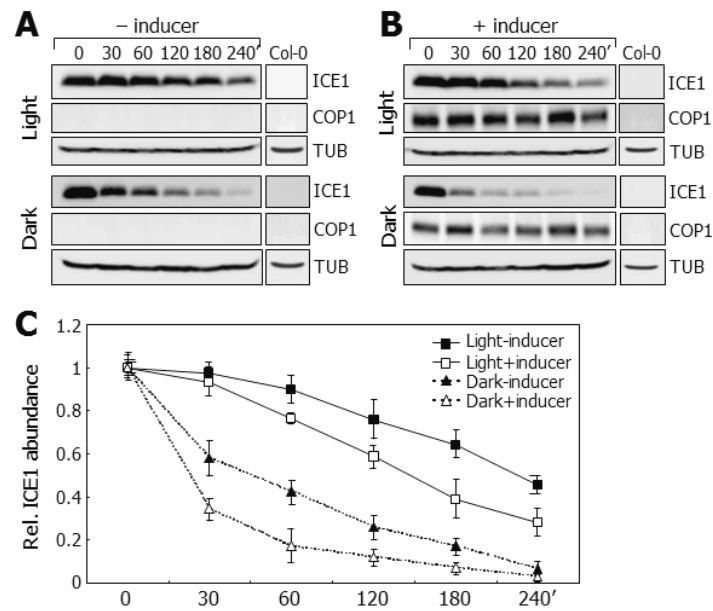


**Figure 37. Light inhibits COP1-mediated degradation of ICE1**

Five-day-old *35S:HA-ICE1 pXVE:COP1-MYC* seedlings were pretreated with 50  $\mu$ M MG132 in the absence (A) or presence (B) of 25  $\mu$ M  $\beta$ -estradiol for 16 h and subsequently incubated in the presence of 0.5 mM cycloheximide either in the light or darkness. Whole seedlings were harvested at the indicated time points for total protein extraction. Anti-HA and anti-MYC antibodies were used to detect ICE1 and COP1 proteins, respectively. Nontransformed Col-0 seedlings were also included in the assays.

Blots on the membranes were quantitated using the ImageJ software (C). Quantitations of three blots of biological triplicates from independent plant samples incubated under identical conditions were averaged. Bars indicate SE.

production, owing to the presence of endogenous COP1 produced in the *35S:HA-ICE1 pXVE:COP1-MYC* plants.

### **Light-mediated stabilization of ICE proteins is critical for stomatal development**

A critical question was whether the light-mediated stabilization of ICE proteins is essential for the induction of stomatal development. I measured the stomatal index (SI) for transgenic plants overexpressing a GFP-ICE1 fusion driven by the CaMV 35S promoter in Col-0 and *cop1-4* backgrounds. It has been reported that Col-0 plants and *cop1-4* mutants do not exhibit any differences in stomatal phenotypes under normal light conditions (Kang et al., 2009), which is certainly due to the saturated accumulation of ICE proteins (Figure 33B). Therefore, plants were grown under dim light conditions ( $1.5 \mu\text{mol m}^{-2}\text{s}^{-1}$ ), when ICE1 levels were different in Col-0 plants and *cop1-4* mutants (Figure 38A).

The *35S:GFP-ICE1* seedlings exhibited enhanced stomatal development compared with Col-0 plants under dim light conditions, as verified by SI measurements (Figures 38C and 38D). The *cop1-4* mutant exhibited higher SI than Col-0 plants under both dim light and dark conditions, consistent with the negative regulatory role of COP1 in stomatal development (Kang et al., 2009). Notably, *ICE1* overexpression further enhanced the *cop1-4* stomatal phenotype in *35S:GFP-ICE1 cop1-4* seedlings (Figures 38C and 38D), producing adjacent stomata and increasing number

of small cells, which are known to readily differentiate into guard cells (Wang et al., 2007). A similar enhancement of stomatal phenotype has also been observed for the severe COP1-defective allele *cop1-5* (Kang et al., 2009). Meanwhile, I found no discernible differences in the levels of *GFP-ICE1* transcripts between the *cop1-4* mutants and Col-0 plants (Figure 38B).

Time sequence analysis of stomatal differentiation revealed that the 35S:*GFP-ICE1 cop1-4* plants produced compact, division-competent cells during early stages of stomatal differentiation, at 4 days after germination (DAG) (Figure 39). It was evident that the transgenic plants produced adjacent stomata and small cells at DAG 9, demonstrating that light-induced ICE1 accumulation is critical for stomatal development.

To further verify that the light-mediated inhibition of COP1 function in inducing ICE1 accumulation is important for stomatal development, a GFP-ICE1 fusion was overexpressed driven by the strong CaMV 35S promoter in the *cop1-5* mutant on Ws-2 background, which exhibits severe stomatal phenotypes (Kang et al., 2009). The transgenic plants were grown in darkness, and the SI was measured. The results showed that ICE1 overexpression does not enhance the stomatal phenotype of the *cop1-5* seedlings (Figures 40A to 40C), which would be because ICE1 accumulation is already higher in this phenotypically severe mutant compared to that in the *cop1-4* mutant having mild phenotypes.

To further investigate the functional relationship between ICE

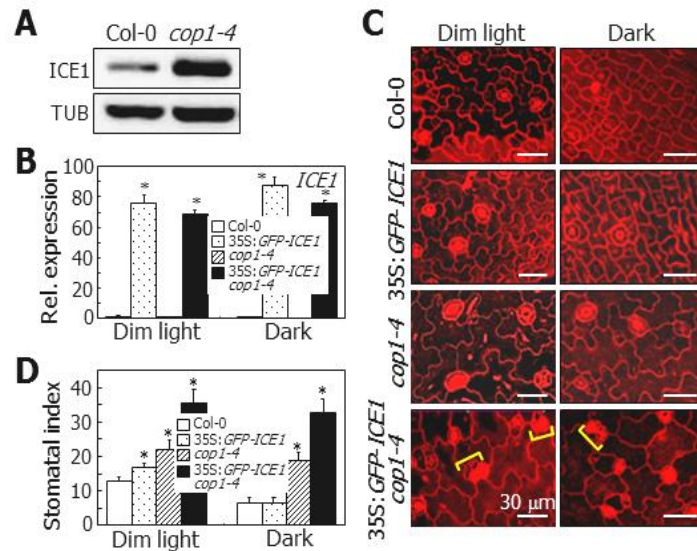


**Figure 38. Light-mediated stabilization of ICE1 is important for stomatal development**

**(A)** ICE1 accumulation in *cop1-4* mutant. Col-0 and *cop1-4* seedlings overexpressing a MYC-ICE1 fusion driven by the CaMV 35S promoter were grown in dim light ( $1.5 \mu\text{mol}\cdot\text{m}^{-2}\cdot\text{s}^{-1}$ ) for 5 d before extracting total proteins from whole seedlings. ICE1 was immuno-detected using an anti-MYC antibody.

**(B)** Transcript levels of *GFP-ICE1* transgene in *cop1-4* background. Seedlings were grown for 5 d on MS-agar plates under either dim light or dark conditions. Transcript levels were examined by RT-qPCR. Biological triplicates using independent seedling samples grown under identical conditions were statistically analyzed (*t*-test,  $*P < 0.01$ ). Bars indicate SE.

**(C and D)** Stomatal phenotypes in dim light. Seedlings were grown under either dim light or dark conditions for 5 d. Confocal images of abaxial

epidermal cells of cotyledons were obtained **(C)**. Yellow brackets mark adjacent stomata. Stomatal index (SI) was measured **(D)**. Three independent measurements, each consisting of ten seedlings, were averaged and statistically analyzed (*t*-test, \**P* < 0.01). Bars indicate SE.

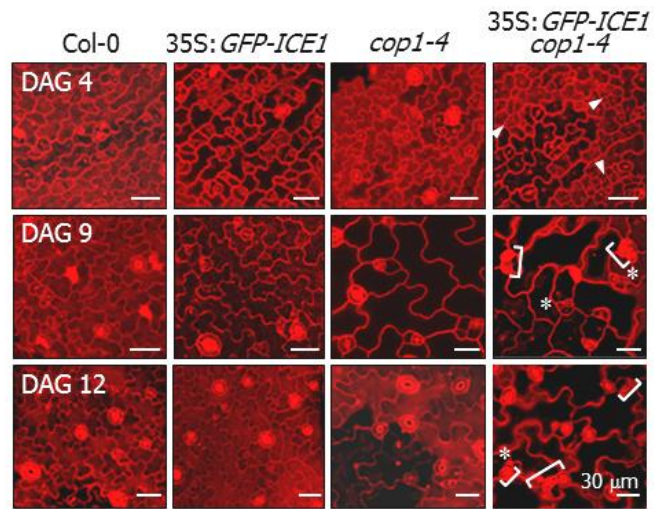


**Figure 39. Kinetics of stomatal differentiation in 35S:*GFP-ICE1 cop1-4* plants**

Seedlings were grown on MS-agar plates in dim light. Confocal images of abaxial epidermal cells of cotyledons were obtained. DAG, days after germination. Arrowheads indicate compact division-competent cells. Asterisks indicate small cells, which readily differentiate into guard cells. Brackets indicate adjacent stomata.

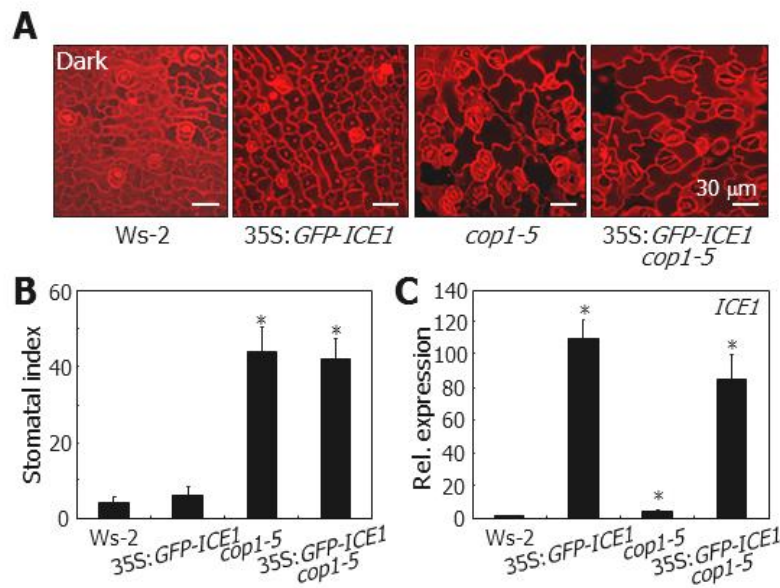


**Figure 40. Stomatal phenotype of 35S:GFP-ICE1 *cop1-5* plants in darkness**

**(A and B)** Stomatal phenotypes in darkness. The 35S:GFP-ICE1 *cop1-5* transgenic seedlings were grown on MS-agar plates in darkness for 8 d. Confocal images of abaxial epidermal cells of cotyledons were obtained **(A)**. Three independent measurements of SI, each consisting of ten seedlings, were statistically analyzed (*t*-test,  $*P < 0.01$ ) **(B)**. Bars indicate SE.

**(C)** Transcript levels of *GFP-ICE1* transgene in *cop1-5* background. Transcript levels were analyzed by RT-qPCR using dark-grown seedlings described in **(A)**. Whole seedlings were used for total RNA extraction. Biological triplicates using independent seedling samples grown under identical conditions were statistically analyzed (*t*-test,  $*P < 0.01$ ). Bars indicate SE.

transcription factors and COP1 in regulating stomatal development, the *ice1-2 scrm2-2* double mutant was crossed with the *cop1-4* and *cop1-5* mutants, and the stomatal phenotypes of the resultant plants were analyzed. The *ice1-2 scrm2-2* double mutant exhibited no symptoms of stomatal development in abaxial epidermal cells of cotyledons under both dim-light and dark conditions (Figures 41A and 41B). Notably, the *ice1-2 scrm2-2* double mutation compromised the constitutive stomatal development of the dark-grown *cop1-4* and *cop1-5* mutants (Figures 41A and 41B and Figure 42), confirming that suppression of the COP1-mediated ICE degradation is required for light-induced stomatal development.

Light induces the division of stomatal lineage cells, but its effects are not prominent before entering the stomatal lineage (Kang et al., 2009). Therefore, it was speculated that the suppression of the *cop1-4* stomatal phenotype by the *ice1-2 scrm2-2* double mutation occurs because the double mutant does not have stomatal lineage cells capable of responding to light. In support of this notion, it has been reported that *spch* mutations, which block the entry into stomatal lineage, suppress the *cop1-5* stomatal phenotype (Kang et al., 2009).

To resolve this uncertainty, we prepared *ice1-2 scrm2-2/+* seedlings, in which the entry into stomatal lineage occurs properly but division of stomatal lineage cells is aborted, unlike *ice1-2 scrm2-2* seedlings (Kanaoka et al., 2008). It was found that the *ice1-2 scrm2-2/+* mutation still compromised the constitutive stomatal phenotype of the *cop1-4* mutant

(Figures 41A and 41B), further supporting the physiological significance of the light-induced suppression of COP1-mediated ICE degradation during stomatal development.

The MAPKK kinase YODA (YDA) acts downstream of COP1 in repressing the stomatal development, and its defective mutants produce stomata even in darkness (Kang et al., 2009; Balcerowicz et al., 2014). A question was whether YDA is functionally associated with ICE proteins in stomatal development. I observed that the stomatal phenotype of the YDA-defective *yda-10* mutant is still light-responsive, producing more stomata in the light than in darkness (Balcerowicz et al., 2014) (Figure 43A). The *yda-10* mutant harbors more cells that express ICE1 than Col-0 plants under both light and dark conditions (Balcerowicz et al., 2014). To examine whether the stomatal phenotype of the mutant is associated with ICE1 accumulation, I produced transgenic plants expressing a GFP-ICE1 fusion in Col-0 and *yda-10* backgrounds. While the number of green fluorescent nuclei was larger in *yda-10* background than in Col-0 background, it further increased following light exposure in *yda-10* background (Figures 43B and 43C), consistent with the stomatal phenotype of the mutant. Immunological assays also showed that ICE1 accumulation is still light-responsive in *yda-10* background but with a lesser degree compared to that in Col-0 background (Figures 43D and 43E). These observations suggest that YDA is functionally independent of ICE-mediated light signaling in regulating stomatal development. It is likely that YDA



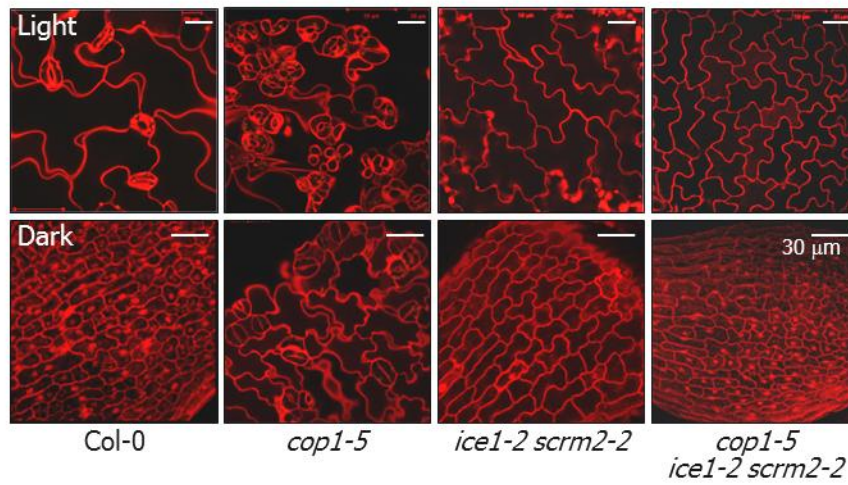


**Figure 42. Stomatal phenotypes of *ice1-2 scrm2-2* mutants harboring *cop1-5* mutation**

The *ice1-2 scrm2-2* double mutant was crossed with the *cop1-5* mutant. Seedlings were grown for 10 d on MS-agar plates under either light or dark conditions. Confocal images of abaxial epidermal surfaces of cotyledons were obtained to visualize guard cells.

and ICE1 function in parallel during stomatal development.

### **ICE proteins integrate light and developmental signals into stomatal development**

My data indicated that light triggers ICE accumulation to direct stomatal development. Meanwhile, it is known that ICE and SPCH transcription factors cooperatively regulate genes that modulate stomatal development, such as *EPIDERMAL PATTERNING FACTOR 2 (EPF2)* and *TOO MANY MOUTH (TMM)* (Horst et al., 2015). Therefore, I examined whether the ICE targets are involved in the light-mediated stomatal development.

RT-qPCR analysis revealed that light promotes the transcription of *EPF2* gene. Its transcript levels gradually elevated in the light, reaching the peak 12 h following light illumination (Figure 44A). The transcription of *TMM* gene was also induced, albeit to a lesser degree, by light exposure.

Spatial regulation of initial stomatal development is conducted by ICE/SPCH transcription factors and its target *EPF2* (Horst et al., 2015). Light-induced *EPF2*, which functions as a secreted signaling peptide, specifically restricts the entry into stomatal lineage in neighboring cells (Hunt and Gray, 2009). Consequently, *EPF2*-defective mutants exhibit small-clustering-cell phenotypes under light conditions (Hunt and Gray, 2009; Yamamuro et al., 2014). Notably, dark-grown wild-type seedlings exhibited numerous small clustering cells (Figure 44B), similar to those observed in *EPF2*-defective mutants, suggesting that the ICE-mediated

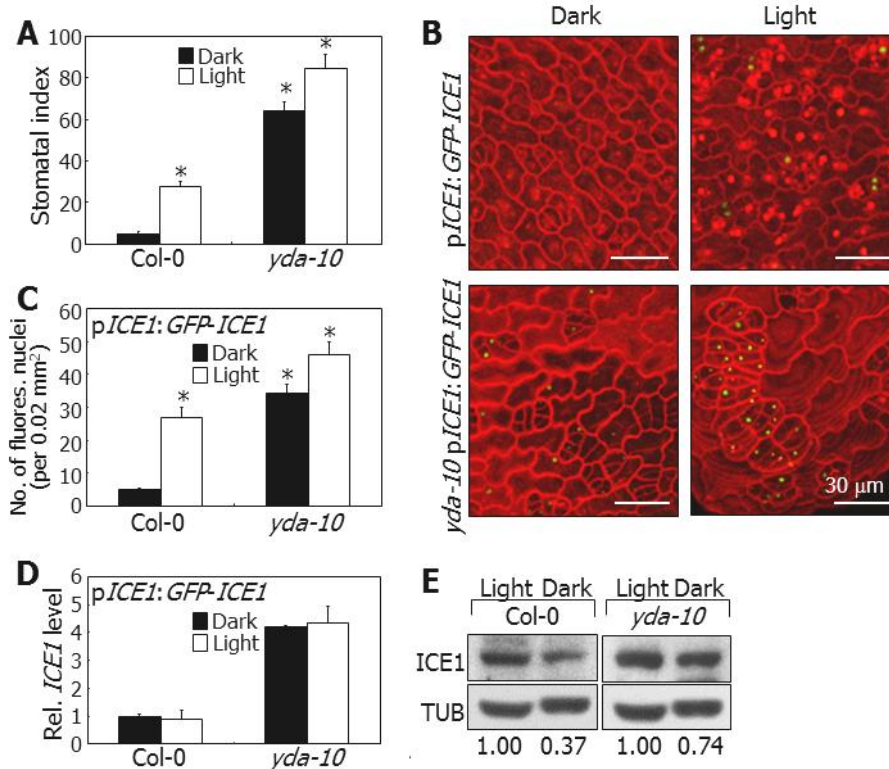


**Figure 43. Functional relationship between YDA and ICE1 in light-induced stomatal development**

**(A)** SI of *yda-10* mutant. Seedlings were grown for 10 d on MS-agar plates under either light or dark conditions. Three independent measurements of SI, each consisting of ten seedlings, were averaged and statistically analyzed (*t*-test,  $*P < 0.01$ ). Bars indicate SE.

**(B and C)** ICE1 accumulation in *yda-10* stomatal lineage cells. Three-day-old *pICE1:GFP-ICE1* and *yda-10 pICE1:GFP-ICE1* seedlings grown in darkness were exposed to white light for 6 h before obtaining confocal images **(B)**. Three independent measurements, each consisting of ten countings of fluorescent nuclei in abaxial epidermal cells, were

averaged and statistically analyzed ( $t$ -test,  $*P < 0.01$ ) (C). Bars indicate SE.

**(D)** Transcript levels of *GFP-ICE1* transgene. Three-day-old *pICE1:GFP-ICE1* and *yda-10 pICE1:GFP-ICE1* transgenic seedlings grown in darkness were exposed to white light for 6 h before harvesting cotyledons for total RNA extraction. Transcript levels were examined by RT-qPCR, as described in Figure 3. Biological triplicates using independent seedling samples grown under identical conditions were averaged. Bars indicate SE.

**(E)** ICE1 accumulation in *yda-10* mutant. Five-day-old *pICE1:GFP-ICE1* seedlings grown in the light were incubated under either light or dark conditions for 12 h before extracting total proteins from cotyledons. Immunological detection of ICE1 proteins was performed as described in Figure 22. Blots on the membranes were quantitated using the ImageJ software.

activation of *EPF2* gene is associated with light regulation of stomatal development.

To examine whether the light-mediated induction of *EPF2* gene is related with ICE transcription factors, I examined the levels of *EPF2* transcripts in *ice1-2* and *cop1-6* mutants grown in the light. It was found that while the transcript levels were elevated in Col-0 plants, they were not elevated in the *ice1-2* and *ice1-2 cop1-6* mutants (Figure 44C). Meanwhile, high levels of *EPF2* transcripts were maintained in *cop1-6* mutant, in which ICE/SCRM proteins accumulate (Figure 33B). These observations demonstrate that ICE/SCRM transcription factors mediate the light-mediated induction of *EPF2* gene.

In conclusion, my data demonstrated that COP1 degrades the ICE transcription factors through ubiquitin/proteasome pathways in darkness, inhibiting stomatal development. Accordingly, ICE proteins accumulate in the nuclei of abaxial epidermal cells in COP1-defective mutants even in darkness. However, light suppresses the COP1-mediated degradation of ICE proteins, underlying the induction of stomatal development in light-grown plants. My data provide a molecular mechanism by which light signals are integrated into the ICE-SPCH/MUTE/FAMA-mediated developmental programs during stomatal development (Figure 45).

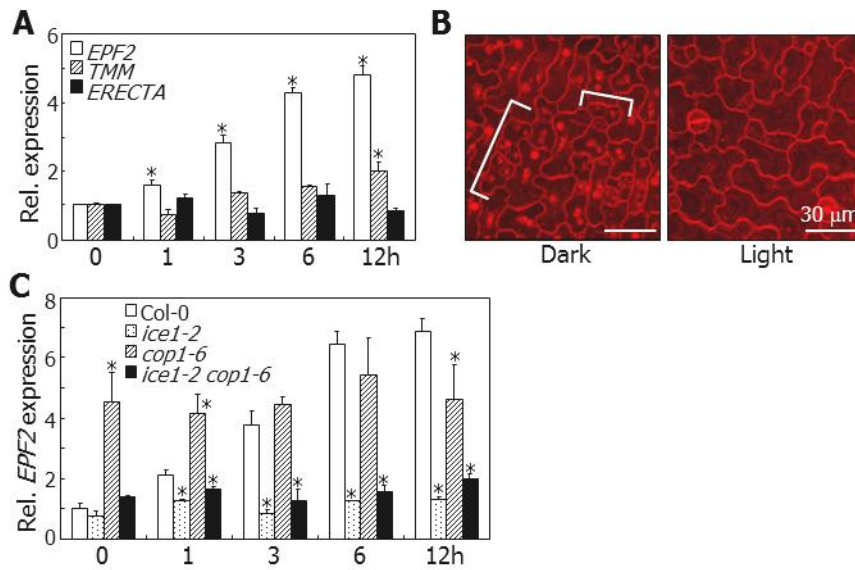


**Figure 44. ICE proteins integrate light signals into stomatal development**

**(A)** Effects of light on the transcription of stomatal regulator genes. Col-0 plants were grown in darkness for 3 d and then exposed to white light for the indicated time periods before harvesting whole seedlings. Transcript levels were examined by RT-qPCR. Biological triplicates using independent seedling samples grown under identical conditions were statistically analyzed (*t*-test,  $*P < 0.01$ ). Bars indicate SE. The *ERECTA* gene was used as negative control (Horst et al., 2015).

**(B)** Stomatal spacing and distribution. Col-0 plants were grown under either dark or light conditions for 3 d. Confocal images of abaxial epidermal surfaces of cotyledons were obtained. Brackets indicate small clustering cells that occur only in etiolated seedlings.

**(C)** Transcript levels of *EPF2* gene in *ice1-2* and *cop1-6* mutant. Seedling growth and RT-qPCR were performed as described in (A).

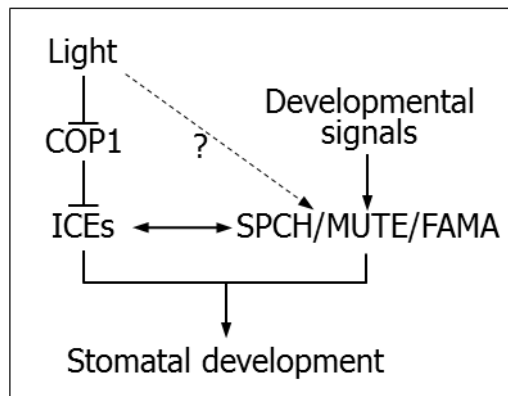


**Figure 45. ICE-mediated light signaling scheme during stomatal development**

In this signaling scheme, ICE transcription factors integrate light signals into stomatal development. Light would also stabilize SPCH via a COP1-independent pathway.

## **DISCUSSION**

### **Post-translational modification of ICE proteins in light-mediated stomatal development**

It has been known that ICE transcription factors are modified at the post-translation level. HOS1 degrades ICE proteins to prevent the exaggerated cold response, thus attenuating cold response during cold acclimation (Dong et al., 2006; Kim et al., 2015). Moreover, cold temperature enhances the ICE1 activity, through promoting their DNA binding and transcriptional activation activity (Lee et al., 2015). Recent studies revealed that OPEN STOMATA 1 (OST1), also known as SNF1-RELATED PROTEIN KINASE 2.6 (SnRK 2.6), phosphorylates ICE1 during cold acclimation (Ding et al., 2015). This molecular event promotes the ICE1 activity on target genes and prevents HOS1-mediated degradation of ICE1 proteins during cold acclimation. However, the transcript level of *ICE1* is not largely affected by cold temperatures (Chinnusamy et al., 2003; Kim et al., 2015).

In this study, apart from the cold response in ICE1 modulation, I demonstrated that inhibition of degradation of ICE proteins, via a COP1-mediated ubiquitin/proteasome-dependent pathway, is critical for light-induced stomatal development. My data represented that light rapidly induces ICE protein in the stomatal lineage cell and this event occurs through light inhibition of COP1 activity. Light in the red, blue, and

far-red wavelength ranges induced ICE protein accumulation, thus inducing stomatal development. Therefore, light-mediated inhibition of COP1-mediated degradation of ICE proteins, via a ICE-directed signaling module, is directly linked with stomatal development. Also, I think that the translational modification of ICE proteins ensures rapid regulatory process during stomatal development. Together with previous reports and my own data, these results indicate that post-translation modification of ICE proteins would be a crucial molecular events that regulate diverse plant developmental process in plants.

#### **Distinct mechanism of light-induced stabilization of bHLH transcription factors in stomatal development**

I found that ICE proteins are rapidly induced by light-mediated inhibition of the ubiquitin/proteasome-mediated protein degradation pathways. ICEs and SPCH/MUTE/FAMA transcription factors coordinate the transitional steps of stomatal differentiation by forming heterodimeric protein complexes (Kanaoka et al., 2008). Notably, I found that SPCH proteins are also modulated by exposure of light irradiance. Interestingly, the potent ubiquitin/proteasome inhibitor MG132 did not block the degradation of SPCH in darkness, unlike that of ICE proteins. Therefore, I concluded that light induces the accumulation of SPCH proteins by COP1- and ubiquitin/proteasome-independent pathways. It is worth identifying the regulators that modulate the abundance of SPCH proteins in dark

conditions. I propose that it is plausible light-mediated initial stomatal development is modulated by two distinct protein surveillance systems: COP1-mediated ubiquitin/proteasome-dependent pathways and ubiquitin-independent protein surveillance systems, which are not yet unidentified. These distinct molecular events contribute to the accurate and rapid responses of plants to environmental changes for their development. Additional investigations into the MUTE and FAMA proteins need to be undertaken to better understand light-mediated stomatal development.

#### **Integration of environmental signals into stomatal development by ICE transcription factors**

YODA (YDA) is a negative regulator of stomatal development and constitutes developmental pathways in stomatal development. The constitutively active form of YDA exhibits no stomata in abaxial leaf epidermis. YDA acts as an upstream regulator of MAPK cascade (MacAlister et al., 2007; Wang et al., 2007). MPK3 and MPK6 phosphorylate SPCH proteins, thus inhibiting stomatal development (Lampard et al., 2008). Notably, the SPCH/ICE complex activates *EPF2* in specification of early stomatal development (Horst et al., 2015). However, it is unknown how light signaling is closely associated with the developmental pathways that govern stomatal development.

My data showed that the ICE-mediated signaling network is directly linked to light signaling. While COP1 degraded ICE proteins in abaxial

epidermal and stomatal lineage cells in darkness, light induced accumulation of ICE proteins, thus inducing stomatal development. I also found that light induced level of *EPF2* transcripts and this regulation depends on light-induced ICE1 accumulation. Meanwhile, *EPF2*, which functions as a signaling peptide, restricts entry into the stomatal lineage (Hara et al., 2009; Hunt and Gray, 2009), thereby constituting early developmental pathways. Accordingly, I found that while light-grown plants exhibit proper stomatal spacing and distribution, the etiolated seedlings possess small-clustering cells in the leaves. Therefore, it is likely that the ICE-mediated signaling module integrates environmental information, such as light, into the developmental pathways to modulate stomatal development. It will be worth investigating whether and how various environmental cues interact with the ICE-mediated signaling network during stomatal development.

#### **Promising role of ICE1 in the epigenetic control of the development**

My data revealed the light-mediated accumulation of ICE proteins, thus elevating *EPF2* transcription, which ensures proper stomatal spacing and distribution in light-grown seedlings. Notably, transcript level of *EPF2* is regulated at the chromatin level (Yamamuro et al., 2014). REPRESSOR OF SILENCING1 (ROS1) is required for prevention of hyper-methylation in the genome and ROS1-mediated DNA methylation is critical for *EPF2* reduction during stomatal development (Yamamuro et al., 2014). When the

*EPF2* gene is hyper-methylated, the expression level is greatly reduced, thus producing small-cell-clustering phenotype (Yamamuro et al., 2014). It is found that the *EPF2* gene possesses a transposable element (TE) in its promoter region. TEs have been known to link with changes in the DNA methylation status (Yamamuro et al., 2014). The region of the *EPF2* promoter proximal to the TE exhibits hyper-methylation status in the *ROSI*-defective mutant (Yamamuro et al., 2014). My data revealed that light induces *EPF2*. It is worth investigating whether and how light-mediated stabilization of ICE transcription factors affects the methylation status of *EPF2*. Additionally, whether ICE transcription factors interact with chromatin modification factors needs to be defined. In fact, several transcription factors recruit chromatin modification factors to target loci (Xiao et al., 2017). Elucidation of functional linkage between the transcription factors and chromatin modification factors, which are not yet unidentified, will provide a direct and distinct mechanism of transcriptional regulation in environmental adaptation of plant development.

## REFERENCES

- Ang, L.H., Chattopadhyay, S., Wei, N., Oyama, T., Okada, K., Batschauer, A., and Deng, X.W. (1998). Molecular interaction between COP1 and HY5 defines a regulatory switch for light control of *Arabidopsis* development. *Mol. Cell* 1: 213-222.
- Ausín, I., Alonso-Blanco, C., Jarillo, J.A., Ruiz-García, L. and Martínez-Zapater, J.M. (2004). Regulation of flowering time by FVE, a retinoblastoma-associated protein. *Nat. Genet.* 36: 162–166.
- Balcerowicz, M., Ranjan, A., Rupprecht, L., Fiene, G., and Hoecker, U. (2014). Auxin represses stomatal development in dark-grown seedlings via Aux/IAA proteins. *Development* 141: 3165-3176.
- Bergmann, D.C., Lukowitz, W., and Somerville, C.R. (2004). Stomatal development and pattern controlled by a MAPKK kinase. *Science* 304: 1494-1497.
- Bergmann, D.C., and Sack, F.D. (2007). Stomatal development. *Annu. Rev. Plant Biol.* 58: 163-181.
- Blázquez, M.A., Soowal, L.N., Lee, I. and Weigel, D. (1997). *LEAFY* expression and flower initiation in *Arabidopsis*. *Development* 124: 3835–3844.
- Blázquez, M.A. and Weigel, D. (2000). Integration of floral inductive signals in *Arabidopsis*. *Nature* 404: 889–892.

- Blázquez, M.A., Ahn, J.H. and Weigel, D. (2003). A thermosensory pathway controlling flowering time in *Arabidopsis thaliana*. *Nat. Genet.* 33: 168–171.
- Boccalandro, H.E., Rugnone, M.L., Moreno, J.E., Ploschuk, E.L., Serna, L., Yanovsky, M.J., and Casal, J.J. (2009). phytochrome B enhances photosynthesis at the expense of water-use efficiency in *Arabidopsis*. *Plant Physiol.* 150: 1083-1092.
- Bond, D.M., Dennis, E.S. and Finnegan, E.J. (2011). The low temperature response pathways for cold acclimation and vernalization are independent. *Plant Cell Environ.* 34: 1737–1748.
- Casson, S.A., Franklin, K.A., Gray, J.E., Grierson, C.S., Whitlam, G.C., and Hetherington, A.M. (2009). phytochrome B and PIF4 regulate stomatal development in response to light quantity. *Curr. Biol.* 19: 229-234.
- Casson, S.A., and Hetherington, A.M. (2014). phytochrome B is required for light-mediated systemic control of stomatal development. *Curr. Biol.* 24: 1216-1221
- Chen, L., Chen, Y., Jiang, J., Chen, S., Chen, F., Guan, Z. and Fang, W. (2012). The constitutive expression of *Chrysanthemum dichrum ICE1* in *Chrysanthemum grandiflorum* improves the level of low temperature, salinity and drought tolerance. *Plant Cell Rep.* 31: 1747–1758.
- Chinnusamy, V., Ohta, M., Kanrar, S., Lee, B.H., Hong, X., Agarwal, M. and Zhu, J.K. (2003). ICE1: a regulator of cold-induced transcriptome

- and freezing tolerance in *Arabidopsis*. *Genes Dev.* 17: 1043–1054.
- Clough, S.J., and Bent, A.F. (1998). Floral dip: a simplified method for *Agrobacterium*-mediated transformation of *Arabidopsis thaliana*. *Plant J.* 16: 735-743.
- Crawford, A.J., McLachlan, D.H., Hetherington, A.M., and Franklin, K.A. (2012). High temperature exposure increases plant cooling capacity. *Curr. Biol.* 22: R396-397.
- Dello Ioio, R., Galinha, C., Fletcher, A.G., Grigg, S.P., Molnar, A., Willemsen, V., Scheres, B., Sabatini, S., Baulcombe, D., Maini, P.K. and Tsiantis, M. (2012). A PHABULOSA/cytokinin feedback loop controls root growth in *Arabidopsis*. *Curr. Biol.* 22: 1699–1704.
- Denay, G., Creff, A., Moussu, S., Wagnon, P., Thévenin, J., Gérentes, M.F., Chambrier, P., Dubreucq, B. and Ingram, G. (2014). Endosperm breakdown in *Arabidopsis* requires heterodimers of the basic helix-loop-helix proteins ZHOUP1 and INDUCER OF CBF EXPRESSION 1. *Development*, 141: 1222–1227.
- Deng, X.W., Caspar, T., and Quail, P.H. (1991). *cop1*: a regulatory locus involved in light-controlled development and gene expression in *Arabidopsis*. *Genes Dev.* 5: 1172-1182.
- Dong, C.H., Agarwal, M., Zhang, Y., Xie, Q., and Zhu, J.K. (2006). The negative regulator of plant cold responses, HOS1, is a RING E3 ligase that mediates the ubiquitination and degradation of ICE1. *Proc. Natl. Acad. Sci. USA* 103: 8281-8286.

- Dong, J., and Bergmann, D.C. (2010). Stomatal patterning and development. *Curr. Top. Dev. Biol.* 91: 267-297.
- Ding, Y., Li, H., Zhang, X., Xie, Q., Gong, Z., and Yang, S. (2015). OST1 kinase modulates freezing tolerance by enhancing ICE1 stability in *Arabidopsis*. *32*: 278-289.
- Driscoll, S.P., Prins, A., Olmos, E., Kunert, K.J., and Foyer, C.H. (2006). Specification of adaxial and abaxial stomata, epidermal structure and photosynthesis to CO<sub>2</sub> enrichment in *maize* leaves. *J. Exp. Bot.* 57: 381-390.
- Engineer, C.B., Ghassemian, M., Anderson, J.C., Peck, S.C., Hu, H., and Schroeder, J.I. (2014). Carbonic anhydrases, EPF2 and a novel protease mediate CO<sub>2</sub> control of stomatal development. *Nature* 513: 246-250.
- Fowler, S., Lee, K., Onouchi, H., Samach, A., Richardson, K., Morris, B., Coupland, G. and Putterill, J. (1999). *GIGANTEA*: a circadian clock-controlled gene that regulates photoperiodic flowering in *Arabidopsis* and encodes a protein with several possible membrane-spanning domains. *EMBO J.* 18: 4679–4688.
- Geisler, M., Nadeau, J., and Sack, F.D. (2000). Oriented asymmetric divisions that generate the stomatal spacing pattern in *Arabidopsis* are disrupted by the too many mouths mutation. *Plant Cell* 12: 2075-2086.
- Geisler, M.J., Deppong, D.O., Nadeau, J.A., and Sack, F.D. (2003). Stomatal neighbor cell polarity and division in *Arabidopsis*. *Planta* 216: 571-579.

- Gilmour, S.J., Zarka, D.G., Stockinger, E.J., Salazar, M.P., Houghton, J.M. and Thomashow, M.F. (1998). Low temperature regulation of the *Arabidopsis* CBF family of AP2 transcriptional activators as an early step in cold-induced *COR* gene expression. *Plant J.* 16: 433–442.
- Gray, J.E., Holroyd, G.H., van der Lee, F.M., Bahrami, A.R., Sijmons, P.C., Woodward, F.I., Schuch, W., and Hetherington, A.M. (2000). The HIC signalling pathway links CO<sub>2</sub> perception to stomatal development. *Nature* 408: 713-716.
- Gutierrez, L., Mauriat, M., Guénin, S., Pelloux, J., Lefebvre, J.F., Louvet, R., Rusterucci, C., Moritz, T., Guerineau, F., Bellini, C. and Van Wuytswinkel, O. (2008). The lack of a systematic validation of reference genes: a serious pitfall undervalued in reverse transcription-polymerase chain reaction (RT-PCR) analysis in plants. *Plant Biotechnol. J.* 6: 609–618.
- Guy, C.L. (1990). Cold acclimation and freezing stress tolerance: Role of protein metabolism. *Annu. Rev. Plant Physiol. Plant Mol. Biol.* 41: 187–223.
- Guy, C., Kaplan, F., Kopka, J., Selbig, J., and Hinch, D.K. (2008). Metabolomics of temperature stress. *Physiol. Plant* 132:220-235.
- Hetherington, A.M., and Woodward, F.I. (2003). The role of stomata in sensing and driving environmental change. *Nature* 424: 901-908.
- Henderson, I.R. and Dean, C. (2004). Control of *Arabidopsis* flowering: the chill before the bloom. *Development*, 131: 3829–3838.

- Horst, R.J., Fujita, H., Lee, J.S., Rychel, A.L., Garrick, J.M., Kawaguchi, M., Peterson, K.M., and Torii, K.U. (2015). Molecular framework of a regulatory circuit initiating two-dimensional spatial patterning of stomatal lineage. *PLoS Genet.* 11: e1005374.
- Hunt, L., and Gray, J.E. (2009). The signaling peptide EPF2 controls asymmetric cell divisions during stomatal development. *Curr. Biol.* 19: 864-869.
- Jang, I.C., Henriques, R., Seo, H.S., Nagatani, A., and Chua, N.H. (2010). *Arabidopsis* PHYTOCHROME INTERACTING FACTOR proteins promote phytochrome B polyubiquitination by COP1 E3 ligase in the nucleus. *Plant Cell* 22: 2370-2383.
- Jang, I.C., Yang, J.Y., Seo, H.S., and Chua, N.H. (2005). HFR1 is targeted by COP1 E3 ligase for post-translational proteolysis during phytochrome A signaling. *Genes Dev.* 19: 593-602.
- Jefferson, R.A., Kavanagh, T.A. and Bevan, M.W. (1987). GUS fusions: beta-glucuronidase as a sensitive and versatile gene fusion marker in higher plants. *EMBO J.* 6: 3901–3907.
- Jung, J.H., Park, J.H., Lee, S., To, T.K., Kim, J.M., Seki, M., and Park, C.M. (2013). The cold signaling attenuator HIGH EXPRESSION OF OSMOTICALLY RESPONSIVE GENE1 activates *FLOWERING LOCUS C* transcription via chromatin remodeling under short-term cold stress in *Arabidopsis*. *Plant Cell* 25: 4378-4390.
- Jung, J.H., Ju, Y., Seo, P.J., Lee, J.H. and Park, C.M. (2012). The

- SOC1-SPL module integrates photoperiod and gibberellic acid signals to control flowering time in *Arabidopsis*. *Plant J.* 69: 577–588.
- Jung, J.H., Seo, P.J. and Park, C.M. (2012). The E3 ubiquitin ligase HOS1 regulates *Arabidopsis* flowering by mediating CONSTANS degradation under cold stress. *J. Biol. Chem.* 287: 43277–43287.
- Kanaoka, M.M., Pillitteri, L.J., Fujii, H., Yoshida, Y., Bogenschutz, N.L., Takabayashi, J., Zhu, J.K. and Torii, K.U. (2008). *SCREAM/ICE1* and *SCREAM2* specify three cell-state transitional steps leading to *Arabidopsis* stomatal differentiation. *Plant Cell*, 20: 1775–1785.
- Kang, C.Y., Lian, H.L., Wang, F.F., Huang, J.R., and Yang, H.Q. (2009). Cryptochromes, phytochromes, and COP1 regulate light-controlled stomatal development in *Arabidopsis*. *Plant Cell* 21: 2624-2641.
- Kang, J.Y., Choi, H.I., Im, M.Y., and Kim, S.Y. (2002). *Arabidopsis* basic leucine zipper proteins that mediate stress-responsive abscisic acid signaling. *Plant Cell* 14: 343-357.
- Kim, H.J., Hyun, Y., Park, J.Y., Park, M.J., Park, M.K., Kim, M.D., Kim, H.J., Lee, M.H., Moon, J., Lee, I. and Kim, J. (2004). A genetic link between cold responses and flowering time through *FVE* in *Arabidopsis thaliana*. *Nat. Genet.* 36: 167–171.
- Kim, Y.S., Kim, S.G., Park, J.E., Park, H.Y., Lim, M.H., Chua, N.H., and Park, C.M. (2006). A membrane-bound NAC transcription factor regulates cell division in *Arabidopsis*. *Plant Cell* 18: 3132-3144.
- Kim, Y.S., Lee, M., Lee, J.H., Lee, H.J., and Park, C.M. (2015). The

- unified ICE-CBF pathway provides a transcriptional feedback control of freezing tolerance during cold acclimation in *Arabidopsis*. *Plant Mol. Biol.* 89: 187-201.
- Klermund, C., Ranftl, Q.L., Diener, J., Bastakis, E., Richter, R., and Schwechheimer, C. (2016). LLM-domain B-GATA transcription factors promote stomatal development downstream of light signaling pathways in *Arabidopsis thaliana* hypocotyls. *Plant Cell* 28: 646-660.
- Kumar, S.V. and Wigge, P.A. (2010). H2A.Z-containing nucleosomes mediate the thermosensory response in *Arabidopsis*. *Cell* 140: 136–147.
- Lampard, G.R., Macalister, C.A., and Bergmann, D.C. (2008). *Arabidopsis* stomatal initiation is controlled by MAPK-mediated regulation of the bHLH SPEECHLESS. *Science* 322: 1113-1116.
- Lau, O.S., and Deng, X.W. (2012). The photomorphogenic repressors COP1 and DET1: 20 years later. *Trends Plant Sci.* 17: 584-593.
- Lawson, T., and Blatt, M.R. (2014). Stomatal size, speed, and responsiveness impact on photosynthesis and water use efficiency. *Plant Physiol.* 164: 1556-1570.
- Lee, B.H., Henderson, D.A., and Zhu, J.K. (2005). The *Arabidopsis* cold-responsive transcriptome and its regulation by ICE1. *Plant Cell* 17: 3155-3175.
- Lee, C.M. and Thomashow, M.F. (2012). Photoperiodic regulation of the C-repeat binding factor (CBF) cold acclimation pathway and freezing tolerance in *Arabidopsis thaliana*. *Proc. Natl. Acad. Sci. USA* 109:

15054–15059.

- Lee, D.H., and Goldberg, A.L. (1998). Proteasome inhibitors: valuable new tools for cell biologists. *Trends Cell Biol.* 8: 397-403.
- Lee, H., Suh, S.S., Park, E., Cho, E., Ahn, J.H., Kim, S.G., Lee, J.S., Kwon, Y.M. and Lee, I. (2000). The AGAMOUS-LIKE 20 MADS domain protein integrates floral inductive pathways in *Arabidopsis*. *Genes Dev.* 14: 2366–2376.
- Lee, I., Michaels, S.D., Masshardt, A.S. and Amasino, R.M. (1994). The late-flowering phenotype of *FRIGIDA* and mutations in *LUMINIDEPENDENS* is suppressed in the Landsberg *erecta* strain of *Arabidopsis*. *Plant J.* 6: 903–909.
- Lee, J.H., Jung, J.H., and Park, C.M. (2015). INDUCER OF CBF EXPRESSION 1 integrates cold signals into FLOWERING LOCUS C-mediated flowering pathways in *Arabidopsis*. *Plant J.* 84: 29-40.
- Lee, J.H., Yoo, S.J., Park, S.H., Hwang, I., Lee, J.S. and Ahn, J.H. (2007). Role of *SVP* in the control of flowering time by ambient temperature in *Arabidopsis*. *Genes Dev.* 21: 397–402.
- Lian, H.L., He, S.B., Zhang, Y.C., Zhu, D.M., Zhang, J.Y., Jia, K.P., Sun, S.X., Li, L., and Yang, H.Q. (2011). Blue-light-dependent interaction of cryptochrome 1 with SPA1 defines a dynamic signaling mechanism. *Genes Dev.* 25: 1023-1028.
- Liang, C.H., and Yang, C.C. (2015). Identification of ICE1 as a negative regulator of ABA-dependent pathways in seeds and seedlings of

- Arabidopsis*. Plant Mol Biol. 88: 459-470.
- Li, D., Liu, C., Shen, L., Wu, Y., Chen, H., Robertson, M., Helliwell, C.A., Ito, T., Meyerowitz, E. and Yu, H. (2008). A repressor complex governs the integration of flowering signals in *Arabidopsis*. Dev. Cell 15: 110–120.
- Liu, B., Zuo, Z., Liu, H., Liu, X., and Lin, C. (2011). *Arabidopsis* cryptochrome 1 interacts with SPA1 to suppress COP1 activity in response to blue light. Genes Dev. 25: 1029-1034.
- Liu, C., Xi, W., Shen, L., Tan, C., and Yu, H. (2009). Regulation of floral patterning by flowering time genes. Dev. Cell 16: 711-722.
- Lu, X.D., Zhou, C.M., Xu, P.B., Luo, Q., Lian, H.L., and Yang, H.Q. (2015). Red-light-dependent interaction of phyB with SPA1 promotes COP1-SPA1 dissociation and photomorphogenic development in *Arabidopsis*. Mol. Plant 8: 467-478.
- MacAlister, C.A., Ohashi-Ito, K., and Bergmann, D.C. (2007). Transcription factor control of asymmetric cell divisions that establish the stomatal lineage. Nature 445: 537-540.
- McNellis, T.W., von Arnim, A.G., Araki, T., Komeda, Y., Miséra, S., and Deng, X.W. (1994). Genetic and molecular analysis of an allelic series of *cop1* mutants suggests functional roles for the multiple protein domains. Plant Cell 6: 487-500.
- Medina, J., Catalá, R., and Salinas, J. (2011). The CBFs: three *arabidopsis* transcription factors to cold acclimate. Plant Sci. 180: 3-11.

- Michaels, S.D. and Amasino, R.M. (1999). *FLOWERING LOCUS C* encodes a novel MADS domain protein that acts as a repressor of flowering. *Plant Cell* 11: 949–956.
- Michaels, S.D. and Amasino, R.M. (2001). Loss of *FLOWERING LOCUS C* activity eliminates the late-flowering phenotype of *FRIGIDA* and autonomous pathway mutations but not responsiveness to vernalization. *Plant Cell* 13: 935–941.
- Michaels, S.D., Himelblau, E., Kim, S.Y., Schomburg, F.M. and Amasino, R.M. (2005). Integration of flowering signals in winter-annual *Arabidopsis*. *Plant Physiol.* 137: 149–156.
- Miura, K., Jin, J.B., Lee, J., Yoo, C.Y., Stirn, V., Miura, T., Ashworth, E.N., Bressan, R.A., Yun, D.J. and Hasegawa, P.M. (2007). SIZ1-mediated sumoylation of ICE1 controls *CBF3/DREB1A* expression and freezing tolerance in *Arabidopsis*. *Plant Cell* 19: 1403–1414.
- Molkentin, J.D., and Olson, E.N. (1996). Combinatorial control of muscle development by basic helix-loop-helix and MADS-box transcription factors. *Proc. Natl. Acad. Sci. USA* 93: 9366-9373.
- Nadeau, J.A., and Sack, F.D. (2002). Control of stomatal distribution on the *Arabidopsis* leaf surface. *Science* 296: 1697-1700.
- Ohashi-Ito, K., and Bergmann, D.C. (2006). *Arabidopsis* FAMA controls the final proliferation/differentiation switch during stomatal development. *Plant Cell* 18: 2493-2505.
- Oraby, H. and Ahmad, R. (2012). Physiological and biochemical changes of

- CBF3* transgenic oat in response to salinity stress. *Plant Sci.* 185–186: 331–339.
- Osterlund, M.T., Hardtke, C.S., Wei, N., and Deng, X.W. (2000). Targeted destabilization of HY5 during light-regulated development of *Arabidopsis*. *Nature* 405: 462-466.
- Pacín, M., Legris, M., and Casal, J.J. (2014). Rapid decline in nuclear constitutive photomorphogenesis1 abundance anticipates the stabilization of its target elongated hypocotyl5 in the light. *Plant Physiol.* 164: 1134-1138.
- Page, T., Macknight, R., Yang, C.H. and Dean, C. (1999). Genetic interactions of the *Arabidopsis* flowering time gene *FCA*, with genes regulating floral initiation. *Plant J.* 17: 231–239.
- Pastore, J.J., Limpuangthip, A., Yamaguchi, N., Wu, M.F., Sang, Y., Han, S.K., Malaspina, L., Chavdaroff, N., Yamaguchi, A. and Wagner, D. (2011). LATE MERISTEM IDENTITY2 acts together with LEAFY to activate *APETALA1*. *Development* 138: 3189–3198.
- Pastore, J.J., Limpuangthip, A., Yamaguchi, N., Wu, M.F., Sang, Y., Han, S.K., Malaspina, L., Chavdaroff, N., Yamaguchi, A. and Wagner, D. (2011). LATE MERISTEM IDENTITY2 acts together with LEAFY to activate *APETALA1*. *Development* 138: 3189–3198.
- Pillitteri, L.J., Sloan, D.B., Bogenschutz, N.L., and Torii, K.U. (2007). Termination of asymmetric cell division and differentiation of stomata. *Nature* 445: 501-505.

- Pillitteri, L.J., and Torii, K.U. (2012). Mechanisms of stomatal development. *Annu. Rev. Plant Biol.* 63: 591-614.
- Raissig, M.T., Abrash, E., Bettadapur, A., Vogel, J.P., and Bergmann, D.C. (2016). Grasses use an alternatively wired bHLH transcription factor network to establish stomatal identity. *Proc. Natl. Acad. Sci. USA* 113: 8326-8331.
- Reichler, S.A., Balk, J., Brown, M.E., Woodruff, K., Clark, G.B., and Roux, S.J. (2001). Light differentially regulates cell division and the mRNA abundance of *pea* nucleolin during de-etiolation. *Plant Physiol.* 125: 339-350.
- Saijo, Y., Sullivan, J.A., Wang, H., Yang, J., Shen, Y., Rubio, V., Ma, L., Hoecker, U., and Deng, X.W. (2003). The COP1-SPA1 interaction defines a critical step in phytochrome A-mediated regulation of HY5 activity. *Genes Dev.* 17: 2642-2647.
- Sawa, M. and Kay, S.A. (2011). GIGANTEA directly activates *FLOWERING LOCUS T* in *Arabidopsis thaliana*. *Proc. Natl. Acad. Sci. USA* 108: 11698-11703.
- Seo, E., Lee, H., Jeon, J., Park, H., Kim, J., Noh, Y.S. and Lee, I. (2009). Crosstalk between cold response and flowering in *Arabidopsis* is mediated through the flowering-time gene *SOC1* and its upstream negative regulator *FLC*. *Plant Cell* 21: 3185-3197.
- Seo, H.S., Yang, J.Y., Ishikawa, M., Bolle, C., Ballesteros, M.L., and Chua, N.H. (2003). LAF1 ubiquitination by COP1 controls

- photomorphogenesis and is stimulated by SPA1. *Nature* 423: 995-999.
- Sheerin, D.J., Menon, C., zur Oven-Krockhaus, S., Enderle, B., Zhu, L., Johnen, P., Schleifenbaum, F., Stierhof, Y.D., Huq, E., and Hiltbrunner, A. (2015). Light-activated phytochrome A and B interact with members of the SPA family to promote photomorphogenesis in *Arabidopsis* by reorganizing the COP1/SPA complex. *Plant Cell* 27: 189-201.
- Shinozaki, K., Yamaguchi-Shinozaki, K., and Seki, M. (2003). Regulatory network of gene expression in the drought and cold stress responses. *Curr. Opin. Plant Biol.* 6: 410-417.
- Shpak, E.D., McAbee, J.M., Pillitteri, L.J., and Torii, K.U. (2005). Stomatal patterning and differentiation by synergistic interactions of receptor kinases. *Science* 309: 290-293.
- Stacey, M.G., Hicks, S.N., and von Arnim, A.G. (1999). Discrete domains mediate the light-responsive nuclear and cytoplasmic localization of *Arabidopsis* COP1. *Plant Cell* 11: 349-364.
- Suárez-López, P., Wheatley, K., Robson, F., Onouchi, H., Valverde, F. and Coupland, G. (2001). *CONSTANS* mediates between the circadian clock and the control of flowering in *Arabidopsis*. *Nature* 410: 1116–1120.
- Sung, S. and Amasino, R.M. (2004). Vernalization in *Arabidopsis thaliana* is mediated by the PHD finger protein VIN3. *Nature* 427: 159–164.
- Takada, S. and Goto, K. (2003). *TERMINAL FLOWER2*, an *Arabidopsis* homolog of *HETEROCHROMATIN PROTEIN1*, counteracts the activation of *FLOWERING LOCUS T* by *CONSTANS* in the vascular

- tissues of leaves to regulate flowering time. *Plant Cell* 15: 2856–2865.
- Thomashow, M.F. (1999). PLANT COLD ACCLIMATION: Freezing tolerance genes and regulatory mechanisms. *Annu. Rev. Plant Physiol. Plant Mol. Biol.* 50: 571-599.
- Torii, K.U., McNellis, T.W., and Deng, X.W. (1998). Functional dissection of *Arabidopsis* COP1 reveals specific roles of its three structural modules in light control of seedling development. *EMBO J.* 17: 5577-5587.
- Tricker, P.J., Gibbins, J.G., Rodríguez López, C.M., Hadley, P., and Wilkinson, M.J. (2012). Low relative humidity triggers RNA-directed de novo DNA methylation and suppression of genes controlling stomatal development. *J. Exp. Bot.* 63: 3799-3813.
- Udvardi, M.K., Czechowski, T., and Scheible, W.R. (2008). Eleven golden rules of quantitative RT-PCR. *Plant Cell* 20: 1736-1737.
- Valverde, F., Mouradov, A., Soppe, W., Ravenscroft, D., Samach, A. and Coupland, G. (2004). Photoreceptor regulation of CONSTANS protein in photoperiodic flowering. *Science* 303: 1003–1006.
- von Arnim, A.G., Osterlund, M.T., Kwok, S.F., and Deng, X.W. (1997). Genetic and developmental control of nuclear accumulation of COP1, a repressor of photomorphogenesis in *Arabidopsis*. *Plant Physiol.* 114: 779-788.
- Wang, J.W., Czech, B. and Weigel, D. (2009). miR156-regulated SPL transcription factors define an endogenous flowering pathway in

- Arabidopsis thaliana*. Cell 138: 738–749.
- Wang, Y., Jiang, C.J., Li, Y.Y., Wei, C.L. and Deng, W.W. (2012). CsICE1 and CsCBF1: two transcription factors involved in cold responses in *Camellia sinensis*. Plant Cell Rep. 31: 27–34.
- Wang, H., Ngwenyama, N., Liu, Y., Walker, J.C., and Zhang, S. (2007). Stomatal development and patterning are regulated by environmentally responsive mitogen-activated protein kinases in *Arabidopsis*. Plant Cell 19: 63-73.
- Weintraub, H. (1993). The MyoD family and myogenesis: redundancy, networks, and thresholds. Cell 75: 1241-2143.
- Xiao, J., Jin, R., Yu, X., Shen, M., Wagner, J.D., Pai, A., Song, C., Zhuang, M., Klasfeld, S., He, C., Santos, A.M., Helliwell, C., Pruneda-Paz, J.L., Kay, S.A., Lin, X., Cui, S., Garcia, M.F., Clarenz, O., Goodrich, J., Zhang, X., Austin, R.S., Bonasio, R., and Wagner, D. (2017). Cis and trans determinants of epigenetic silencing by Polycomb repressive complex 2 in *Arabidopsis*. Nat. Genet. 49: 1546-1552.
- Xu, F., Liu, Z., Xie, H., Zhu, J., Zhang, J., Kraus, J., Blaschnig, T., Nehls, R. and Wang, H. (2014). Increased drought tolerance through the suppression of *ESKMOI* gene and overexpression of *CBF*-related genes in *Arabidopsis*. PLoS One 9: e106509.
- Yamamuro, C., Miki, D., Zheng, Z., Ma, J., Wang, J., Yang, Z., Dong, J., and Zhu, J.K. (2014). Overproduction of stomatal lineage cells in *Arabidopsis* mutants defective in active DNA demethylation. Nat.

Commun. 5: 4062.

Yoo, S.D., Cho, Y.H., and Sheen, J. (2007). *Arabidopsis* mesophyll protoplasts: a versatile cell system for transient gene expression analysis. Nature Protoc. 2: 1565-1572.

Yoo, S.K., Chung, K.S., Kim, J., Lee, J.H., Hong, S.M., Yoo, S.J., Yoo, S.Y., Lee, J.S. and Ahn, J.H. (2005). CONSTANS activates *SUPPRESSOR OF OVEREXPRESSION OF CONSTANS 1* through *FLOWERING LOCUS T* to promote flowering in *Arabidopsis*. Plant Physiol. 139: 770–778.

Zarka, D.G., Vogel, J.T., Cook, D. and Thomashow, M.F. (2003). Cold induction of *Arabidopsis CBF* genes involves multiple ICE (inducer of *CBF* expression) promoter elements and a cold-regulatory circuit that is desensitized by low temperature. Plant Physiol. 133: 910–918.

Zuo, J., Niu, Q.W., and Chua, N.H. (2000). Technical advance: An estrogen receptor-based transactivator XVE mediates highly inducible gene expression in transgenic plants. Plant J. 24: 265-273.

Zuo, Z., Liu, H., Liu, B., Liu, X., and Lin, C. (2011). Blue light-dependent interaction of CRY2 with SPA1 regulates COP1 activity and floral initiation in *Arabidopsis*. Curr. Biol. 21: 841-847.

## PUBLICATION LIST

1. Lee, J.H., Jung, J.H., Park, C.M. (2017). Light inhibits COP1-mediated degradation of ICE transcription factors to induce stomatal development in *Arabidopsis*. **Plant Cell** pii: tpc.00371.
2. Lee, J.H., Park, C.M. (2015). Integration of photoperiod and cold temperature signals into flowering genetic pathways in *Arabidopsis*. **Plant Signal Behav.** 10: e1089373.
3. Kim, Y.S., Lee, M., Lee, J.H., Lee, H.J., Park, C.M. (2015). The unified ICE-CBF pathway provides a transcriptional feedback control of freezing tolerance during cold acclimation in *Arabidopsis*. **Plant Mol. Biol.** 89: 187-201.
4. Lee, J.H., Jung, J.H., Park, C.M. (2015). INDUCER OF CBF EXPRESSION 1 integrates cold signals into FLOWERING LOCUS C-mediated flowering pathways in *Arabidopsis*. **Plant J.** 84: 29-40.
5. Jung, J.H., Ju, Y., Seo, P.J., Lee, J.H., Park, C.M. (2012). The SOC1-SPL module integrates photoperiod and gibberellic acid signals to control flowering time in *Arabidopsis*. **Plant J.** 69: 577–588.

## ABSTRACT IN KOREAN (국문초록)

특정장소에 고착되어 살아가는 식물은 다양한 외부환경 변화에 반응하여야만 한다. 식물은 생존과 번식을 위하여 환경적 제약을 견뎌야 한다. 이러한 환경적 제약을 극복하기 위하여, 식물은 유전자 조절 기작을 통한 다양한 형태의 적응전략들을 진화적으로 발전시켜 왔다. 환경변화에 따른 유전자 발현은 전사인자를 포함한 수많은 전사조절인자에 의해 직접적으로 조절된다. 환경변화에 따른 ICE 전사인자에 의한 유전자 발현 조절현상이 알려져 있었다. 하지만, 어떻게 외부 환경변화 관련 조절 신호가 식물의 발달 조절경로에 통합되는지에 대한 이해는 부족한 실정이었다.

본 연구에서는 외부 환경변화 관련 신호와 식물 발달 조절경로와의 통합에 있어 ICE 전사인자의 기능을 규명하였다. 온도와 빛 반응성에 있어 핵심적인 역할을 하는 전사인자의 작용메커니즘 조절 기작이 규명되었다.

1장에서는 계절변화에 따른 온도 및 빛 주기 변화가 어떻게 개화시기 조절경로에 통합되는지에 대해서 알아보았다. 이 연구를 통하여 식물 개화시기를 면밀히 조절하는 향상된 신호 전달 체계를 규명하였다. 비교적 짧은 시기동안의 저온에 의한 개화시기 늦춤 현상은 주로 ICE1 전사인자를 통해 매개된다는 사실을 발견하였다. 또한 ICE1은 직접적으로 *FLC* 발현 증가에 관련한다는 사실을 밝혀냈다. 반면, 개화시기 유발조건에서 개화시기 촉진인자로 알려진 *SOC1* 단백질에 의한

ICE1의 *FLC* 및 *CBF3* promoter 지역에서의 결합 억제 현상을 규명함으로써, 개화시기 촉진과 저온저항성 감소현상을 확인하였다. 이러한 결론도출을 통하여 변화하는 자연환경 조건에서 식물의 개화시기 조절현상이 ICE1-*FLC*-*SOC1* 신호전달체계에 의해 면밀히 조절된다는 사실을 제시하였다.

2장에서는 어떻게 빛이 식물의 기공발달 촉진현상에 관여하는지를 연구하였다. 이번 연구를 통하여 빛이 없는 조건하에서 COP1에 의한 ICE 단백질의 분해현상과 유비퀴틴화 현상을 규명하였다. 또한, 빛은 COP1에 의한 ICE 단백질 분해현상을 억제한다는 사실을 표피세포에서 증명하였다. 이러한 결론도출을 통하여, 빛에 의해 증진되는 ICE 단백질 작용기작은 식물 기공발달에 있어 중요하다는 사실을 규명하였다.

**주요어:** 전사인자, 개화시기, 저온, 빛 신호전달 체계, 기공발달, 적응반응

**학번:** 2010-23096